

EFFECT OF THE PARTICLE SIZE OF ZIF-8 ON THE SEPARATION
PERFORMANCE OF ZIF-8/PNA/PES MEMBRANES

A THESIS SUBMITTED TO
THE GRADUATE SCHOOL OF NATURAL AND APPLIED SCIENCES
OF
MIDDLE EAST TECHNICAL UNIVERSITY

BY
İLHAN AYAS

IN PARTIAL FULFILLMENT OF THE REQUIREMENTS
FOR
THE DEGREE OF MASTER OF SCIENCE
IN
CHEMICAL ENGINEERING

SEPTEMBER 2014

Approval of thesis:

**EFFECT OF THE PARTICLE SIZE OF ZIF-8 ON THE SEPARATION
PERFORMANCE OF ZIF-8/PNA/PES MEMBRANES**

submitted by **İLHAN AYAS** in partial fulfillment of the requirements for the degree
of **Master of Science in Chemical Engineering Department, Middle East
Technical University** by,

Prof. Dr. Canan Özgen
Dean, Graduate School of **Natural and Applied Sciences**

Prof. Dr. Halil Kalıpçılar
Head of Department, **Chemical Engineering**

Prof. Dr. Halil Kalıpçılar
Supervisor, **Chemical Engineering Dept., METU**

Prof. Dr. Levent Yılmaz
Co-Supervisor, **Chemical Engineering Dept., METU**

Examining Committee Members:

Assoc. Prof. Dr. Yusuf Uludağ
Chemical Engineering Dept., METU

Prof. Dr. Halil Kalıpçılar
Chemical Engineering Dept., METU

Prof. Dr. Levent Yılmaz
Chemical Engineering Dept., METU

Asst. Prof. Dr. P. Zeynep Çulfaz Emecen
Chemical Engineering Dept., METU

Asst. Prof. Dr. Berna Topuz
Chemical Engineering Dept., Ankara University

Date: 05.09.2014

I hereby declare that all information in this document has been obtained and presented in accordance with academic rules and ethical conduct. I also declare that, as required by these rules and conduct, I have fully cited and referenced all material and results that are not original to this work.

Name, Last name : İlhan AYAS

Signature :

ABSTRACT

EFFECT OF THE PARTICLE SIZE OF ZIF-8 ON THE SEPARATION PERFORMANCE OF ZIF-8/PNA/PES MEMBRANES

Ayas, İlhan

M. S, Department of Chemical Engineering

Supervisor: Prof. Dr. Halil Kalıpçılar

Co-supervisor: Prof. Dr. Levent Yılmaz

September 2014, 128 pages

Membrane based separation processes have great potential of acquiring a significant role in the gas separation processes in the coming future. In this study, the effect of the particle size of ZIF-8 on the gas separation performance of PES/pNA/ZIF-8 mixed matrix membranes (MMMs) was investigated. MMMs were prepared by solvent evaporation method, and polyethersulfone (PES) was used as the polymer, p-nitro aniline (pNA) as the low molecular weight additive and Zeolitic Imidazolate Framework-8 (ZIF-8) as filler material.

Various particle sizes of ZIF-8 crystals were synthesized by using 1 hour stirring method at room temperature. ZIF-8s with particle sizes of 65, 144 and 262 nm were synthesized by using different MeOH/Zn⁺² molar ratios. Recycling of the mother liquor method was used to synthesize ZIF-8s with particle sizes of 14 and 23 nm. Synthesized ZIF-8 crystals were characterized by X-ray diffractometer, nitrogen

adsorption/desorption (BET), scanning electron microscopy (SEM) and transmission electron microscopy (TEM).

PES/pNA/ZIF-8 MMMs with two different ZIF-8 loadings for varying particle sizes were also investigated to understand the combined effect of particle size and loading. The single gas permeation performances of the MMMs were determined for H₂, CO₂ and CH₄ gases at feed pressures of 3 bar. Also, the single gas permeabilities of the selected PES/pNA(4%)/ZIF-8(10%, 23 nm) MMM were measured at feed pressures of 6, 10, 12 and 15 bar in order to investigate the effect of the feed pressure on the separation performance. The binary gas separation performances of selected MMM were also investigated with CO₂/CH₄ mixtures for different feed gas compositions at feed pressures of 3 and 10 bar. Moreover, MMMs were characterized by scanning electron microscopy (SEM) analysis.

The single gas permeabilities of all gases and ideal selectivities for all gas pairs of 10% (wt/wt) ZIF-8 loaded PES/pNA(4%)/ZIF-8 MMMs increased with decreasing particle sizes of ZIF-8 except for 14 nm ZIF-8 loaded membrane. Also, the single gas permeabilities increased significantly when the loading amount of ZIF-8 rose from 10% to 20% (wt/wt). For the 20% (wt/wt) ZIF-8 loaded PES/pNA(4%)/ZIF-8 MMMs, the single gas permeabilities had an descending trend when the particle sizes of ZIF-8s were increasing; however, the ideal selectivities increased. A significant improvement was obtained in permeabilities and ideal selectivities by using the particle size of 23 nm ZIF-8 loaded PES/pNA(4%)/ZIF-8(10%) MMM. The single gas permeations of the selected MMM were measured with increasing feed pressure from 3 bar to 15 bar. The H₂ permeability was not affected by changing feed pressure and might be said as pressure independent. However, the CO₂ and CH₄ permeabilities decreased with increasing feed pressure. Also, the ideal selectivity of H₂/CH₄ pair showed the highest selectivity improvement when the feed pressure increased from 3 bar to 15 bar. It was observed that selected MMM had good gas separation performance at high pressure conditions.

The binary gas separation performance of the selected MMM showed that the separation factors of CO₂/CH₄ pair remained nearly constant with increasing feed composition of CO₂ at 3 bar, and it was similar to ideal selectivity. Also, the separation factors at 10 bar had two types of behavior according to CO₂ composition of the feed. The behavior of separation factors at 10 bar had similar behavior at 3 bar until the feed was 22.5 % CO₂ in the first section. However, the separation factors at 10 bar were higher than the ideal selectivity when the CO₂ composition of the feed was more than 22.5% in the second section.

Keywords: Gas Separation, Mixed matrix membranes, Polyethersulfone, Zeolitic Imidazolate Framework-8 (ZIF-8), Low molecular weight additive

ÖZ

ZIF-8 PARTİKÜL BOYUTLARININ ZIF-8/PNA/PES MEMBRANLARIN AYIRMA PERFORMANSINA ETKİLERİ

Ayas, İlhan

Yüksek Lisans, Kimya Mühendisliği Bölümü

Tez Yöneticisi: Prof. Dr. Halil Kalıpçılar

Ortak Tez Yöneticisi: Prof. Dr. Levent Yılmaz

Eylül 2014, 128 sayfa

Membran bazlı ayırma prosesleri ilerleyen yıllarda gaz ayırma proseslerinde önemli bir rol elde edebilecek potansiyele sahiptirler. Bu çalışmada ZIF-8 partikül boyutunun PES/pNA/ZIF-8 karışık matrisli membranların ayırma performanslarına etkisi incelenmiştir. Karışık matrisli membranlar çözücü buharlaştırma yöntemiyle hazırlanmıştır. Bu çalışmada polimer olarak polietersülfon (PES), düşük molekül ağırlıklı uyumlaştırıcı olarak p-nitro anilin (pNA) ve dolgu malzemesi olarak Zeolitik Imidazolat Kafes-8 (ZIF-8) kullanılmıştır.

Farklı partikül boyutlarında ZIF-8 kristalleri 1 saatlik karıştırma yöntemi kullanılarak oda sıcaklığında sentezlenmiştir. 65, 144 ve 262 nm partikül boyutlarındaki ZIF-8 kristalleri farklı MeOH/Zn⁺² molar oranları kullanılarak sentezlenmiştir. Ayrıca ana çözeltinin geri dönüşüm metodu kullanılarak 14 ve 23 nm partikül boyutlarında ZIF-8 kristalleri elde edilmiştir. Sentezlenen farklı partikül boyutlarındaki ZIF-8

kristalleri X-ray ışınım kırınımı (XRD), azot adsorpsiyon/desorpsiyon (BET), taramalı elektron mikroskobu (SEM), geçirimli elektron mikroskobu (TEM) ile karakterize edilmişlerdir.

Farklı partikül boyutlarındaki ZIF-8 kristallerinin yükleme miktarı ile birlikte gaz ayırma performansına etkisinin araştırılması için PES/pNA/ZIF-8 karışık matrisli membranlar hazırlanmıştır. Hazırlanan membranlar ağırlıkça %4 pNA ve farklı partikül boyutlarındaki ZIF-8 kristallerinden (14 ile 262 nm aralığında) ağırlıkça %10 ve %20 miktarlarda eklenmiştir. Karışık matrisli membranların tekli gaz geçirgenlik performansları 3 bar besleme basıncında H₂, CO₂ ve CH₄ gazları ile belirlenmiştir. Ayrıca besleme basıncının ayırma performansına etkisini incelemek amacıyla seçilen PES/pNA(4%)/ZIF-8(10%, 23 nm) karışık matrisli membranı 6, 10, 12, 15 bar besleme basınçlarında tekli gaz geçirgenlikleri ölçülmüştür. Seçilen karışık matrisli membranın 3 ve 10 bar besleme basınçlarında ve farklı besleme kompozisyonlarında CO₂/CH₄ gaz çifti için ikili gaz ayırma performansı incelenmiştir. Ayrıca sentezlenen karışık matrisli membranlar SEM analizi ile karakterize edilmişlerdir.

Hazırlanan ağırlıkça %10 ZIF-8 içeren PES/pNA(%4)/ZIF-8 membranlarının tüm gazlar için geçirgenlik ve tüm gaz çiftleri için ideal seçicilik değerleri kullanılan ZIF-8' in partikül boyutunun azaldıkça arttığı görülmüştür. 14 nm ZIF-8 kullanılarak hazırlanan membran bu trendin içinde yer almamaktadır. Ayrıca eklenen ZIF-8 miktarı ağırlıkça %10'dan %20'ye arttığında tekli gaz geçirgenlik değerleri önemli derecede artmıştır. Ağırlıkça %20 ZIF-8 içeren PES/pNA(%4)/ZIF-8 membranlarının eklenen ZIF-8 partikül boyutu arttıkça tekli gaz geçirgenlik değerlerinde azalan bir trend görülmüştür. Fakat ideal seçicilik değerlerinde ise artış olmuştur. Tekli gaz geçirgenliği ve ideal seçicilik değerlerindeki en önemli miktarda artış 23 nm partikül boyutunda ağırlıkça %10 miktarında ZIF-8 kullanılarak hazırlanan membranda olduğu belirlenmiştir. Seçilen PES/pNA(%4)/ZIF-8(10, 23 nm) membranı kullanılarak 3 bar ile 15 bar besleme basınç aralığında tekli gaz geçirgenlikleri ölçülmüştür. H₂ geçirgenliği besleme basıncının değişiminden etkilenmemiştir ve basınçtan bağımsız olduğu söylenebilir. Ancak CO₂ ve CH₄

geçirgenlikleri besleme basıncının etkisi ile azalmıştır. Seçilen PES/pNA(%4)/ZIF-8(%10, 23 nm) membranının yüksek basınç koşullarında yüksek gaz ayırma performansına sahip olduğu görülmüştür.

Seçilen membranın ikili CO₂/CH₄ gaz ayırma performansı sonucunda 3 bar besleme basıncı geçirgenliğinde elde edilen ayırım seçiciliği değeri ile ideal seçicilik değerinin benzer olduğu görülmüştür. Ayrıca 10 bar besleme basıncında yürütülen geçirgenlik ölçümünde beslemedeki CO₂ kompozisyonuna bağlı olarak iki farklı davranış gözlenmiştir. İlk aşamada 10 bar besleme basıncındaki geçirgenlik ölçümünde ayırım seçiciliği değerleri 3 bar besleme basıncındaki ayırım seçiciliği değerlerine benzer değerlere sahiptirler. Fakat ikinci aşamada beslemedeki CO₂ kompozisyonu %22.5 oranından fazla olduğunda 10 bar besleme basıncındaki ayırım seçicilik değerleri ideal seçicilik değerlerinden yüksek davranış göstermişlerdir.

Anahtar Kelimeler: Gaz ayırımı, Karışık matrisli membran, Polietersülfon, Zeolitik Imidazolat Kafes-8 (ZIF-8), Düşük molekül ağırlıklı uyumlaştırıcı

To my family

ACKNOWLEDGEMENTS

First of all, I'm deeply grateful to my supervisor Prof. Dr. Halil Kalıpçılar for his significant contributions and guidance during this study. I would like to show my appreciation to my co-supervisor Prof. Dr. Levent Yılmaz for his precious suggestions and support. It was a pleasing honor for me to work with them.

I would like to present my sincere thanks to my dear lab colleagues Elif İrem Şenyurt, Fırat Ozanırk, Gülçin Kaltalı, Melis Kargılı, Nilay Keser and Burcu Tüzün for their kind friendship, help and useful cooperation.

I would also like to thank to my dear friends Cihan Can, Suna Sop and Sefa Taşaltın for their endless friendship. Also, I sincerely thanks to all my friends who were beside me during my graduate study.

My very special thanks go to my family for their great support, encouragement and unlimited patience.

TABLE OF CONTENTS

ABSTRACT	v
ÖZ	viii
ACKNOWLEDGEMENTS	xii
TABLE OF CONTENTS	xiii
LIST OF FIGURES	xv
LIST OF TABLES	xviii
LIST OF SYMBOLS AND ABBREVIATIONS	xx
CHAPTERS	
1. INTRODUCTION	1
2. LITERATURE SURVEY	7
2.1 Polymeric Gas Separation Membranes	7
2.2 Mixed Matrix Membranes (MMMs).....	11
2.3 Metal Organic Frameworks (MOF)	14
2.3.1 Metal Organic Framework-Mixed Matrix Membranes.....	15
2.3.2 Zeolitic Imidazolate Framework-8 (ZIF-8).....	16
2.3.3 ZIF-8 based Mixed Matrix Membranes	19
2.4 Effect of the Particle Size of Filler on the Gas Separation Performance	23
2.5 Separation of Binary Gas Mixtures with Mixed Matrix Membranes	24
3. EXPERIMENTAL	27
3.1 Synthesis of ZIF-8.....	27
3.1.1 Materials.....	27
3.1.2 Preparation of ZIF-8.....	27
3.1.3 Characterization of ZIF-8.....	28
3.2 Membrane Preparation	29
3.2.1 Materials for Membrane Preparation	29
3.2.2 Membrane Preparation Methodology	30
3.2.3 Membrane Characterization	31
3.3 Gas Permeation Measurements	33
3.3.1 Gas Permeation System and Procedure of Measurement	33
3.3.2 Binary Gas Permeation System and Procedure of Measurement.....	35
4. RESULTS AND DISCUSSION	39
4.1 Characterization of ZIF-8.....	39
4.2 Membrane Characterization	47
4.2.1 SEM Results.....	47

4.3 Single Gas Permeation Results of PES/pNA/ZIF-8 MMMs.....	51
4.4 Effect of Feed Pressure on the Gas Separation Performance of PES/pNA(4%)/ZIF-8(10%, 23 nm).....	62
4.5 Binary Gas Permeation Results of PES/pNA(4%)/ZIF-8(10%, 23 nm) MMM ..	67
5. CONCLUSIONS	71
6. RECOMMENDATIONS	73
REFERENCES.....	75
APPENDICES	
APPENDIX A: THE AMOUNTS OF CHEMICALS FOR THE SYNTHESIS OF ZIF-8.....	81
APPENDIX B: THE AMOUNTS OF MATERIALS IN MEMBRANE PREPARATION	83
APPENDIX C: CALCULATION OF SINGLE PERMEABILITIES	85
APPENDIX D: CALIBRATION OF GAS CHROMATOGRAPHY.....	87
APPENDIX E: A SAMPLE CALCULATION FOR DETERMINATION OF PERMEABILITIES AND SELECTIVITIES OF BINARY GAS MIXTURES	89
APPENDIX F: SAMPLE CALCULATION OF YIELD AND COMPOSITIONS OF ZIF-8 SYNTHESIS SOLUTIONS.....	93
APPENDIX G: SAMPLE CALCULATION OF PARTICLE SIZE BY USING SCHERRER EQUATION.....	103
APPENDIX H: REPRODUCIBILITY OF ZIF-8 SYNTHESIS	105
APPENDIX I: THE NUMBER OF ZIF-8 PARTICLES PER GRAM CALCULATION	107
APPENDIX J: DETERMINATION OF AVERAGE PARTICLE SIZES OF ZIF-8 BY USING SEM IMAGES.....	109
APPENDIX-K: SEM IMAGES OF ZIF-8 SAMPLES.....	111
APPENDIX-L: SEM IMAGES OF PES/pNA(4%)/ZIF-8(10%, 23nm) MMM.....	115
APPENDIX-M: REPRODUCIBILITIES OF SINGLE GAS PERMEATION EXPERIMENTS	117
APPENDIX-N: REPRODUCIBILITIES OF HIGH PRESSURE PERMEATION EXPERIMENTS	123
APPENDIX-O: REPRODUCIBILITIES OF BINARY GAS PERMEATION EXPERIMENTS	125

LIST OF FIGURES

FIGURES

Figure.2.1 Upper bound correlation for H ₂ /CH ₄ separation.....	10
Figure.2.2 The sodalite topology (left) and narrow six-membered-ring opening through which molecules have to pass (right).....	17
Figure.2.3 (a) XRD pattern and (b) N ₂ adsorption-desorption isotherm of ZIF-8 crystals.....	18
Figure.2.4 Adsorption isotherms of (a) CO ₂ and (b) CH ₄ in ZIF-8 at 298 K.....	18
Figure.2.5 Adsorption isotherms of CO ₂ /CH ₄ (50:50 mol/mol) gas mixture	19
Figure.3.1 The structure of repeating unit of polyethersulfone (PES).....	29
Figure.3.2 The structural formula of p-Nitro Aniline	30
Figure.3.3 The preparation methodology of PES/pNA/ZIF-8 MMMs	32
Figure.3.4 The schematic drawing of the gas permeability set-up	34
Figure.3.5 The six port injection valve in GC.....	36
Figure.4.1 XRD patterns of ZIF-8 crystals with different particle sizes.....	41
Figure.4.2 N ₂ adsorption/desorption isotherms of ZIF-8 crystals with different particle sizes.....	44
Figure.4.3 SEM images of ZIF-8 crystals: (a) 14 nm, (b) 23 nm, (c) 65 nm, (d) 144 nm, (e) 262 nm	45
Figure.4.4 TEM images of ZIF-8 crystals: (a1) and (a2) 14 nm, (b1) and (b2) 23 nm, (c1) and (c2) 65 nm	46

Figure.4.5 Cross-sectional SEM images of PES/pNA(4%)/ZIF-8(10%) MMMs with respect to increasing particle size of ZIF-8 (a) 23 nm, (b) 65 nm, (c) 262 nm	47
Figure.4.6 Cross-sectional SEM images of PES/pNA(4%)/ZIF-8(20%) MMMs with respect to increasing particle size of ZIF-8 (a) 23 nm, (b) 65 nm, (c) 144 nm	48
Figure.4.7 Cross-sectional SEM images of (a) PES/pNA(4%)/ZIF-8(10%) (23 nm), (b) PES/pNA(4%)/ZIF-8(20%) (23 nm)	50
Figure.4.8 Effect of particle size of ZIF-8 on the single gas separation performance of PES/pNA(4%)/ZIF-8(10%) MMMs	53
Figure.4.9 Effect of particle size of ZIF-8 on the single gas separation performance of PES/pNA(4%)/ZIF-8(20%) MMMs	55
Figure.4.10 The permeation results of PES/pNA(4%)/ZIF-8(10%) MMMs on the Robeson's upper bound curves for H ₂ /CO ₂ , CO ₂ /CH ₄ and H ₂ /CH ₄ gas pairs.....	59
Figure.4.11 The permeation results of PES/pNA(4%)/ZIF-8(20%) MMMs on the Robeson's upper bound curves for H ₂ /CO ₂ , CO ₂ /CH ₄ and H ₂ /CH ₄ gas pairs.....	60
Figure.4.12 The permeation results of PES/pNA(4%)/ZIF-8(10%) (23 nm) and PES/pNA(4%)/ZIF-8(20%) (23 nm) MMMs on the Robeson's upper bound curves for H ₂ /CH ₄ gas pair	61
Figure.4.13 The permeabilities for H ₂ , CO ₂ and CH ₄ for PES/pNA(4%)/ZIF-8(10%) (23 nm) MMM with different feed pressures.....	63
Figure.4.14 The ideal selectivities for H ₂ /CO ₂ , CO ₂ /CH ₄ and H ₂ /CH ₄ gas pairs for PES/pNA(4%)/ZIF-8(10%) (23 nm) MMM with different feed pressures.....	64
Figure.4.15 The effect of the feed pressure on PES/pNA(4%)/ZIF-8(10%)(23 nm) in Robeson's upper bound curves for H ₂ /CO ₂ , CO ₂ /CH ₄ and H ₂ /CH ₄ gas pairs.....	66
Figure.4.16 Effect of the feed composition on the permeabilities of CO ₂ /CH ₄ gas mixture for PES/pNA(4%)/ZIF-8(10%) (23 nm) MMM	67
Figure.4.17 Effect of the feed composition of CO ₂ on the separation factor for CO ₂ /CH ₄ mixture and CH ₄ amount in permeate for PES/pNA(4%)/ZIF-8(10%) (23 nm) MMM with different feed pressures	69
Figure C.1 The pressure change versus time graph for H ₂ permeation test for PES/ZIF-8(144nm)(10%)/pNA(4%).....	85
Figure C.2. Algorithm for single gas permeability calculation.....	86

Figure D.1. The calibration curve of CO ₂	88
Figure D.2. The calibration curve of CH ₄	88
Figure H.1 XRD patterns of the second trial synthesis of ZIF-8s.....	105
Figure.J.1 Used SEM images for counting particle sizes of ZIF-8 crystals.....	109
Figure.K.1 SEM images of ZIF-8 crystals (a) 14 nm, (b) 23 nm, (c) 65 nm, (d) 144 nm,(e) 262 nm	111
Figure.L.1 SEM images of PES/pNA(4%)/ZIF-8(10%, 23nm) MMM.....	115

LIST OF TABLES

TABLES

Table.2.1 Gas separation membrane applications in the industry	9
Table.2.2 The ideal selectivities of ZIF-8 loaded MMMs in literature	22
Table.3.1 Operating conditions of GC	36
Table.4.1 Yields, normalized crystallinities and calculated crystallite sizes of ZIF-8 crystals and average particle sizes of ZIF-8 based on SEM images with synthesis molar ratios.....	41
Table.4.2 BET surface areas, external surface areas, volume adsorbed values and number of particles per gram values of ZIF-8 crystals with different particle sizes.	43
Table.4.3 Gas permeation performances of pure PES, PES/pNA and ZIF-8 loaded PES/pNA MMMs.....	57
Table A.1 Weights of used chemicals during the synthesis of ZIF-8 with different average particle sizes.....	81
Table B.1 Weights of used polymer, filler, low molecular weight additive and volume of solvent during the preparation of membranes.....	83
Table H.1 Yields, crystallinities and calculated particle size of the second trial synthesis of ZIF-8 crystals with synthesis molar ratios	106
Table.J.1 Particle sizes of each crystals and average particle sizes of ZIF-8 samples.....	110
Table M.1 Reproducibility data for pure PES, PES/pNA(4%) and ZIF-8 loaded PES/pNA(4%) MMMs.....	117
Table N.1 Reproducibility data of high pressure permeation measurements for PES/pNA(4%)/ZIF-8(10%, 23nm) MMMs	123

Table O.1 Reproducibility data of binary gas permeation measurements for PES/pNA(4%)/ZIF-8(10%, 23nm) MMMs	125
--	-----

LIST OF SYMBOLS AND ABBREVIATIONS

A : Effective membrane area (cm^2)

D: diffusion coefficient

dn/dt : Molar flow rate (mol/s)

dp/dt : Pressure increase

J : Flux ($\text{cm}^3/\text{cm}^2.\text{s}$)

L : thickness of the membrane (μm)

M : Molecular weight of the gas

P : Permeability (Barrer)

P_f : Feed side pressure (cmHg)

P_p : Permeate side pressure (cmHg)

R : Ideal gas constant

S: Solubility (cm^3 (STP)/ $\text{cm}^3.\text{atm}$)

T : Temperature ($^{\circ}\text{C}$)

T_g : Glass transition temperature ($^{\circ}\text{C}$)

V_d : Dead volume (cm^3)

X: mole fraction of the components

Y: mole fraction of the components

Greek Letters

α : Selectivity

ρ : Density of the gas

Δp : Transmembrane pressure difference (cmHg)

θ : Bragg Angle ($^{\circ}$)

CHAPTER 1

INTRODUCTION

Membrane technology is an advancing separation process due to its advantages that are ease of operation, low energy requirements, low cost [1-3]. Membrane technology is applicable in various separation processes such as CO_2/CH_4 in natural gas purification, CO_2/H_2 separation in purification of synthesis gas, oxygen enrichment from O_2/N_2 , recovery of landfill gas, H_2/N_2 separation in ammonia purge gas [2-4].

Membrane is a selective barrier between phases. The retentate is part of the feed that cannot pass through the membrane. Components pass through the membrane are called as permeate. Permeability and selectivity are typical properties that determine the efficiency of a gas separation membrane. The transport through a membrane can take place due to the pressure gradient. In polymeric dense membranes gas separation is achieved by solution-diffusion mechanism. Solution-diffusion mechanism is described in three steps. Firstly, the gas molecules are sorbed at one interphase of the membrane. In second step, the gas molecules are passed through the polymer matrix by diffusion. Finally, they are desorbed at the other interphase. There are two parameters that affect solution-diffusion mechanism; namely, the diffusion coefficient and the solubility coefficient [1, 5, 6].

The permeability of a membrane is expressed and can be found based on flux measurements through the membrane by

$$P = \frac{Jl}{P_f - P_p} \quad (1.1)$$

where P_f is the partial pressure of the feed side, P_p is the partial pressures of the permeate side, l is the thickness of the membrane and J is flux of gas passing through the membrane. Barrer is generally used as a unit of permeability.

Ideal selectivity is defined as the ratio of the individual gas permeabilities. Ideal selectivity determines the membrane efficiency, and also is expressed as,

$$\alpha_{AB} = \frac{P_A}{P_B} \quad (1.2)$$

Separation performance of a membrane for gas mixture is represented with separation factor instead of ideal selectivity, defined as,

$$\alpha_{A/B} = \frac{(y_A/y_B)_p}{(x_A/x_B)_f} \quad (1.3)$$

where x is the feed side mole fraction of the component, y is the permeate side mole fraction of the component.

Polymeric materials are dominant membrane materials in gas separation due to their desirable properties. Polymeric membranes have good mechanical properties, the flexibility to be produced different module types, low cost and ease of fabrication [3, 7, 8]. The relationship between permeability and selectivity was examined by Robeson [9], and represented by a trade-off line. It was indicated permeability-selectivity trade-off curves of many polymeric membranes for different gas pairs. In the permeability-selectivity trade-off, it was observed that the polymeric membranes have a limit of their gas separation performances despite of their desired properties [9, 10].

The inorganic membranes can be more favorable due to their high permeability, selectivity, thermal and chemical stability properties. Nevertheless they have limited by high fabrication costs, low reproducibility, low mechanical resistance and breakability [9, 10].

A new type of organic-inorganic membrane, mixed matrix membrane (MMM), has been developed to incorporate the desired properties of polymeric and inorganic membranes. Mixed matrix membranes consist of two phases such as the dispersed phase (inorganic materials) and the continuous phase (polymer) [7, 10]. MMM is expected to exhibit better performance than polymeric membrane. However, poor adhesion of inorganic filler with polymer matrix causes undesirable voids, and poor dispersion of inorganic filler in polymer matrix. Gas molecules pass through these non-selective voids during the transportation due to their low resistance. Therefore, the selectivity decreases with increasing permeability [3, 7, 11]. Some methods were proposed in the literature to eliminate non-interfacial voids such as modification of the external surface of filler by silylation, addition of low molecular weight additive and annealing of MMM above glass transition temperature [11-13]. Properties of mixed matrix membrane can be affected by particle size, pore size, loading amount of inorganic material and properties of polymeric materials [3, 7, 11].

Many types of materials can be used as the inorganic filler in MMMs that are carbon molecular sieves, microporous molecular sieves, mesoporous materials, silica nanoparticles, carbon nanotubes, metal organic frameworks and activated carbons [7, 10, 11]. Metal organic frameworks (MOFs) are formed from the functional groups that are the organic ligands and the metal ions or clusters. MOFs are widely used in gas storage and gas separation processes. They have desirable properties such as high surface area and tunable porosity properties [10, 14]. Zeolitic Imidazolate Frameworks (ZIFs) have arisen as a new type of crystalline nanoparticles, and they are sub-family of MOFs. ZIFs comprise desirable characteristics from both zeolites and metal organic frameworks. ZIFs possess some characteristics for gas separation applications such as high microporosity, high surface area, and high thermal and chemical stability. ZIF-8, which has mostly studied as a subclass of zeolitic imidazolate frameworks, has greatly potential for gas storage of CO₂, H₂, gas separations and catalysis. ZIF-8 has sodalite zeolite type structure and highly porous open framework [14-16]. Properties of filler materials in the MMM must be relevant to gas molecules such as pore size distribution, surface area and surface chemistry [11]. ZIF-8 crystals have great separation ability to gases of H₂ and

CO₂ from larger gases because of their narrow pore size (0.34 nm in diameter) [1, 14, 17]. Some researches were investigated the effects of ZIF-8 in mixed matrix membranes [10, 18, 19, 21]. The gas separation performances of MMMs were enhanced by addition of ZIF-8 up to 30% (w/w), generally. Also 10 and 20% (w/w) ZIF-8 loaded MMMs had better separation performances and mechanical stability [10, 21]. On the other hand, it was shown in literature that addition of low molecular weight additive improved the selectivities of MMMs [16, 19, 20].

In this study, the effect of the particle size of ZIF-8 on the gas separation performance of ZIF-8/pNA/PES MMMs was investigated. Synthesized ZIF-8 crystals were characterized by X-ray diffractometer, N₂ adsorption/desorption analysis (BET), scanning electron microscopy (SEM) and transmission electron microscopy (TEM). Then, ternary MMMs were produced with ZIF-8 crystals as dispersed phase, polyethersulfone (PES) as polymer matrix and p-nitroaniline (pNA) as a low molecular weight additive (LMWA). In order to investigate effect of particle size of ZIF-8 crystals on the gas separation performances, ternary MMMs were prepared with particle sizes of ZIF-8 crystals between 14 nm and 262 nm. ZIF-8 crystals with different particle sizes were synthesized at room temperature from mixtures with different methanol molar ratio method and recycling mother liquor methodology. The objective of the addition of ZIF-8 with small particle sizes was to have improved compatibility between the ZIF-8 and PES. When the particle sizes of filler are smaller, its interfacial voids can be reduced. The change in particle volume is proportional to the change in particle diameter in third order. That means, the number of particle in a unit mass are affected significantly by changing particle size. In this study, pure PES membrane, PES/pNA (4% w/w) membrane and PES/ZIF-8 (10, 20% w/w)/pNA (4% w/w) MMMs were investigated. The separation performances of membranes were determined by single gas permeation measurements of H₂, CO₂ and CH₄ gases at feed pressure of 3 bar. Also single gas permeation experiments were measured at feed pressures of 3, 6, 10, 12 and 15 bar to examine the effect of feed pressure on the separation performance of the selected ternary MMM. Binary gas permeation measurements with different compositions of CO₂/CH₄

gas mixtures were conducted at feed pressure of 10 bar. The membrane morphologies were also evaluated by scanning electron microscopy (SEM) analysis.

CHAPTER 2

LITERATURE SURVEY

2.1 Polymeric Gas Separation Membranes

The membrane can be described as an interphase between phases [1]. Membranes can be used as a thin barrier for selective removal of one or more component from a mixture in the membrane based separation processes. The retentate is the part of the feed that could not pass through the membrane. The other part does pass through the membrane that is called as permeate. Driving force allows transport of feed components through the membrane during the separation processes. Driving force can be based on concentration or pressure difference. Two common characteristics used to describe the performance of membranes are the permeability (the ability of component to pass across the membrane) and selectivity (the ratio of the permeabilities of the components). A higher permeability reduces the membrane area required for separation, while high selectivity results in a product with higher purity [1, 22]. The permeability can be expressed as Eqn.2.1,

$$P = \frac{Jl}{P_f - P_p} \quad (2.1)$$

where l is the thickness of the membrane, J is flux of gas passing through the membrane, P_f is the partial pressure of the each sides. The barrer is the unit of the permeability, and it is expressed by Eqn.2.2,

$$1 \text{ Barrer} = \frac{10^{-10} \text{ cm}^3 \text{ STP} \cdot \text{cm}}{\text{cm}^2 \cdot \text{s} \cdot \text{cm-Hg}} \quad (2.2)$$

The ideal selectivity indicates the efficiency of the membrane, and is described as the ratio of the gas permeabilities of the individual components, and expressed by Eqn.2.3,

$$\alpha_{AB} = \frac{P_A}{P_B} \quad (2.3)$$

For a gas mixture, separation factor is used for defining separation performance of a membrane instead of ideal selectivity. The ratio of the permeate side mole fractions to the feed side mole fractions gives the separation factor. The separation factor is expressed by Eqn.2.4,

$$\alpha_{A/B} = \frac{(y_A/y_B)_P}{(x_A/x_B)_f} \quad (2.4)$$

where x_A and x_B are the feed side mole fractions of the components, y_A and y_B are the permeate side mole fractions of the components [1, 5].

Membrane technology has various advantages when compared to other separation processes; such as minimum energy requirements, low cost, ease of operation and being environment friendly. Due to these advantages, membranes have potential of acquiring a significant role in gas separation area for the coming future. Some potential applications of the gas separation processes are given in Table.2.1. Some important membrane requirements for industrial processes include mechanical stability, and high permeability and selectivity. However, in order to be used effectively in industrial processes a mechanically stable membrane with high permeability and selectivity is required [1-3, 5].

Polymeric membranes have various advantages over inorganic membranes and will be the focus of this introduction. Polymeric membranes have great potential for separation processes because of their advantages such as being inexpensive and being economically processable and having low operating costs [3, 5, 23]. Many different polymer families have been used as membrane matrix such as polycarbonates, polyesters, polysulfones, polyimides, cellulose derivatives and polypyrrolones [3, 5, 24]. Among these polymers

glassy ones are more suitable for separation of permanent gases because of their size dependent separation characteristics and mechanical properties. Moreover, high glass transition temperature and high melting point make a polymer more preferable for permanent gas separation. Glassy polymers have stiffer polymer backbones, so smaller gas molecules can rapidly pass through the membrane [25].

Table.2.1 Gas separation membrane applications in the industry [1-3, 5]

Gas Mixture	Application
H ₂ /CO	Purification of hydrogen
H ₂ /Hydrocarbons	Hydrogen purification in refinery
O ₂ /N ₂	Oxygen enrichment
CO ₂ /Hydrocarbons	CO ₂ recovery from associated gas, landfill gas upgrading
H ₂ /N ₂	Hydrogen recovery
H ₂ S/Hydrocarbons	Sour gas treating
H ₂ O/Hydrocarbons	Dehydration of natural gas
He/Hydrocarbons	Separation of helium
He/N ₂	Helium recovery
H ₂ O/Air	Dehydration of the air
Hydrocarbons/Air	Cryogenic air separation

For dense polymeric membranes, the solution-diffusion mechanism is applied for the transport of the gas molecule. The solution-diffusion mechanism includes three steps. The gas molecule is sorbed by membrane surface in the first step. Then, the gas molecules diffuse through the membrane. The gas molecules desorbed from the other interphase of the membrane in the last step of this mechanism. In this model,

permeability of a molecule, P , is expressed as the function of diffusivity coefficient, D , and solubility coefficient, S , such by Eqn.2.5,

$$P = D \cdot S \quad (2.5)$$

The sorbed amount of penetrant is defined by the solubility that is a thermodynamic parameter. The diffusivity is related to the transportation speed of a penetrant through the membrane [1, 5, 6].

The relation between permeability and selectivity for polymeric membranes were associated with each other by Robeson, and represented by a trade-off line that was given for H_2/CH_4 gas pair in Figure.2.1. The Trade-off lines are called as polymer upper-bound limits for many gas pairs. According to the trade-off trend, when the permeability of gas increases, the expected selectivity of gas pair decreases, and vice versa. Glassy polymers are close to the upper bound line because of their high separation performances. Besides, their mechanical properties are desirable [9]. The inorganic molecular sieves reach well above the trade-off line, and near the commercially desirable region. However, inorganic molecular sieve materials are expensive and hard to process [26].

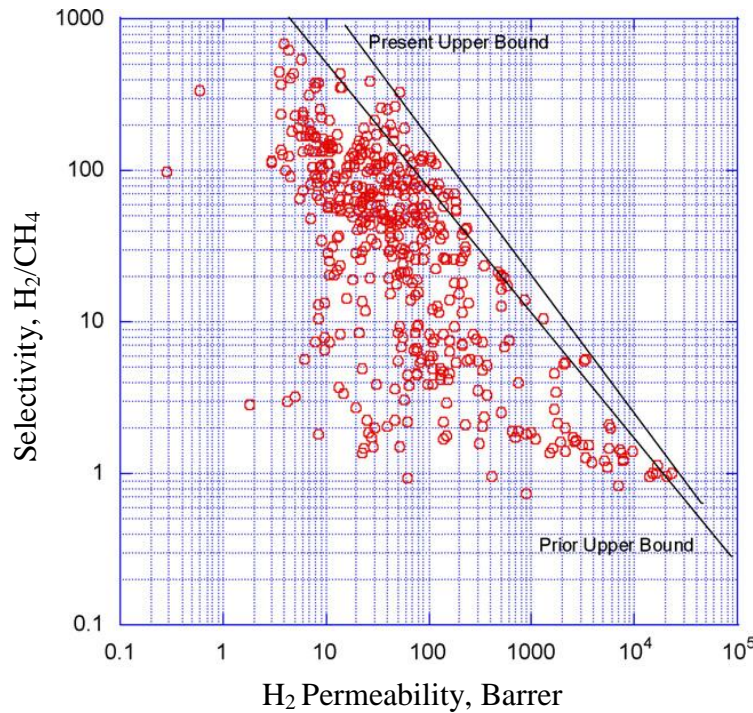


Figure.2.1 Upper bound correlation for H_2/CH_4 separation [9]

2.2 Mixed Matrix Membranes (MMMs)

For gas separation applications, the polymeric membranes have been researched extensively. The main reason behind this is polymeric membranes have attained the upper bound limit in the trade-off line. Inorganic membranes have good thermal stability, chemical stability and high permeability and selectivity. However, the inorganic membranes are limited by fabrication costs. Therefore, a new membrane material, which is convenient material for industrial separations, has become an important research issue in recent years [27, 28]. This new type of organic-inorganic membrane material has been improved to overcome these limitations, which is called as mixed matrix membrane (MMM). Mixed matrix membranes contain a continuous phase and a dispersed phase. They theoretically combine the advantages of both polymers (processibility, low cost etc.) and molecular sieves (separation performance) [26, 29]. MMMs have potential to reach upper bound limit of trade off line when compared to polymeric membranes. Glassy or rubbery polymers can be used as the bulk continuous phase. Many types of fillers can be used as dispersed phase such as; microporous molecular sieves (zeolites), mesoporous molecular sieves, carbon molecular sieves, silicas and metal organic frameworks. Number of researches examined the effects of the filler materials on the gas separation performances [2, 5, 7, 11, 30-33].

There are still many challenges such as interface defects during the preparation of the MMMs. These defects can be the consequences of the weak polymer-sieve interaction and properties of the polymer and sieve phase. The gas separation performances of the MMMs can be affected negatively due to these defects. This is divided into three sections such as interface voids, pore blockage and chain rigidification. Firstly, incompatibility between polymer phase and filler can cause formation of interfacial voids that is called as sieve-in-a cage morphology. As a result of formation of interfacial voids, the permeability increases with decreasing selectivity. Secondly, the pore entrances of the porous filler can be clogged up due to polymer chains, solvent or contaminant, which is called as partial pore blockage. The selectivity can be increase

with decreasing permeability when partial pore blockage occurs. Lastly, non-selective interfacial voids can form due to poor adhesion between filler material and polymer phase. Gas molecules pass through these nonselective voids during the transportation because of its low resistance. Therefore, the selectivity decreases with increasing permeability [11, 33, 34].

Recently, mixed matrix membranes have been subject of many research because of their potential of improved gas separation performance. However, the problem of interface defects between filler and polymer matrix is still under investigation. In literature scientist try to improve the performance of MMMs by observing the effect of different parameters and using different approaches.

Another study, which related to the surface modification with silane coupling agents, was examined by Mahajan et al. [29]. Matrimid/Zeolite-4A MMM produced with modified and unmodified zeolites. When modified Zeolite-4A was used into the MMM, the selectivity of O_2/N_2 was the same as the O_2/N_2 selectivity of pure Matrimid membrane. However, both the permeability and selectivity were increased by using unmodified Zeolite-4A into the membranes. They concluded that the surface modification with silane coupling agents did not enhance the separation performances of the membranes due to unreduced non-selective voids in the polymer phase.

Ismail et al. [36] studied separation performances of the polyethersulfone/polyimide (PES/PI)/Zeolite-4A MMMs. The loading amounts of Zeolite-4A were varied between 10 and 50 wt % of the polymer. For mixed matrix membranes that were annealed above T_g , the permeability of O_2 and N_2 gases decreased compared to below T_g annealed membranes. Also, the ideal O_2/N_2 selectivity was improved by a factor of 5 for the mixed matrix membranes which were annealed above T_g . When annealing temperature was above T_g , the polymer chains became flexible, and adhesion of the filler particles was better into the polymer chains. Thus, the separation performances of the MMMs were improved due to annealing above T_g .

Süer et al. [34] studied the preparation method effects of polyethersulfone (PES)/ Zeolite 13X or 4A MMM with different amount of zeolite loadings. The permeation analyses were carried out for N₂, O₂, Ar, CO₂ and H₂ gases. Permeability and selectivity values were improved at high loading amounts of Zeolites 13X and 4A (50 w%). However, permeabilities decreased in both PES/zeolite 13X and PES/Zeolite-4A MMM when zeolite loading increased. Permeabilities started to increase at certain amount of zeolite loadings which were above 8 wt % and 25 wt % for Zeolite-13X and Zeolite-4A, respectively. They concluded that the membrane morphology and gas separation performance was affected by zeolite type, significantly. Also, formation of microvoids and partial incompatibility between polymer matrix and zeolite were observed.

Duval et al. [37] studied as an objective to improve the adhesion between zeolite and polymer phase and they proposed two methods. These were annealing above T_g of the polymer and modifying zeolite surface with silane coupling agents. Cellulose acetate, polysulfone, polyetherimide and polyimide were used as a polymer phase. According to the results of the modifying zeolite surface, the selectivities of CO₂/CH₄ gas pair was not improved significantly; although, SEM images showed good interaction between polymer phase and zeolite.

Yong et al. [13] examined the effect of 2,4,6-triaminopyrimidine (TAP) as a low molecular weight additive on the separation performance of Matrimid/zeolite MMMs. The low molecular weight additive was used as compatibilizer that linked zeolite particles to the polymer chains. Many types of zeolites were used such as 4A, 5A, 13X, NaY and NaZS390HUA. When TAP used as a compatibilizer in Matrimid/Zeolite 4A MMM, the permeabilities of He, O₂, N₂, CO₂ and CH₄ gases reduced. The CO₂/CH₄ selectivity of Matrimid/zeolite 4A/TAP MMM increased from 1.22 to 617 compared to pure Matrimid membrane. Also, the selectivity values of CO₂/N₂ and O₂/N₂ gas pairs improved significantly. They concluded that addition of TAP into the Matrimid/Zeolite MMM improved the separation performance due to better interaction of filler with the polymer chains that were formed hydrogen bonds between them.

Şen et al. [12] examined the effect of p-nitroaniline (pNA) in polycarbonate (PC)/Zeolite-4A MMM on the gas separation performance. pNA was used as a LMWA into the MMM. MMMs were produced by using PC, Zeolite-4A and pNA concentrations of 20% wt/v, 5-30% wt/wt and 1-5% wt/wt, respectively. For PC/pNA (1 wt %)/Zeolite-4A (20 wt %) MMM, the selectivity of H₂/CH₄ and CO₂/CH₄ gas pairs improved from 40.9 to 121.3 and from 23.6 to 51.8, respectively. However, the permeabilities of all gasses decreased with addition of pNA into the PC/Zeolite-4A (20 wt %) MMM. DSC analysis showed that the glass transition temperatures of membranes increased with the addition of Zeolite-4A into PC/ pNA. However, the addition of Zeolite-4A into pure PC did not change the glass transition temperature. They concluded that only small amount of pNA (1 wt %) changed the polycarbonate membrane morphology with Zeolite-4A filler materials. It was a necessary agent because of the effects on interaction between filler particles and the polymer phase.

In another study of our research group, Karatay et al. [38] examined the effect of LMWA loading of the binary and ternary MMMs. MMMs were prepared by using polyethersulfone as polymer matrix, 2-hydroxy 5-methyl aniline (HMA) as LMWA and SAPO-34 with constant amount of loading (20 % wt/wt) as filler. The addition of the SAPO-34 into PES membrane improved permeability of H₂, CO₂ and CH₄ gases. However, this membrane was less selective than pure PES membrane due to the formation of nonselective voids between SAPO-34 particles and polymer matrix. The addition of HMA (10 % wt/wt) into PES/SAPO-34(20 % wt/wt) membrane increased ideal selectivity values of H₂/CO₂, CO₂/CH₄ and H₂/CH₄ as 93 %, 27 % and 146 %, respectively. However, permeability values of all gases reduced. They concluded that HMA was a essential agent to improve of the interaction between SAPO-34 particles and PES phase.

2.3 Metal Organic Frameworks (MOF)

Metal Organic Frameworks are a newer class of hybrid materials consist of metal ions and organic ligands. The metal ions function as connectors and the organic ligands

function as linkers. There are strong bonds between connectors and linkers, with the aid of these bonds, one, two or three-dimensional porous frameworks are formed. The structures of MOFs are enlarged also their surface area and pore volumes are extremely high. Unlike zeolitic fillers, MOFs have high surface areas, and high flexibility due to their crystal structures and chemical composition. These properties of MOFs makes the bonding of functional groups in selected linkers possible. By this way both pore size and chemical properties of MOFs can be changed. Also, MOFs have precisely sized cavities which can adsorb and store specific gas molecules. MOFs have been asserted for many applications that are drug delivery, catalysis, the storage of gases such as CO₂ and H₂, and gas separations especially for clean energy applications [39, 40]

2.3.1 Metal Organic Framework-Mixed Matrix Membranes

In recent years, Metal Organic Frameworks have attracted great attention as a filler material for fabrication of MMMs due to high surface area, ease of synthesis and availability of different structures. Also, MOFs are composed of metal ions connected by organic linkers, which organic linkers help to improve the interfacial interactions [32, 33, 41].

Perez et al. [32] studied separation performance of Matrimid/MOF-5 MMMs. MOF-5 nanoparticles have high surface area and particle size of 100 nm. The loading amounts of MOF-5 nanoparticles into Matrimid polymer were between 0 and 30 % wt/wt. The permeability values of gases improved 120 % for the loading amount of 30% w/w MOF-5 compared to pure Matrimid. However, ideal selectivities of all gas pairs did not change. They proposed that the mixed matrix membrane was free of non-selective voids. SEM images showed that the plastic deformations of the polymer that caused polymer veins occurred by the adhesion between polymer phase and MOF-5. Also, MOF-5 nanocrystals were not well dispersed in the polymer phase for strong interaction between the nanoparticles.

Adams et al. [42] investigated improvement of gas separation performance by using MOFs as filler in a polymer phase. Copper and terephthalic acid (CuTPA) was synthesized, and used as filler with constant loading amount of 15 % wt/wt into poly(vinyl acetate) (PVAc) polymer. The permeabilities of He, N₂, O₂, CO₂ and CH₄ gases were analyzed. The permeabilities and ideal selectivities of CuTPA/PVAc MMM had better separation performance than pure PVAc membrane. They suggested that CuTPA/PVAc MMM were free of interfacial voids; therefore, the gas molecules interacted with CuTPA crystals, easily.

2.3.2 Zeolitic Imidazolate Framework-8 (ZIF-8)

Zeolitic Imidazolate Frameworks (ZIFs) are a sub-family of Metal Organic Frameworks which have extremely desirable properties from both MOFs and zeolites. High crystallinities, microporosity, high surface areas, rich structural diversity and high thermal and chemical stability are highly desirable properties of ZIFs. ZIFs are constructed from metal ions and rigid organic linkers. A framework is created the five membered imidazolate ring by bridging the Zn(II) and Co centers to the N atoms in the 1,3-positions of the ring. M-Im-M (M: Co and Zn) bridges are constructed with the 145° angle. The Im links functionalized to produce neutral framework. Also, this provides tunable nanosized pores to be created [15, 16, 43].

The framework of ZIF-8 is sodalite (SOD) topology that its structure of was given in Figure.2.2. ZIF-8 has pores of 3.4 Å in diameter which allows adsorption of small gas molecule. The pore cavity has a diameter of 11.6 Å. The thermal stability of ZIF-8 is up to 400 °C. The surface area of ZIF-8 is nearly 900-1600 m²/g. Also, ZIF-8 has hydrophobic property [15-17, 43].

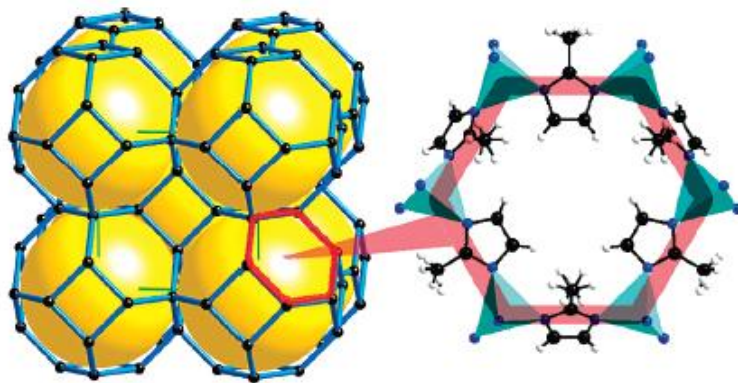


Figure.2.2 The sodalite topology (left) and narrow six-membered-ring opening through which molecules have to pass (right) [17]

ZIFs can be used for emerging functional applications such as catalysis, gas storage and gas separation. ZIF membranes for gas separation of H_2/CO_2 , CO_2/CH_4 and CO_2/CO gas pairs have reported in some studies [15, 17].

Venna et al. [15] synthesized ZIF-8 crystals to investigate CO_2/CH_4 gas mixture separation performance of ZIF-8 membranes. The particle sizes of synthesized ZIF-8 crystals were approximately 55 nm. XRD pattern and N_2 adsorption-desorption isotherm was given in Figure.2.3. Figure.2.3-a showed that the relative intensity and peak positions in XRD pattern were in agreement with XRD pattern of ZIF-8 crystals. Also, Type-I isotherm is observed in the range of P/P_0 of 0.01- 0.3 in the nitrogen adsorption-desorption isotherm, this situation indicated that ZIF-8 crystals had microporous structure.

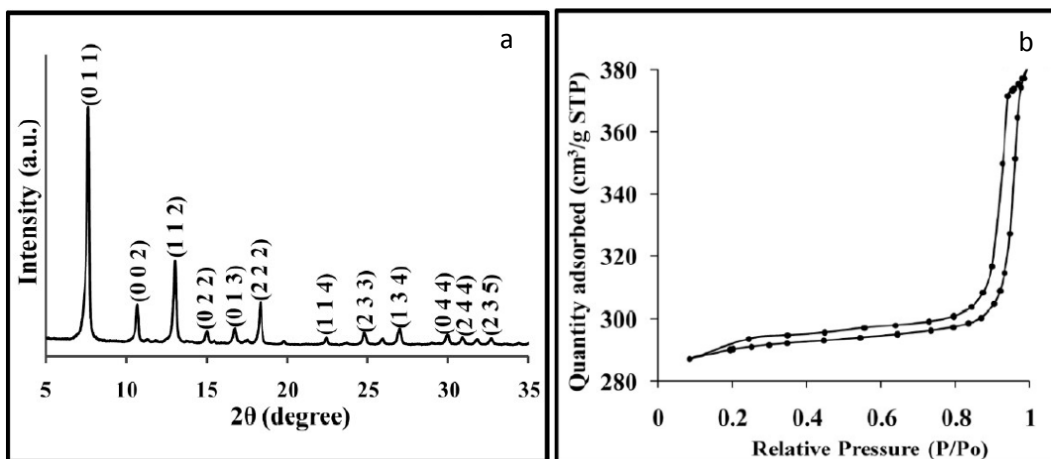


Figure.2.3 (a) XRD pattern and (b) N₂ adsorption-desorption isotherm of ZIF-8 [15]

In another study, Zhang et al. [44] studied adsorption of CO₂ and CH₄ by using ZIF-8 crystals at 298 K. They showed that simulated isotherms for pure CO₂ and CH₄ gases were in good agreement with experimental isotherms. The isotherms of CO₂ and CH₄ were given in Figure.2.4. They concluded that the negligible effect of flexibility of structure on adsorption might base on the low pressure range at 298 K.

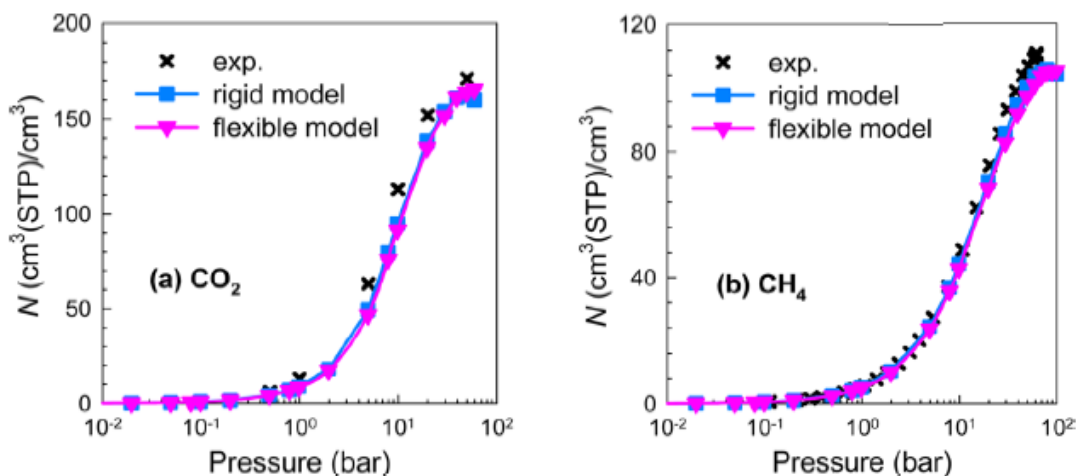


Figure.2.4 Adsorption isotherms of (a) CO₂ and (b) CH₄ in ZIF-8 at 298 K [44]

The adsorption isotherms of CO₂/CH₄ (50:50 mol/mol) gas mixtures in ZIF-8 at 298 K were given in Figure.2.5. ZIF-8 framework interacted with CO₂ in a stronger way when

compared to CH₄. They showed that adsorbed CO₂ from the mixture was closed to pure species. Also, diffusivity of CH₄ was reduced due to blockage of its diffusion pathway of CH₄ by strongly adsorbed CO₂ species.

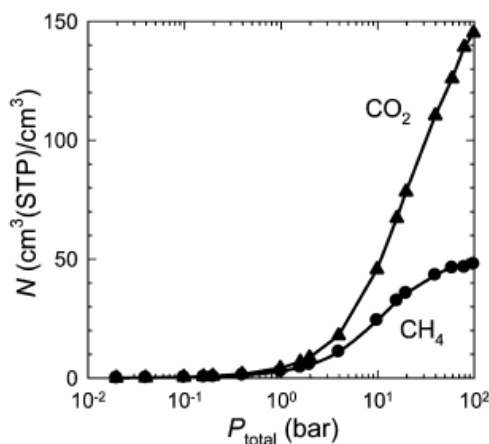


Figure.2.5 Adsorption isotherms of CO₂/CH₄ (50:50 mol/mol) gas mixture [44]

2.3.3 ZIF-8 based Mixed Matrix Membranes

In literature, the usage of ZIF-8 crystals as a filler in MMMs has become an important research objective in recent years due to its promising molecular sieve performances. There are limited numbers of research for ZIF-8 loaded MMMs in literature, and their results are tabulated in Table.2.2. Ordonez et al. [10] prepared ZIF-8/Matrimid mixed matrix membranes that loading amounts of ZIF-8 were between 0 and 80 % (wt/wt). The particle sizes of ZIF-8 crystals were 50- 150 nm. The permeabilities of H₂, CO₂, O₂, N₂, CH₄, C₃H₈ gases and H₂/CO₂, CO₂/CH₄ gas mixtures were tested. When ZIF-8 loading was increased from 0 to 40 % (wt/wt), permeabilities increased for all gases. However, the permeabilities decreased at higher ZIF-8 loadings of 50 % and 60 % (wt/wt). The ideal selectivities for gas pairs increased with ZIF-8 loading especially gas pairs of containing small gases. The increase of ZIF-8 loading of 50 and 60 % (wt/wt) to the gas separation was arised transition to ZIF-8 controlled gas transport process. When the

addition of ZIF-8 was more than 60 % (wt/wt), mechanical strength and flexibility of ZIF-8/Matrimid membranes became very low.

Basu et al. [45] studied dense and asymmetric Matrimid mixed matrix membranes with three different MOFs for separation of binary gas mixtures. $[\text{Cu}_3(\text{BTC})_2]$, ZIF-8 and MIL-53(Al) were used as filler up to 40 % (wt/wt). The particle size of ZIF-8 was 250-500 nm. Thermal and mechanical stabilities of MMMs were improved by using MOF fillers except of filler loading of 40 % (wt/wt). For dense membranes, the permeability and selectivity of gas pairs, which were CO_2/CH_4 and CO_2/N_2 , improved with the addition of filler. The improvement of both permeabilities and selectivities showed good interactions between particles and polymer chains. So, mechanical properties of dense MMMs were improved with addition of particles.

Song et al. [21] prepared Matrimid membranes with ZIF-8 particles up to loadings of 30 wt %. Pure gas permeation tests were done for H_2 , CO_2 , O_2 , N_2 and CH_4 . The permeabilities of gases increased when the loading amount of ZIF-8 increased. Especially, the permeability of H_2 and CO_2 for the ZIF-8 loading of 20 wt % membrane increased two times when compared to pure Matrimid membrane. The selectivity of CO_2/CH_4 remained same as the pure Matrimid membrane. It was concluded that the pure gas permeabilities improved with negligible losses in selectivities when ZIF-8 crystals were loaded into the nanocomposite membranes.

Diaz et al. [18] studied effects of ZIF-8 on gas transport performances of hybrid membranes which contained poly(1,4-phenylene ether-ether-sulfone) (PPEES) as polymer matrix. Loading amounts of ZIF-8 particles that have particle size of 4.9 μm were 10, 20 and 30 % (wt/wt). The permeability analysis was done for different gases such as O_2 , N_2 , H_2 , CO_2 , CH_4 , C_2H_6 , C_2H_4 . Also, permeabilities of all gases improved with the addition of ZIF-8. Also, the loading of 10 % (wt/wt) ZIF-8 into the hybrid membrane improved ideal selectivity values for H_2/CO_2 , CO_2/CH_4 and H_2/CH_4 pairs. The ideal selectivities started to decrease for all gas pairs when the ZIF-8 loading was more than 10 % (wt/wt). They concluded that the ZIF-8 loading of 30 % (wt/wt) showed

good separation performance due to closeness of its selectivity to the Robeson's upper bound.

Dai et al. [46] prepared dual layer composite Ultem 1000 asymmetric hollow fiber membranes with using ZIF-8 as filler. The particle size of ZIF-8 was around 200 nm. The loading of ZIF-8 was 13 wt % in the selective skin layer of the membrane. The permeation tests were done for pure N₂ and CO₂ gases and mixed gas that included 20 % CO₂ in N₂. The permselectivity for CO₂/N₂ was improved as high as 20 % over pure Ultem 1000 hollow fiber membrane when ZIF-8 particles loaded to Ultem 1000 asymmetric hollow fiber membrane. Also, the permeance of pure CO₂ for ZIF-8/Ultem 1000 hollow fiber membrane increased to two times of pure Ultem 1000 hollow fiber membrane.

Keser et al. [19] investigated effects of ZIF-8 loading amount on the membrane separation performances. MMMs were prepared by polyethersulfone (PES) as polymer phase, ZIF-8 as filler and 2-hydroxy 5-methyl aniline (HMA) as LMWA. The particle size of ZIF-8 was around 60 nm. In binary mixed matrix membranes, ZIF-8 particles were loaded up to 60 % (wt/wt). In ternary mixed matrix membranes, ZIF-8 particles and HMA were loaded up to 30 % (wt/wt) and 10 % (wt/wt), respectively. The permeation tests for pure H₂, CO₂ and CH₄ gases were done at different feed pressures between 3 and 12 bar. When ZIF-8 particles were loaded to pure PES membrane, the permeability values of all gases increased with decreasing ideal selectivities, slightly. PES/ZIF-8(20%)/HMA(7%) was the best membrane composition for separation performance of pure gases among ternary membranes because of improving H₂/CH₄ selectivity, significantly. Also, it was shown that the separation performances of all membranes improved with increasing feed pressure.

Table.2.2 The ideal selectivities of ZIF-8 loaded MMMs in literature [10, 18, 19, 21]

Reference	Membrane Materials					Ideal Selectivities			
	Polymer	Filler	Loading (% w/w)	Average Particle Size	Additive	Loading (w/w)	H ₂ /CO ₂	CO ₂ /CH ₄	H ₂ /CH ₄
Ordonez et. al [10]	Matrimid	ZIF-8	0	50 – 150 nm	-	-	3.0	39.8	120.8
			20				3.5	51.1	176.7
			30				3.3	38.2	128.1
			40				3.1	27.8	80.8
			50				3.8	124.9	471.9
			60				4.4	80.8	356.9
Song et. al [21]	Matrimid	ZIF-8	0	60 nm	-	-	4.1	35.2	142.7
			5				3.8	39.1	148.2
			10				3.8	30.6	117.7
			20				3.8	35.8	137.0
			30				3.9	24.9	97.0
			0				1.4	22.9	31.6
Diaz et. al [18]	PPEES	ZIF-8	10	4.9 μm	-	-	2.2	29.5	64.8
			20				1.8	24.1	43.5
			30				1.9	20.8	38.5
			0				2.1	34.5	72.9
			4				3.1	31.4	97.4
			4				2.8	29.9	83.3
Keser et. al [19]	PES	ZIF-8	10	60 nm	HMA	-	2.7	26.8	70.5
			20				2.7	26.8	70.5
			4				2.2	27.3	62.9
			30				2.2	27.3	62.9

2.4 Effect of the Particle Size of Filler on the Gas Separation Performance

Numerous researchers have indicated that the permeance performances of MMMs are related to particle shape and size, particle pore size and pore size distribution as well as operating conditions. The permeability behavior depends on particle size of fillers due to changing area of filler-polymer interfaces by number of particles. However, effect of the particle size of filler material has not clearly researched yet [3, 47].

Huang et al. [31] investigated the effect of the particle size of Zeolite-4A on the permeation performance. MMMs were produced by using microsized and nanosized Zeolite-4A particles (20 wt % of the polymer) and polyethersulfone that annealed above the T_g of the polymer. The permeabilities for He, H₂, O₂, CO₂, CH₄ and N₂ gases significantly increased when using nanosized Zeolite-4A/PES membrane relative to microsized Zeolite-4A/PES membrane. The permeabilities of all mixed matrix membranes for all gases decreased compared to the permeability of pure PES membrane. Microsized Zeolite-4A/PES membrane and nanosized Zeolite-4A/PES membrane had same selectivity values for H₂/CO₂ and CO₂/CH₄ gas pairs.

Bae et al. [33] synthesized two different particle sizes of ZIF-90 crystals which were approximately 2 μm and 0.81 μm. ZIF-90 crystals were prepared with the solvothermal method, and particle sizes of ZIF-90 crystals were approximately 2.00±0.66 μm that is too large. Also, submicrometer-sized ZIF-90 particles were prepared by the nonsolvent-induced crystallization method. 0.81±0.05 μm particles were obtained by using this method. Three different types of polymers were used to prepare MMMs which were Ultem, Matrimid and 6FDA-DAM. The ZIF-90 loading was constant of 15 % for each membrane. The CO₂ permeabilities of Ultem and Matrimid MMMs improved without any loss of the selectivity of CO₂/CH₄ gas pair. The constant selectivities were explained by the mismatch between the permeability values of polymer phase and permeabilities of ZIF-90. Moreover, the CO₂ permeability performance of 6FDA-DAM membrane was enhanced with a 1.8 times by addition of ZIF-90, significantly. The mixed gas selectivity of CO₂/CH₄ (1:1 pressure ratio) was increased from 24 to 37. ZIF-90/6FDA-DAM

membranes showed good performance for CO₂/CH₄ separation. Also, the submicrometer-sized ZIF-90 crystals showed better gas separation performance.

Ersolmaz et al. [51] investigated the effects of zeolite particle sizes on the performance of silicalite-PDMS mixed matrix membranes. PDMS was rubbery polymer that used as polymer matrix. The O₂, N₂ and CO₂ permeation measurements were done. The silicalite was loaded 20 and 40 wt % into the PDMS membranes. Also, the particle sizes of 0.1, 0.2, 0.7, 0.8, 1.5 and 8 μm silicalite were used by MMM preparation. The permeability values of all gases improved with increasing particle size of silicalite for all of the silicalite loaded MMMs. The ideal selectivities were less affected with changing particle size of silicalite. They concluded that the behavior of permeabilities related to the improved area and number of interfaces around silicalite particles with the smaller particle sizes.

Bushell et al. [40] prepared two different particle sizes of ZIF-8 crystals which had 2-10 μm and 40-60 nm. Gas separation performances were analyzed for ZIF-8/PIM-1 MMMs. The volume percent of filler in the membranes were 11 with microZIF-8 and 16, 28, 36 and 43 with nanoZIF-8. The permeation tests of pure gases such as He, H₂, O₂, N₂, CO₂ and CH₄ were done for prepared ZIF-8/PIM-1 membranes. For nanoZIF-8/PIM-1 membranes, the permeability improved as well as ideal selectivities with addition of nanoZIF-8 particles. Moreover, gas separation performances of both for nanoZIF-8 and microZIF-8 containing PIM-1 membranes shift above the upper bound limit in the trade-off line for several gas pairs.

2.5 Binary Gas Mixtures Separation with Mixed Matrix Membranes

The binary gas mixture separation performances are mostly studied for CO₂/CH₄ gas pairs due to a wide range of usage area. In this purpose, some researches were done by using different polymer and filler types to show effect of the components in the MMMs. Battal et al. [48] studied effects of feed composition on the transport properties of PES/Zeolite-4A MMM. Permeability and selectivity of gas mixtures of CO₂/CH₄ were

investigated for composition range of 0 to 100% (mol/mol). They observed that separation selectivity decreased linearly when feed concentration of CO₂ increased. They claimed that active sites of zeolite could saturate with increasing CO₂ concentration. So, the separation selectivity decreased due to self-inhibited properties of CO₂ molecules.

Şen et al. [49] investigated effects of feed compositions of CO₂/CH₄ gas mixtures on the separation performance of PC/pNA/Zeolite-4A MMM. The feed concentration of CO₂ was from 0 to 100% (mol), and the feed pressures were 3 bar. They observed that separation factors were similar as ideal selectivities for pure PC and PC/pNA membranes for all of the feed compositions. However, the separation factors decreased with increasing feed composition of CO₂ for PC/Zeolite-4A and PC/pNA/Zeolite-4A membranes. They showed that the ideal selectivity values were higher than the separation factor values due to sorption property of penetrants. Also, addition of pNA enhanced the molecular sieving effects due to arrangement of membrane morphology.

Çakal et al. [50] prepared PES/HMA/SAPO-34 ternary MMMs. Effect of feed gas composition of CO₂/CH₄ mixtures was investigated with the feed concentration of CO₂ varying between 5 to 70 % by volume. The feed pressure was 3 bar. They observed that the separation performances of all types of membranes were independent of the feed composition. PES/HMA(10%)/SAPO-34(20%) had highest separation selectivity among all membranes which was approximately 40 for CO₂/CH₄. Also, the permeabilities increased when feed concentration of CO₂ increased. This could be major advantage for industrial scale.

In another research of our research group, Keser et al. [19] studied separation of binary mixtures of CO₂/CH₄ (50:50 % v/v) for pure PES and PES/ZIF-8(10%), PES/HMA(4%)/ZIF-8(10%) MMMs. The feed pressures were 3 and 12 bar. They showed that the feed pressure was not be important on the separation factors for all membranes, significantly. The separation factors were equal to the ideal selectivities for 3 bar measurements. However, the separation factors were lower than the ideal

selectivities at 12 bar. They explained lower separation factors by resulting of concentration polarization, competition of penetrants and plasticization phenomena.

Perez et al. [32] prepared Matrimid/MOF-5(30%) MMMs to separation of gas mixtures of CO₂/CH₄ with CO₂ feed composition of 10 and 50 % by mol. The feed pressure was 2.7 bar. Separation selectivity of CO₂/CH₄ decreased with increasing the feed concentration of CO₂. This case was explained by the dual mode transport model. According to this model, the competition was between the gases for the fixed free volume in the polymer matrix and the high solubility of CO₂ in the membrane. They concluded that the solubility of CH₄ reduced due to the high solubility of CO₂ in the membrane. So, transportation of CH₄ depended on diffusivity, mostly.

In another study, Ordonez et al. [10] examined Matrimid/ZIF-8(50 and 60 %) mixed matrix membranes for the separation of binary mixtures of CO₂/CH₄ (10:90 mol %). Some variations were observed between ideal selectivities and separation selectivities. This could be results of penetrant competition, gas phase non-ideality, plasticization of the polymer and the gas polarization. Also, an increase in separation selectivity of CO₂/CH₄ gas mixture was expected that compared to ideal selectivity due to the faster diffusion of CO₂. However, the separation selectivities were lower than the ideal selectivity. The pore aperture of ZIF-8 could be blocked by larger in size and higher in concentration of CH₄ molecules.

CHAPTER 3

EXPERIMENTAL

3.1 Synthesis of ZIF-8

3.1.1 Materials

Zinc nitrate hexahydrate [$\text{ZnNO}_3 \cdot 6\text{H}_2\text{O}$, 98% purity] was purchased from Acros Organics and used as zinc source. 2-methylimidazole [$\text{C}_4\text{H}_6\text{N}_2$, 99% purity] and Methanol [MeOH , 98% purity] was purchased from Sigma-Aldrich and used as ligand and solvent, respectively.

3.1.2 Preparation of ZIF-8

A ligand solution which included 5.28 g of 2-methyl imidazolate and 90.4 g of methanol was prepared. A solution consisting of 2.4 g of zinc nitrate hexahydrate and 90.4 g of methanol was mixed with the ligand solution, rapidly. Molar composition of the synthesis solution was $\text{ZnNO}_3 \cdot 6\text{H}_2\text{O} : 7.9\text{Hmim} : 695.1\text{MeOH}$. The synthesis mixture was stirred for 1 hour at room temperature of 20-25 °C. The synthesized ZIF-8 crystals were obtained from the synthesis solution by centrifugation at 6000 rpm. Then, ZIF-8 crystals washed with methanol for two times. The ZIF-8 crystals, which had an average particle size of 65 nm, were dried overnight at 80°C and activated overnight at 180 °C [16]. The

particle sizes of 144 nm and 262 nm ZIF-8 crystals were synthesized from solutions with MeOH/Zn⁺² molar ratios of 347.5 and 86.9, respectively.

The recycling of the mother liquor that is crystallization solution of ZIF-8 was used to synthesize the particle sizes of 14 nm and 23 nm ZIF-8 crystals. The procedure of recycle mother liquor for the synthesis of a new generation of ZIF-8 crystals had been previously developed in our laboratory [19]. The recycling procedure-C of Keser et al. [19] was used. Procedure-C was as follows: in the first step, pH of the mother liquor solution, which was aged for 1 day, was adjusted by adding NaOH. Amount of NaOH was 0.36 g per 100 g of total mother liquor solution. Particle sizes of 23 nm ZIF-8 powder were obtained after 1 hour stirring of this solution. In the second step, initial amount of ZnNO₃.6H₂O was added to second mother liquor. This mother liquor was obtained from synthesis solution of first step after forming crystallization of ZIF-8. Particle sizes of 14 nm ZIF-8 crystals were produced after 1 hour stirring of this solution. The amounts of chemicals for the recycle synthesis method of ZIF-8 are given in Appendix-A.

3.1.3 Characterization of ZIF-8

X-ray diffraction (XRD) patterns of synthesized ZIF-8 crystals were obtained by Philips PW 1840 X-Ray diffractometer between 5-40° Bragg angles by using Cu-K α tube at a 30 kV voltage and 24 mA current. Also, 0.05 °/s was a scan rate. XRD patterns of synthesized ZIF-8 crystals were compared to simulated peak positions of ZIF-8 [16]. The crystallinity of ZIF-8 was determined by using area under the curve of peaks that the planes of (011), (002), (112), (022), (013), (222), (114) and (134) were used. Quantochrome Corporation Autosorb-1-C/MS equipment was used to obtain N₂ adsorption/desorption isotherms of ZIF-8 crystals at 77 K. ZIF-8 was degassed in vacuum at 135°C for 24 hour. The BET (Brunauer-Emmett-Teller) method was used for calculation of the surface area values of ZIF-8 crystals. The morphologies and the particle sizes of crystals were determined by scanning electron microscopy (SEM) at a magnification range of 50,000-300,000x by QUANTA 400F Field Emission equipment.

Average particle sizes were calculated by determining of the numbers of particles (counted between 18 and 30 particles) and their sizes for each SEM images. For defining particle sizes, ImageJ Software was used. Then, the morphologies of the ZIF-8 crystals were evaluated by FEI 120kV HCTEM transmission electron microscopy (TEM) analysis.

3.2 Membrane Preparation

3.2.1 Materials for Membrane Preparation

Polyethersulfone (PES), which has an average molecular weight of 53,000, was used for membrane preparation. A commercial Radel A-100 grade PES was provided by Solvay. The structure of repeating unit of PES is shown in Figure.3.1. The glass transition temperature (T_g) of PES is 220°C [1].

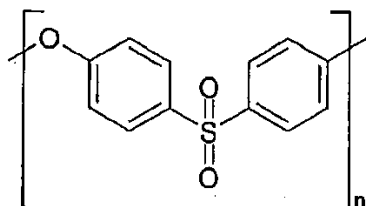


Figure 3.1 The structure of repeating unit of polyethersulfone (PES)

Dimethylformamide (DMF) (C_3H_7ON), used as solvent, was purchased from Lab-Scan Analytical Sciences. Boiling point of DMF is 153°C. The ZIF-8 crystals, which had particle sizes of between 14 and 262 nm, were used as filler to study the effect of particle size of filler on the gas separation performance of the MMMs. p-Nitro aniline (pNA) was used as LMWA in MMMs. pNA was purchased from Acros Organics. Melting point of pNA is 146°C and has a chemical formula of $C_6H_6N_2O_2$. Its structural formula is given in Figure.3.2.

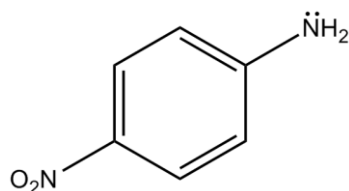


Figure.3.2 The structural formula of p-Nitro Aniline

3.2.2 Membrane Preparation Methodology

In this study, membranes were prepared by solvent evaporation technique. Three types of membranes were prepared which were PES, PES/pNA, and PES/pNA/ZIF-8 membranes. In the preparation of all membranes, the concentration of PES in DMF was kept constant as 20 % (wt/wt).

For pure PES membranes; PES, which dried overnight at 80°C, was added into 10 ml DMF gradually. Then, ultrasonication was used to remove dissolved gases for 10 min before each step of polymer adding. The final solution was stirred overnight at 300 rpm.

For PES/pNA membranes: pNA, which was 4 % (w/w) of total amount of polymer, was dissolved in DMF. Then, 15 w % of total amount of PES was mixed with the mixture. The synthesis solution was stirred overnight at 300 rpm. Remaining PES was added into the solution step by step with ultrasonication for 10 min before each step. The solution was stirred overnight at 300 rpm.

For PES/pNA/ZIF-8 mixed matrix membranes: pNA was dissolved in DMF. Then, ZIF-8 crystals were added into the solution step by step. The solution was ultrasonicated for 30 min and stirred overnight at 300 rpm. 15 w % of the total amount of PES was mixed with the solution, and the synthesis solution was stirred overnight at 300 rpm. The solution was ultrasonicated for 30 min. Then, the remaining PES was added into the solution step by step with ultrasonications for 30 min before each step, and the solution was stirred overnight at 300 rpm. The amount of pNA in the solution was kept constant for all of the mixed matrix membranes which was 4 % (w/w) of total amount of

polymer. The amount of ZIF-8 crystals in MMMs was 10 and 20 % (w/w) of total amount of polymer. Various particle sizes of ZIF-8 crystals (14, 23, 65, 144 and 262 nm) were used to prepare MMMs to investigate the effect of particle sizes of ZIF-8 on the separation performances. The preparation of MMM was shown as flowchart in Figure.3.3. Also, the amounts of materials used in membrane preparation were given in Appendix-B. Although, the procedure for preparation of PES solution was different for all membranes, casting, solvent evaporation, and annealing methods were the same.

All membrane solutions were ultrasonicated for 10 min before casting. The solutions were blade casted on a glass plate at room temperature by using Automatic Film Applicator with a casting knife of 500 μm . The size of liquid film was casted glass plate that sizes of width and length was approximately 25x15cm. The casting was done at room temperature in air atmosphere. The solvent evaporation was accomplished at 80°C and 0.2 bar in N_2 for 8 hour. Then, the membranes were removed from the glass plate, carefully, and annealing was carried out at 100°C and 1 bar in N_2 for 1 week. The residual solvent was removed in annealing step.

3.2.3 Membrane Characterization

Morphologies of PES/pNA/ZIF-8 MMMs were evaluated by using FEI QUANTA 400F series scanning electron microscopy (SEM). The distribution of ZIF-8 crystals into the MMM was determined from the images of membrane cross sections. The SEM analysis was carried out at a magnification of 2,000-100,000x.

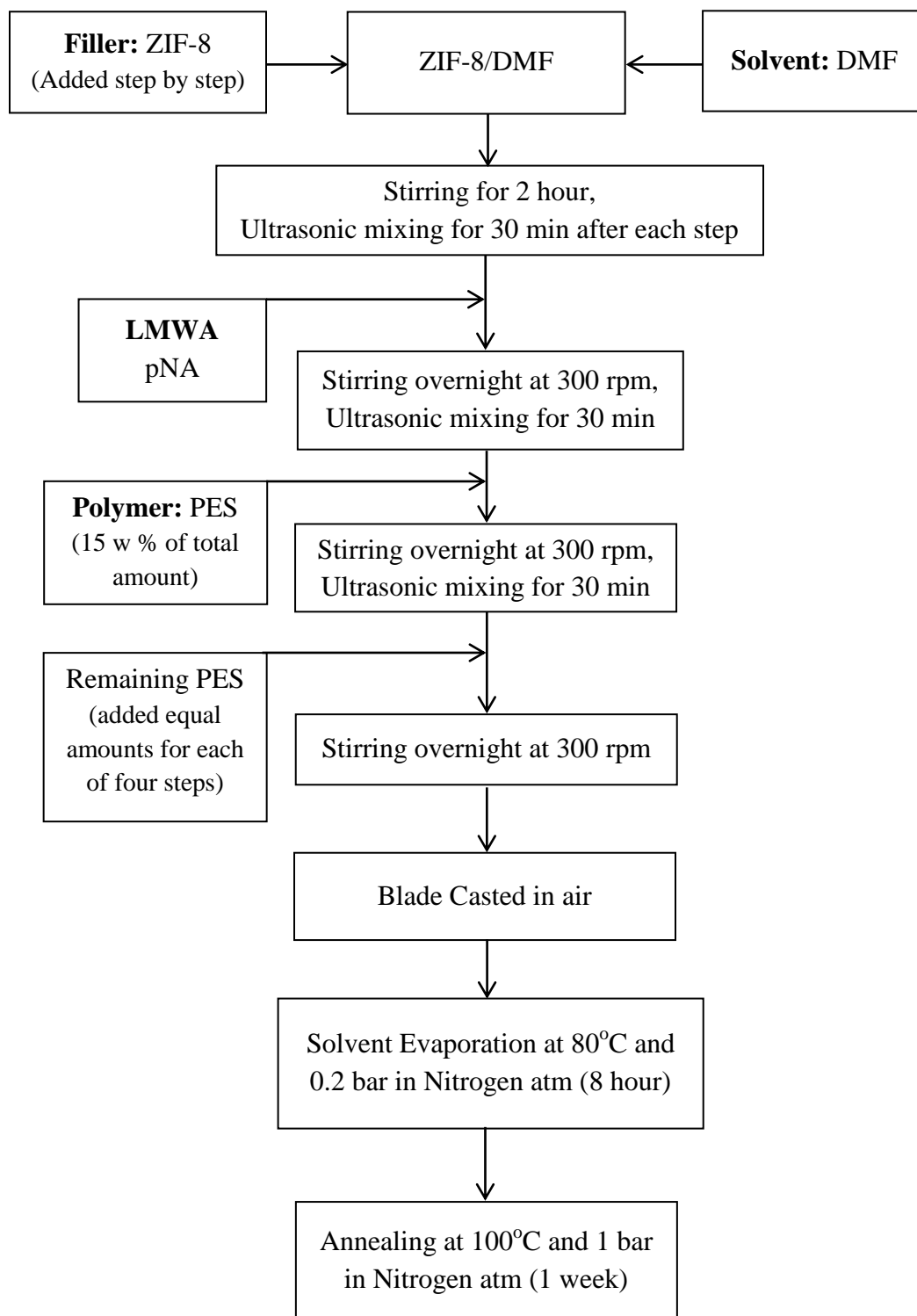


Figure 3.3 The preparation methodology of PES/pNA/ZIF-8 MMMs

3.3 Gas Permeation Measurements

3.3.1 Gas Permeation System and Measurement Method

Schematic drawing of the gas permeability set-up is given in Figure.3.4. The single gas and binary gas mixture permeation experiments were carried out in this set-up. The set-up consists of a gas tank, a membrane cell, a vacuum pump, a pressure transducer, a temperature controller, a heating tape, a gas chromatograph (Varian CP-3800) for binary gas permeation experiments and a computer. Piping (1/4 in) and fitting were stainless steel and purchased from Swagelok and Hoke. A stainless steel Millipore filter holder (part no. XX45047 00) was used as the membrane cell with double Viton O-Rings. In the membrane cell, the effective membrane area was 9.6 cm^2 . The pressure transducer, which was MKS Baratron (0-1000 Torr), measured pressure changes at the permeate side with a sensitivity of 0.1 Torr. The gas permeability set-up had the dead-end volume of 18 cm^3 . The set-up was heated by using Cole Parmer, Barnstead/Thermolyne heating type equipped with a J-type thermocouple and a PID controller to keep the temperature constant. A 2-stage mechanical vacuum pump (Edwards) was used in order to obtain high vacuum. H_2 , CH_4 gases were purchased from Linde, and CO_2 was purchased from Oksan. The purities of penetrant gases were higher than 99%.

The gas permeation system was carried out at constant volume variable pressure. The membrane in the cell was kept in vacuum 1.5-2 hour before each analysis. The penetrant gas, which was filled into the intermediate gas tank, was at pressure of 3 bar. Then, the permeate side including membrane cell was filled with the penetrant gas. The temperature of the gas permeation set-up was kept constant at 35°C . The pressure change at the permeate side was recorded by the pressure transducer. The calculation procedure is shown in Appendix-C. The gas permeation analysis of each gas was carried out twice for each piece of membrane to show the reproducibility of measurement. Also, the gas permeation analysis was performed with two pieces of membrane from a cast to show the uniform structure of membranes. For each formulation, two membranes were casted and performed gas permeation analysis to show the reproducibility of

membranes. Therefore, the single gas permeation measurements of MMMs at 3 bar were performed for 8 membrane piece of each formulation. Also, to show the effects of the feed pressure on the separation performances the single gas permeation measurements of selected MMM were measured for one piece membrane at feed pressures of 6, 10, 12 and 15 bar.

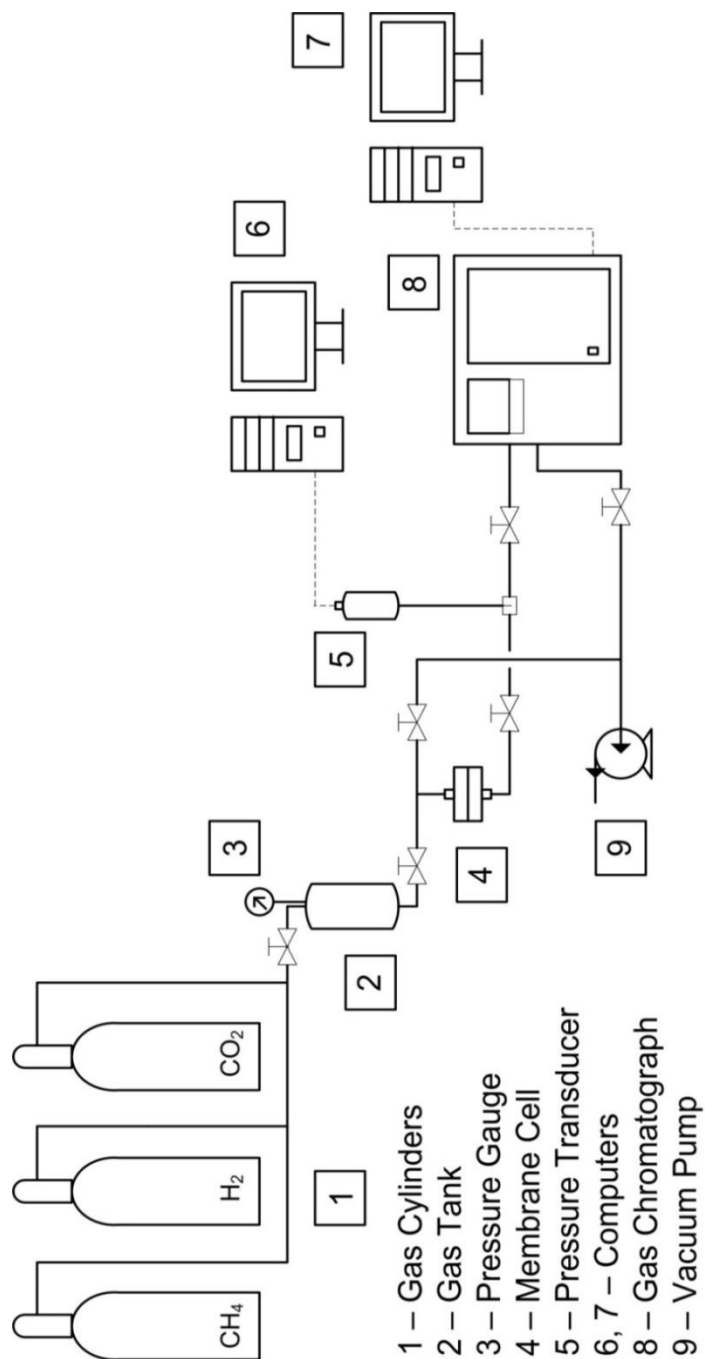


Figure.3.4 The schematic drawing of the gas permeation set-up

3.3.2 Binary Gas Permeability System and Procedure of Measurement

In binary gas mixture analysis, separation performances of CO₂/CH₄ gas pair were measured for the selected membrane. The feed gas mixture composition was changed between 10-50% (mol/mol) CO₂. Measurements were done by constant volume-variable pressure technique at 35°C. In binary gas mixture permeation analysis, the single gas permeation set-up was used with a Gas Chromatograph. The schematic drawing of the set-up is given in Figure.3.4. Feed pressures of binary gas mixtures were 3 and 10 bars. The feed tank was filled the one of the gases up to the corresponding pressure. Then, the other gas was fed to the feed tank to the desired pressure. After the permeate side was kept in vacuum for 1.5-2 hour, the gas mixture was fed to the GC to define feed gas composition. Then, the permeate side was kept in vacuum for 1.5-2 hour, again. The gas mixture was fed to permeate side. The pressure transducer was recorded to the pressure change of downstream pressure. After the permeation experiment, the composition of the permeated gas mixture was analyzed by online GC. After the permeation analysis, the composition of permeated gas mixture was analyzed at least three times by GC to obtain reliable data. The composition of the feed gas stream was analyzed for three times by GC before the permeation experiment. Also, the permeation experiments were repeated at least two times. The compositions of permeate and feed stream were used to calculate separation factor. The separation factor was calculated by using the ratio of the compositions of the permeate stream to the feed stream.

The GC was calibrated before the measurements. The calibration curves were obtained by analyzing pure components in GC at certain pressure. The operating conditions of GC are given in Table.3.1. The pressure versus area under the peak curves was obtained for CO₂ and CH₄ gases. The amount of each gas in binary gas permeation analysis was measured by using GC data and calibration curves. The calibration curves for CO₂ and CH₄ are given in Appendix-D. Also, a sample calculation of permeability and selectivity determination of binary gas mixture are given in Appendix-E.

Table.3.1 Operating conditions of GC.

Column Type	Chromosorp 102, 80-100 mesh
Column Temperature	80 °C
Valve Temperature	80 °C
Detector TCD	TCD
Detector Temperature	100 °C
Sample flow rate	50 ml/min
Reference gas and flow rate	He, 30 ml/min
Column Pressure	50 psi

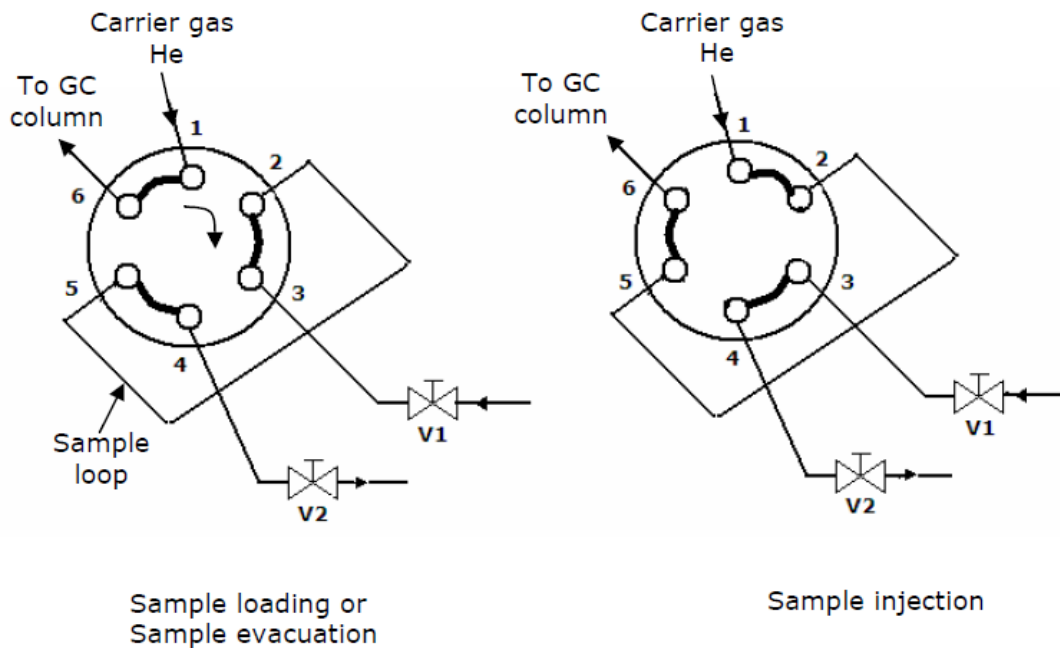


Figure.3.5 The six port injection valve in GC [52]

In this study, the gas compositions of the permeate side and the feed side were analyzed by GC that can be analyzed the relative amounts of the components in the mixtures. A 6-port injection valve operated in GC that is given in Figure.3.5. Firstly, the GC outlet

valve, which was V2, was closed and the GC inlet valve (V1) was opened for 2-3 s during degassing of the sample loop section. The gas sample was sent to the GC column for automatic injection after the V1 was closed. Then, the analysis of the sample was completed, and V2 was opened again to degas sample loop. This measurement was repeated three times per gas sample.

CHAPTER 4

RESULTS AND DISCUSSION

4.1 Characterization of ZIF-8

In this study, ZIF-8 crystals with different particle sizes were synthesized in order to investigate the effects of particle size of ZIF-8 on the gas separation performances of the MMMs. ZIF-8s with particle sizes of 14 and 23 nm were synthesized by using the recycled mother liquor synthesis methodology. Different molar compositions of the solution, $\text{ZnNO}_3 \cdot 6\text{H}_2\text{O}/\text{Hmim}/\text{MeOH}$, were used to synthesize ZIF-8 with particle sizes of 65, 144 and 262 nm. Synthesis compositions of MeOH to $\text{ZnNO}_3 \cdot 6\text{H}_2\text{O}$ and average yield and normalized crystallinity values of ZIF-8 samples were given in Table.4.1.

The yield was calculated by using the maximum possible amount of ZIF-8 that can be produced from the synthesis solution. The ratio of the synthesized amount of ZIF-8 to the maximum producible amount of ZIF-8 gave the yield value. It was observed that ZIF-8 yields, which were synthesized by different molar compositions of the solution method ($\text{ZnNO}_3 \cdot 6\text{H}_2\text{O}$: Hmim: MeOH), increased with the increasing MeOH: $\text{ZnNO}_3 \cdot 6\text{H}_2\text{O}$ molar ratio from 86.9 to 695.1. For the first step of the recycle mother liquor synthesis method, the ZIF-8-2 sample had higher yield value than ZIF-8-1 yield that was the second step synthesis. In the first step, Zn^{+2} source was not added according to the synthesis procedure, so ZIF-8 yield was high in the first step synthesis. The sample calculations of yield and synthesis composition values of ZIF-8 crystals were given in Appendix-F.

XRD measurements were conducted for synthesized ZIF-8 crystals for phase identification and semi-quantitative analysis. XRD patterns of ZIF-8 crystals were given in Figure.4.1. The peak positions of synthesized ZIF-8s were in agreement with the peak positions of simulated pattern of ZIF-8 [53] and also study of Keser et al. [66] whose synthesis procedure was followed in this study [19]. Sharp and intense peaks indicated that highly crystalline ZIF-8 crystals were obtained. The crystallinities of ZIF-8 crystals were determined by the area under the peaks and these values were given in Table.4.1. The particle size of 60 nm ZIF-8 sample of Keser study was used as reference ZIF-8 that assumed 100% crystallinity for this calculation [66]. The areas between baseline and peaks were determined from raw X-ray diffraction pattern data by using Jade Software (version 2.1). The area values of the peaks of (011), (002), (112), (022), (013), (222), (114) and (134) planes as seen in Figure.2.3(a) were used for calculation of the total area values of the samples. The ratio of the total area values of the sample to the total area of the reference sample gives the information of the crystallinity of the sample. The calculated crystallinities were normalized to 100% in Table.4.1, and the calculated crystallinities were given in Appendix-H. In Figure.4.1, the diffraction peaks were widened with decreasing particle sizes of ZIF-8, so the crystallinities of bigger particles were higher. ZIF-8 crystals with the particle sizes of 14 and 23 nm by using recycled mother liquor synthesis method had lower crystallinities than others that may be due to higher $\text{MeOH}/\text{Zn}^{+2}$ molar ratio of the synthesis solution.

The full width value of the characteristic peak at half max indicates the change of peak width, so this is related to the peak sharpness. For ZIF-8 samples, the full width values at half max (integral breadth), which were peaks of (011) planes, were used to calculate particle size of ZIF-8 crystallite by Scherrer equation. The theoretically calculated average particle sizes of ZIF-8 crystallites were tabulated in Table.4.1. It was seen that theoretically calculated particle sizes by using Scherrer equation were close to actual particle sizes of ZIF-8 with decreasing particle size. The sample calculation of particle sizes by using Scherrer equation was given in Appendix-G.

Also, all types of ZIF-8s were synthesized for two times to show the reproducibility of the synthesis. XRD patterns, yield and crystallinity values and theoretically calculated

particle sizes by Scherrer equation of two syntheses of ZIF-8 crystals were given in Appendix-H.

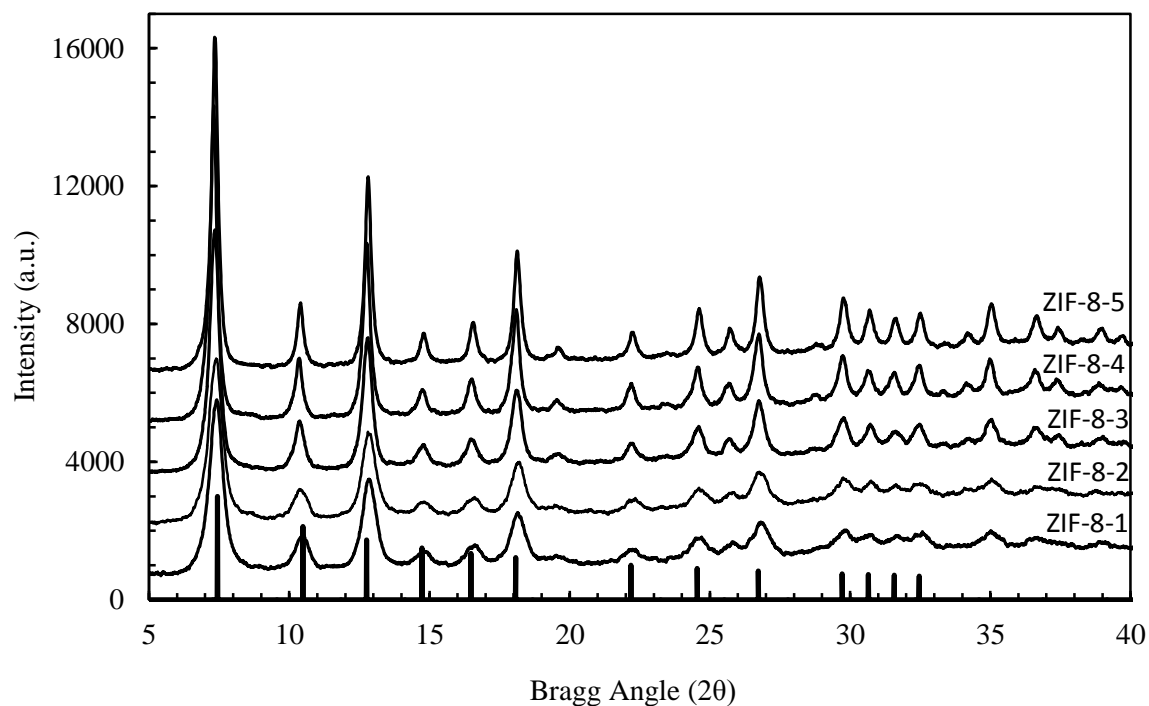


Figure.4.1 XRD patterns of ZIF-8 crystals with different particle sizes

Table.4.1 Yields, normalized crystallinities, calculated crystallite sizes of ZIF-8 crystals and average particle sizes of ZIF-8 based on SEM images with synthesis molar ratios

Sample Code	MeOH to ZnNO ₃ .6H ₂ O Molar Ratio	Yield, %	Normalized Crystallinity, %	The Crystallite Size by using Scherrer Eqn. ((011) plane), nm	Average Particle Size based on SEM, nm
ZIF-8-1	1051	27.1±1.3	75.9±2.8	14.0±1.4	14 ± 2
ZIF-8-2	1130	68.6±2.3	72.0±3.9	15.5±0.7	23 ± 3
ZIF-8-3	695.1	35.6±5.7	92.6±1.2	22.5±2.1	65 ± 5
ZIF-8-4	347.5	32.4±0.7	98.1±2.7	30.5±3.5	144 ± 10
ZIF-8-5	86.9	29.6±0.9	98.6±2.0	31.5±0.7	262 ± 18

Nitrogen adsorption and desorption isotherms (at 77 K) of synthesized ZIF-8 crystals with different particle sizes are given in Figure.4.2. Nitrogen adsorption-desorption isotherms showed that rapidly increased amount of nitrogen was adsorbed by pores of ZIF-8 crystals at low relative pressures. Type-I isotherms were observed for all of the ZIF-8 crystals indicating microporous structure of ZIF-8 crystals when compared to Figure.2.3(b) [15]. However, the particle size of 23 nm ZIF-8 crystals showed Type-II isotherm. Type-II isotherm may arise when there are more than one adsorption site. The second rise of this isotherm represents filling the second site. It might be said that isotherm type of 23 nm ZIF-8 crystals could be related to low crystallinity. The structure of 23 nm ZIF-8 pores might be affected, and they showed Type-II isotherm behavior.

The surface areas of synthesized ZIF-8 crystals were calculated by BET method. The values of BET surface areas and structural characteristics of ZIF-8 crystals with different particle sizes are given in Table.4.2. The BET surface areas of ZIF-8 crystals were approximately 1700 m²/g except of particle size of 14 nm ZIF-8 crystals due to large particles formed as a result of agglomeration of very small particles. The BET surface areas of ZIF-8 crystals were also reported in literature. Keser et al. synthesized ZIF-8 particles with different particle sizes, and the BET surface areas of ZIF-8 crystals were between 1371 and 1781 m²/g [66]. Venna et al. synthesized particle sizes of 60 nm ZIF-8 crystals with same synthesis procedure, and the BET surface area of ZIF-8 was 744 m²/g [16]. The BET surface area of ZIF-8 particles were reported as 1079 m²/g [54], 1478.5 m²/g [55], 962 m²/g [56] and 1630 m²/g [53]. It could be said that the BET surface areas of ZIF-8 crystals in this study conformed to the surface area values of Keser study [66]. Also, the external surface area values were determined from the nitrogen adsorption/desorption data with using t-method external surface area that was calculated by computer software of the analysis. The external surface areas of ZIF-8 crystals were decreased from 490 to 110 m²/g with increasing particle sizes from 23 to 262 nm as expected.

The number of particles per gram in Table.4.2 was calculated by using the average particle sizes and density of ZIF-8 particles that was taken 0.95 g/cm³ [67]. The ZIF-8

particles were assumed as spherical shape. The calculation method was given in Appendix-I.

Table.4.2 BET surface areas, external surface areas, volume adsorbed values and number of particles per gram values of ZIF-8 crystals with different particle sizes

Sample Code	Average Particle Size based on SEM, nm	BET Surface Area, m ² /g	External Surface Area, m ² /g	Volume Adsorbed, cm ³ /g STP	Theoretical Number of Particles per gram
ZIF-8-1	14 ± 2	1144	129	339	7.33x10 ⁺¹⁷
ZIF-8-2	23 ± 3	1728	490	835	1.65 x10 ⁺¹⁷
ZIF-8-3	65 ± 5	1648	207	512	7.32 x10 ⁺¹⁵
ZIF-8-4	144 ± 10	1673	135	561	6.73 x10 ⁺¹⁴
ZIF-8-5	262 ± 18	1753	110	486	1.12 x10 ⁺¹⁴

The morphology of the synthesized ZIF-8 particles with different particle sizes was evaluated with the help of the SEM. Some typical SEM images of synthesized ZIF-8 crystals were given in Figure.4.3. The particle size was determined in each SEM image

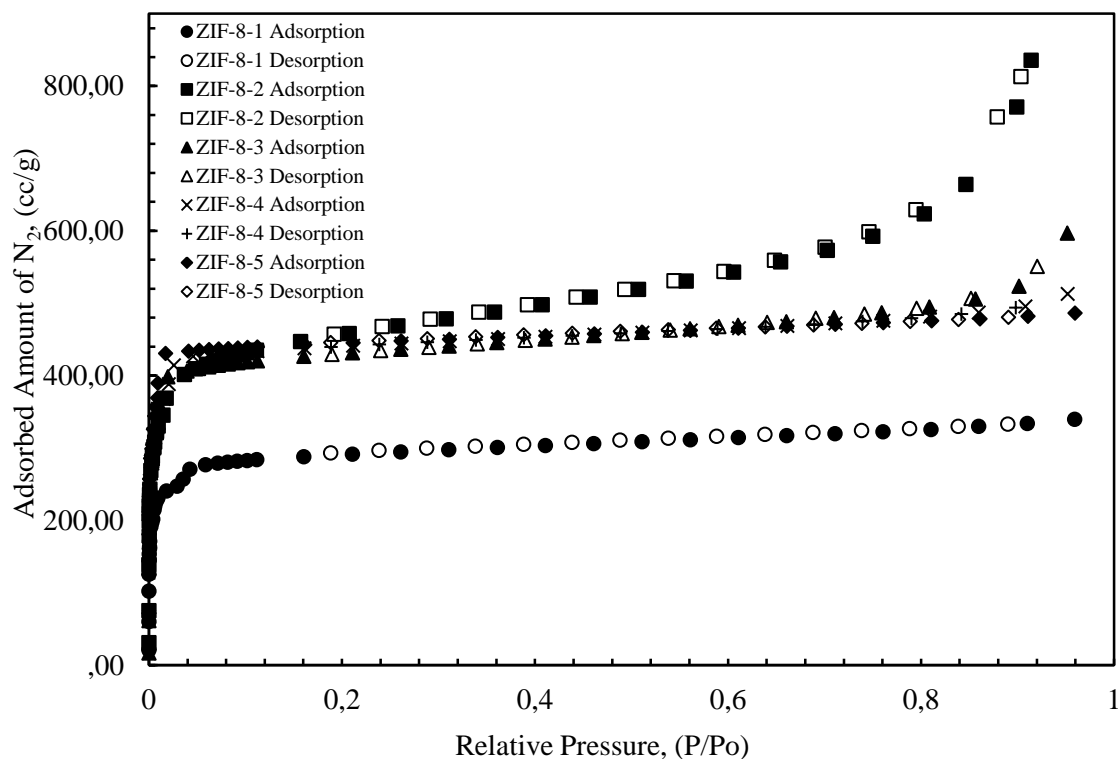


Figure.4.2 N₂ adsorption/desorption isotherms of ZIF-8 crystals with different particle sizes

of ZIF-8 crystals by counting the length of 18 to 30 particles for each sample. Then, average particle sizes of ZIF-8 crystals were given in Table.4.2 were calculated by using these data. The sample calculation was given in Appendix-J. It was observed that the morphology of ZIF-8 crystals were uniform and hexagonal-like if the particle sizes bigger than 65 nm. The morphology of ZIF-8 crystals was become sphere-like with decreasing particle size. Also, the agglomeration of particles was observed significantly for very small particles such as 14 nm ZIF-8 crystals. The agglomeration of smaller ZIF-8 crystals could be related to the decrease in crystallinity that the values were given in Table.4.1. The agglomeration of particles might disrupt crystal structure of particles, so the crystallinity values became lower. Also, the surface area of 14 nm ZIF-8 crystals, which had lower surface area than other samples, could be negatively affected by the highly agglomeration of the particles and low crystallinity.

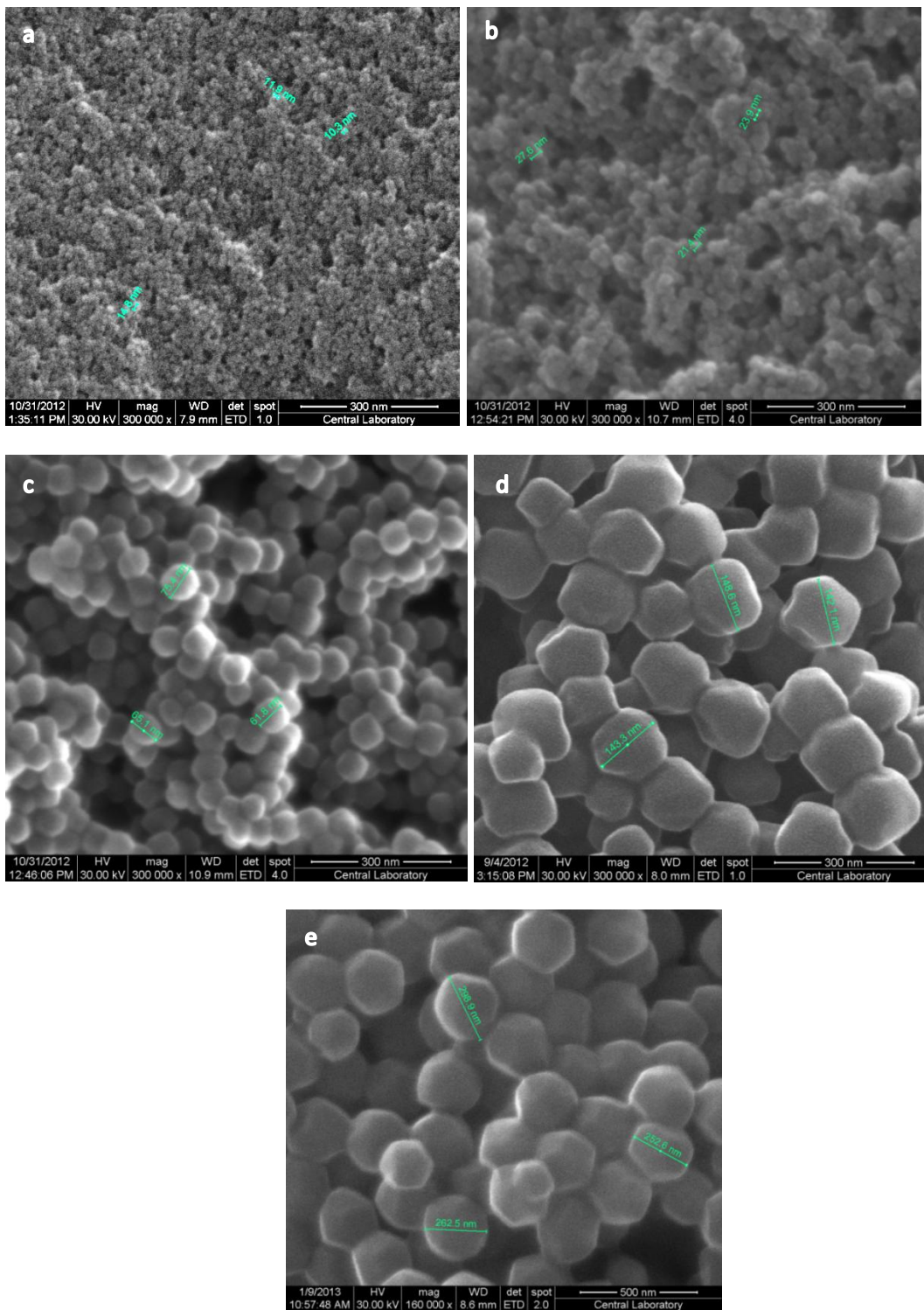


Figure.4.3 SEM images of ZIF-8 crystals: (a) 14 nm, (b) 23 nm, (c) 65 nm, (d) 144 nm, (e) 262 nm (The bigger sizes of these images were given in Appendix-K)

The morphology of the single ZIF-8 crystal with particle sizes of 14, 23 and 65 nm was determined by TEM analysis. The TEM images were given in Figure.4.4. In Figure.4.4 (c1) and (c2), the shape of ZIF-8 with 65 nm had hexagonal-like shape and uniform distribution. The particle sizes of the ZIF-8 crystals were around 60 nm in the Figure.4.4 (c1 and c2). The particle sizes of 14 and 23 nm ZIF-8 crystals, which were synthesized by using synthesis procedure of recycling mother liquor, had sphere-like shape, and agglomerated highly as observed in Figure.4.4 (a and b) in detail. In Figure.4.4 (a and b), the particle sizes of 14 and 23 nm ZIF-8 crystals were around 10-20 nm and 20-30 nm, respectively. The particle sizes of ZIF-8 crystals obtained based on TEM images were in agreement with the SEM images.

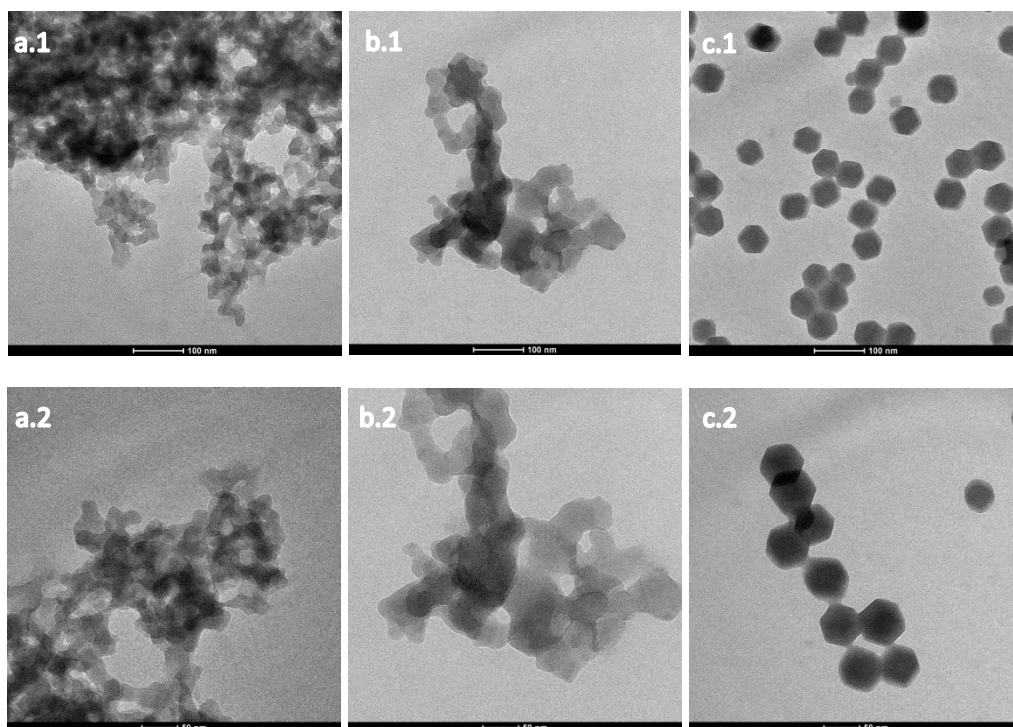


Figure.4.4 TEM images of ZIF-8 crystals: (a1) and (a2) 14 nm, (b1) and (b2) 23 nm, (c1) and (c2) 65 nm.

4.2 Membrane Characterization

4.2.1 SEM Results

The MMMs were characterized by SEM to evaluate the membrane morphologies. The SEM images of the cross-sections of 10 wt % ZIF-8 loaded PES/pNA(4%) MMMs were shown in Figure.4.5. The ternary PES/pNA(4%)/ZIF-8(10%) membranes had heterogeneous structures. The continuous phase was PES and particles were ZIF-8 crystals. It was clearly seen in Figure.4.5 that 23, 65 and 262 nm ZIF-8 crystals distributed in the polymer phase, homogenously, without forming agglomerates.

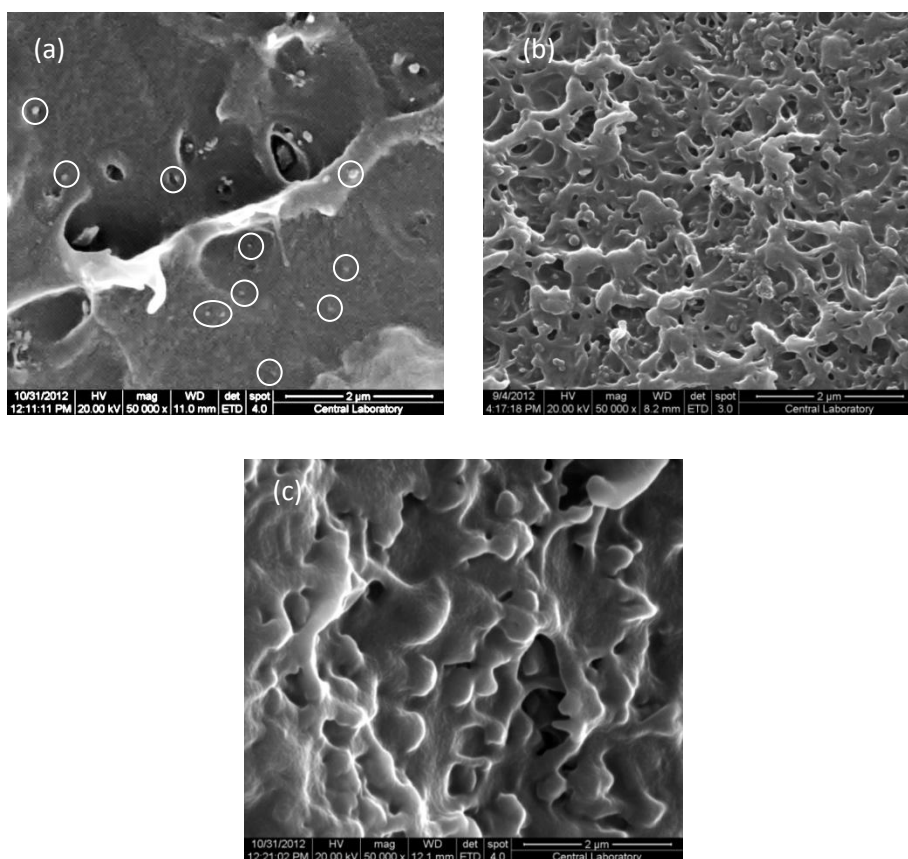


Figure.4.5 Cross-sectional SEM images of PES/pNA(4%)/ZIF-8(10%) MMMs with respect to increasing particle size of ZIF-8 (a) 23 nm, (b) 65 nm, (c) 262 nm

SEM images of the cross-sectional views of PES/pNA(4%)/ZIF-8(20%) MMMs were shown in Figure.4.6. It was observed that interfacial voids formed around ZIF-8 crystals. The amount of interfacial voids increased when loading amount of ZIF-8 was increased from 10 to 20 wt %. The poor compatibility between filler particles and polymer phase caused interfacial non-selective voids [23, 57]. It could be said that the structure of membranes changed with increasing amount of filler material.

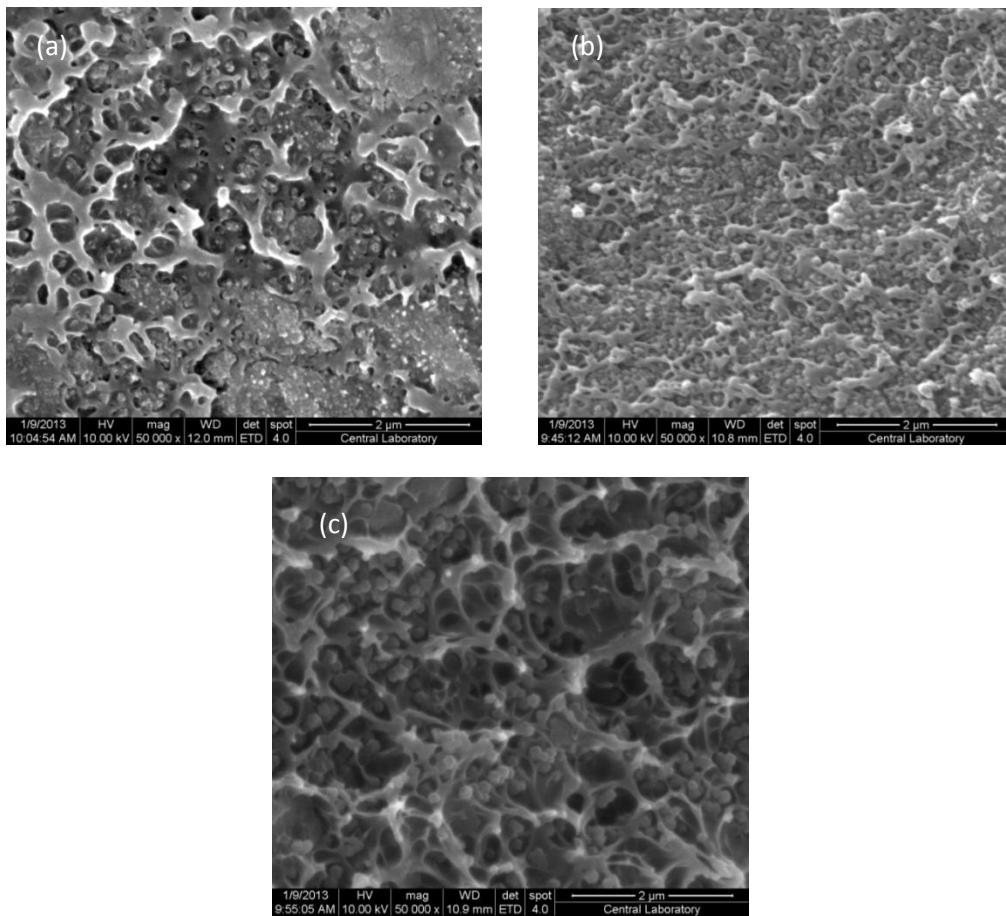


Figure.4.6 Cross-sectional SEM images of PES/pNA(4%)/ZIF-8(20%) MMMs with respect to increasing particle size of ZIF-8 (a) 23 nm, (b) 65 nm, (c) 144 nm

The SEM images of the 10 and 20 wt % ZIF-8 (23 nm) loaded PES/pNA(4%) MMMs were given in Figure.4.7 in order to compare the change in the amount of interfacial voids with increasing ZIF-8 loading. It was observed that 10 wt% ZIF-8 loaded MMM showed better adhesion between polymer matrix and ZIF-8 crystals. However, many interfacial voids formed when the 20 wt% ZIF-8 loaded. It could be said that the addition of pNA did not significantly improve interface morphology for 20 wt% ZIF-8 loaded MMM. The bigger sizes of SEM images of Figure.4.7(a) were given in Appendix-L. Keser et al. [19] reported the SEM images of PES/ZIF-8 MMMs. The interfacial voids were observed around the particles for 10 wt % ZIF-8 (60 nm) loaded membranes. The amount of the interfacial voids increased with increasing loading amount of ZIF-8. They claimed that the incompatibility between filler particles and polymer matrix could cause to these voids. In SEM images of 10 and 20 wt % loaded PES/pNA(4%)/ZIF-8 MMMs, Figure.4.7, the amount of voids decreased with the addition of pNA when compared to SEM images of ZIF-8/PES membrane of Keser study. It could be said that pNA could improve compatibility between ZIF-8 particles and PES matrix in this study.

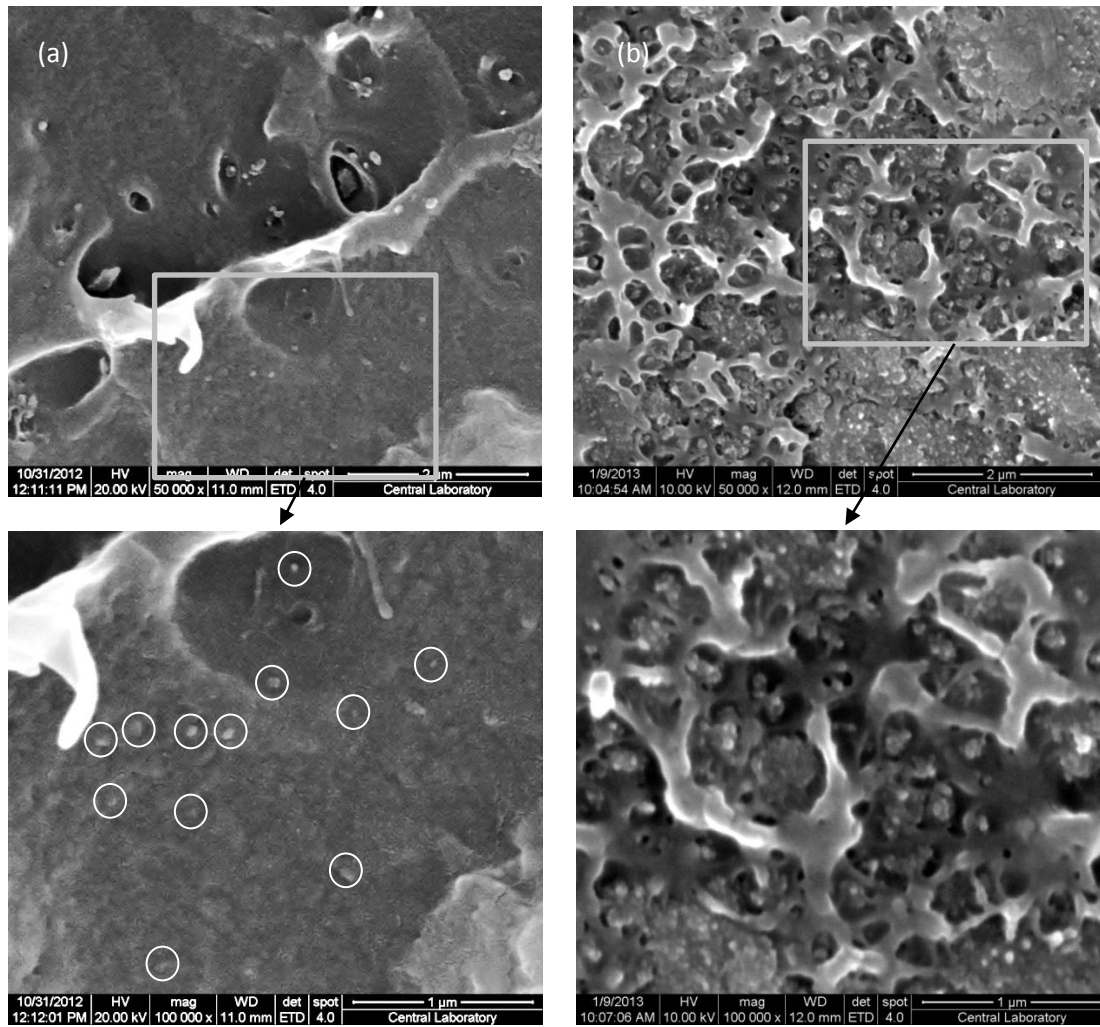


Figure.4.7 Cross-sectional SEM images of (a) PES/pNA(4%)/ZIF-8(10%) (23 nm), (b) PES/pNA(4%)/ZIF-8(20%) (23 nm)

4.3 Single Gas Permeation Results of PES/pNA/ZIF-8 MMMs

For the purpose of the investigation of the effects of particle size and loading amount of the filler of MMMs on the gas separation performances, the single gas permeability values of H₂, CO₂ and CH₄ gases were measured for PES/pNA(4%)/ZIF-8 MMMs. ZIF-8 s with particle sizes of 14, 23, 65, 144 and 262 nm were used in membrane preparation.

For pure PES, PES/pNA(4%) and 10% w/w ZIF-8 loaded PES/pNA(4%) MMMs, the single gas permeability values of H₂, CO₂, and CH₄ and the ideal selectivity values of H₂/CO₂, CO₂/CH₄ and H₂/CH₄ gas pairs were reported in Figure.4.8. It was shown that PES/pNA(4%) membrane had lower permeability values and higher selectivity values compared to neat PES membrane since addition of pNA reduce the free volume of the polymer chain. The permeabilities depend on the kinetic diameters of gas molecules. Kinetic diameters of H₂, CO₂ and CH₄ are 0.289, 0.33 and 0.38 nm, respectively [1]. The kinetic diameter of CH₄ molecule is bigger than other gas molecules; therefore, the permeability of CH₄ can be affected by morphological changes, significantly. When the LMWAs were used, the free volume of the polymer chains reduced so larger gas molecules passed through membrane, in a slower way. It was shown in literature [62, 63] and our research group [19, 20, 38, 58] that the low molecular weight additives showed similar behavior, generally. The addition of low molecular weight additive could lead to reduce the segmental movement of polymer chains, increase stiffness, and reduction of free volume. Therefore, the permeabilities of gases decreased with usage of the low molecular weight additives [19, 50, 58, 59].

Keser et al. [19] prepared PES/ZIF-8 (10%, 60 nm) membrane, and its permeabilities of H₂, CO₂ and CH₄ were 15.4, 7.2 and 0.24 barrer, respectively. It was observed in our study that the addition of pNA improved selectivity values of H₂/CO₂, CO₂/CH₄ and H₂/CH₄ pairs compared with binary and ternary membranes by using binary membrane permeation data of Keser et al. study [19]. Also, the permeabilities of H₂, CO₂ and CH₄ decreased. Çakal et al. [20] reported increasing ideal selectivities with decreasing permeabilities when the SAPO-34 added into the PES/HMA membrane. They claimed

that the low molecular weight additive improved the adhesion between the PES and SAPO-34. Also, the same conclusion was obtained in Karatay et al. [38] study that pNA was used as LMWA. They claimed that the pNA might cause to polymer chain rigidification even at very small concentration.

In this study, it was shown that the particle sizes of ZIF-8 crystals affected both the permeabilities of gases and the ideal selectivities, significantly. Although the effect of the particle size of the filler on the separation performance was studied in limited study in the literature, it has never been investigated systematically as in this study.

Figure.4.8 showed the single gas permeabilities of different particle sizes of ZIF-8 loaded PES/pNA(4%)/ZIF-8(10%) MMMs. The permeabilities of H₂, CO₂ and CH₄ increased significantly with the addition of 14 nm ZIF-8 crystals into the PES/pNA membrane. An ascending trend was observed in H₂ permeability when the particle size of ZIF-8 increased from 14 nm to 23 nm. Then, the H₂ permeability decreased with increasing particle sizes of ZIF-8s that were bigger than 23 nm. A decreasing trend was observed in the CO₂ permeability with increasing particle sizes of ZIF-8s from 14 nm to 262 nm. Moreover, the CH₄ permeability had not a regular trend according to particle sizes of ZIF-8. Still it might be said that CH₄ permeabilities of 14, 23 and 65 nm ZIF-8 loaded MMMs were close to each other. Also same behavior could be observed for 144 and 262 nm ZIF-8 loaded MMMs with a lower CH₄ permeability compared to smaller particle size ZIF-8 loaded ones.

The 14 nm ZIF-8 loaded MMM had almost the same H₂ and CH₄ permeabilities with the 65 nm ZIF-8 loaded MMM. It was shown in Figure.4.3 and Figure.4.4 that the 14 nm ZIF-8 crystals agglomerated highly; therefore these crystals might behave as if they were bigger size. The performance of 14 nm ZIF-8 loaded MMM could be affected by agglomeration of the particles into the MMM. Also, other factors might be low crystallinity and lower surface area of 14 nm ZIF-8 particles than other particle sizes of ZIF-8. The low surface area of 14 nm ZIF-8 might limit the permeation of the MMM, so the separation performance of 14 nm ZIF-8 loaded MMM was lower than 23 nm ZIF-8 loaded MMM.

The permeabilities of all gases decreased significantly with increasing ZIF-8 particle size from 23 nm to 262 nm. This kind of a trend could be related to fact that there were higher numbers of particles when smaller particle size of ZIF-8 was used in the MMM. In one gram, 23 nm ZIF-8 has 1473 times greater number of particle than 262 nm ZIF-8

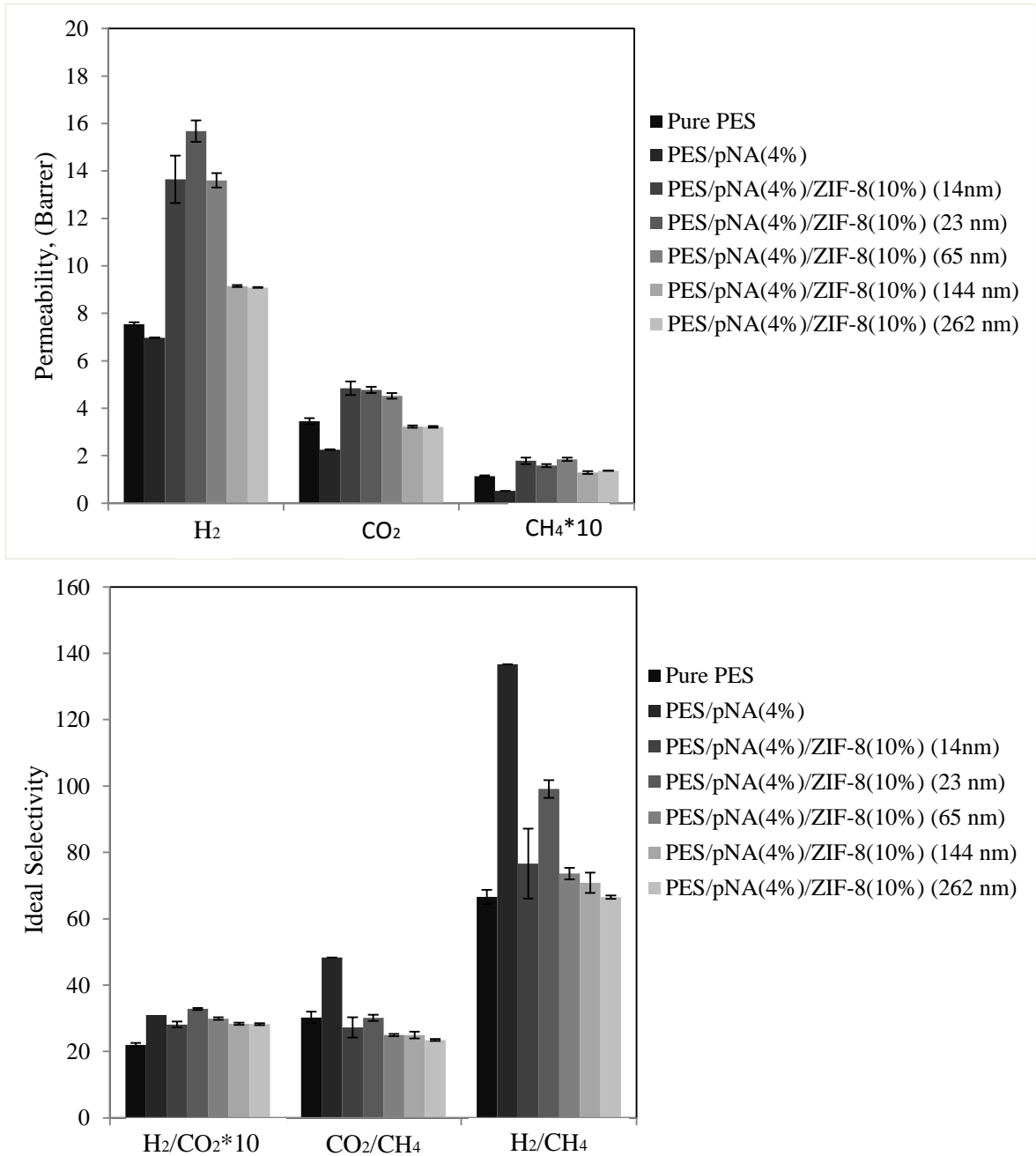


Figure.4.8 Effect of particle size of ZIF-8 on the single gas separation performance of PES/pNA(4%)/ZIF-8(10%) MMMs

according to the number of particle in one gram values of different particle sizes that were given in Table.4.2. In general, the permeabilities of all gases decreased significantly when the particle size of ZIF-8 increased from 65 nm to 144 nm. Also, the permeability values of 144 and 262 nm ZIF-8 loaded MMMs were close to each other. It might be said that the bigger particle sizes of ZIF-8s did not affect permeabilities for all gases.

Figure.4.8 also showed the ideal selectivities for gas pairs of different particle sizes of ZIF-8 loaded PES/pNA(4%)/ZIF-8(10%) MMMs. In general, the increasing trends were observed for the ideal selectivities of all gas pairs when the particle size of ZIF-8 decreased from 262 nm to 23 nm. The adhesion between the particles and the polymer was better for 10% ZIF-8 loaded MMMs when the particle sizes of ZIF-8 were decreased from 262 nm to 23 nm, which SEM images were seen in Figure.4.5 and Figure.4.7(b). The better adhesion might provide the transport of gas molecules through the ZIF-8 pores; therefore, the permeabilities and selectivities could be improved. However, the behavior of 14 nm ZIF-8 loaded MMM did not fit to this trend. The 14 nm ZIF-8 loaded MMM had lower ideal selectivities for all gas pairs than 23 nm ZIF-8 loaded MMM.

For 20 wt% ZIF-8 loaded PES/pNA(4%)/ZIF-8 MMMs, the permeabilities of all gases were presented in Figure.4.9. The 14 nm ZIF-8 particles were not used for 20 wt% loaded MMMs due to the poor separation performance of the 10 wt% 14 nm ZIF-8 loaded MMM. It was observed that effect of particle size on permeabilities were somewhat different when compared to 10 % ZIF-8 loaded MMMs. The permeabilities of H₂, CO₂ and CH₄ had a significant amount of increase with the addition of 23 nm ZIF-8 crystals into the PES/pNA(4%) membrane. For 23 nm ZIF-8 loaded MMM, the percent increments of permeability values of H₂, CO₂ and CH₄ were 462%, 561% and 1604% with respect to PES/pNA(4%) membrane. The largest increase was observed in the CH₄ permeability, so it could be said that the permeability changes could be related to the kinetic diameter of the gas molecule. The permeabilities of all gases decreased notably, when the particle size of ZIF-8 increased from 23 nm to 65 nm. Then, the decreasing trends were observed for permeabilities of all gases with increasing particle sizes of

ZIF-8 particles. However, the 144 nm ZIF-8 loaded MMM did not conform to this trend for H₂ permeability. The percent decrement of permeabilities of H₂, CO₂ and CH₄ were 54%, 58% and 74%, respectively, with increasing particle size of ZIF-8 from 23 nm to 262 nm. This decline could be related to decreasing the number of particles per gram into the membranes due to increase particle sizes of ZIF-8 crystals.

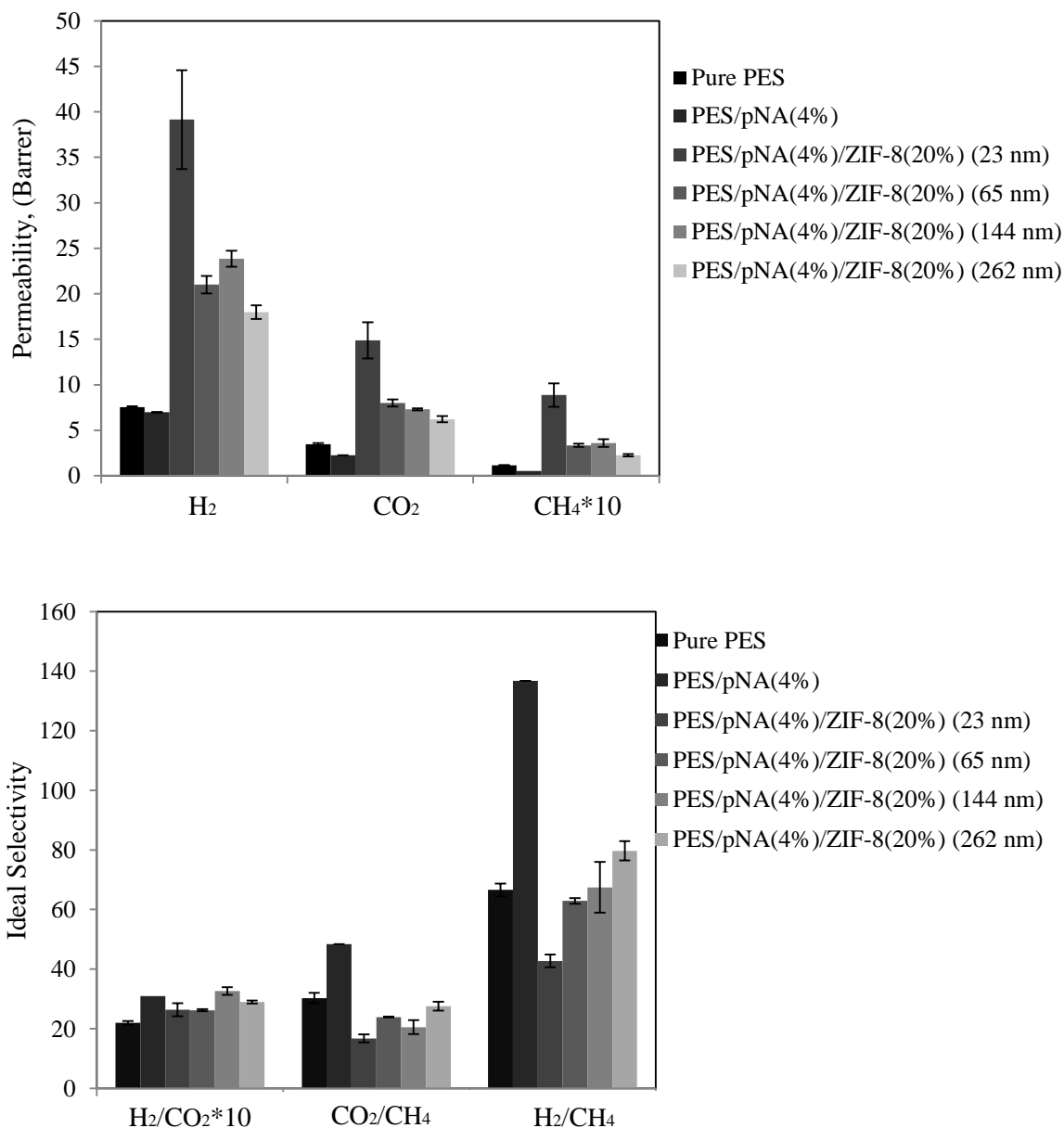


Figure.4.9 Effect of particle size of ZIF-8 on the single gas separation performance of PES/pNA(4%)/ZIF-8(20%) MMMs

Figure.4.9 also showed the ideal selectivity values for H₂/CO₂, CO₂/CH₄ and H₂/CH₄ pairs of 20 wt% ZIF-8 loaded MMMs. The ideal selectivity for H₂/CH₄ gas pair had incremental trend with increasing particle size of ZIF-8. The percent increment of the ideal selectivity of H₂/CH₄ of 262 nm ZIF-8 loaded MMM was nearly 87% with respect to the 23 nm ZIF-8 loaded MMM. The behavior of ideal selectivity values of H₂/CO₂ and CO₂/CH₄ pairs had not a regular trend. It could be said that the 20 wt% ZIF-8 loaded MMMs included big particles had higher ideal selectivities than small particles for H₂/CO₂ and CO₂/CH₄ gas pairs in general.

The single gas permeability values of H₂, CO₂ and CH₄ and the ideal selectivity values for H₂/CO₂, CO₂/CH₄ and H₂/CH₄ pairs were tabulated in Table.4.3 for pure PES, PES/pNA(4%) and PES/pNA(4%)/ZIF-8 MMMs. The results of the reproducibility experiments for all membranes were given in Appendix-M. When 10 and 20 wt% ZIF-8 loaded PES/pNA(4%)/ZIF-8 MMMs were compared, it was seen that the permeabilities increased significantly with increasing loading amount of ZIF-8. However, the behavior of ideal selectivities showed different trends based on loading amount of ZIF-8. The ideal selectivities decreased for 10 wt% ZIF-8 loaded MMMs with increasing particle sizes of ZIF-8. On the contrary, 20 wt% ZIF-8 loaded MMMs showed the incremental ideal selectivity trends with increasing particle sizes of ZIF-8. It was said that the single gas separation performances of MMMs were affected by the loading amounts of ZIF-8 and the particle sizes of ZIF-8 depending on each other.

In SEM pictures of 20% ZIF-8 loaded MMMs (Figure.4.6), it might be said that the interfacial voids between the ZIF-8 and polymer matrix and extent of voids increased. It could be speculated that these interfacial voids around particles may provide an alternative transport pathway for gas molecules; so, the permeabilities may increase. Also, the addition of smaller particle sizes of ZIF-8 could cause more void formation between ZIF-8 particles and PES chains [57, 64]. Another speculation related to the behavior of the permeability change could be the chain rigidification of polymer by addition of ZIF-8 or the pore blockage of the ZIF-8 by the polymer chains. The separation performances could be affected by these possible cases negatively [5, 57, 64].

Table 4.3 Gas permeation performances of pure PES, PES/pNA and PES/pNA/ZIF-8

PES/ZIF-8 (x %)/pNA (y %)		Permeabilities, (Barret)				Ideal Selectivities		
x	y	Average Particle Sizes of ZIF-8	H ₂	CO ₂	CH ₄	H ₂ /CO ₂	CO ₂ /CH ₄	H ₂ /CH ₄
0	0	-	7.6±0.1	3.5±0.1	0.11±0.00	2.2±0.1	30.3±1.7	66.6±2.1
	4	-	8.3±0.0	2.7±0.0	0.06±0.00	3.1±0.0	48.4±0.0	136.7±0.0
10	4	14	13.7±1.0	4.9±0.3	0.18±0.01	2.8±0.1	27.3±3.1	76.6±10.6
	4	23	15.7±0.5	4.8±0.1	0.16±0.01	3.3±0.0	30.1±0.9	99.1±2.7
	4	65	13.6±0.3	4.5±0.1	0.19±0.01	3.0±0.0	25.0±0.4	73.6±1.8
	4	144	9.2±0.0	3.2±0.1	0.13±0.01	2.8±0.0	25.0±1.0	70.9±3.1
20	4	262	9.1±0.0	3.2±0.0	0.14±0.00	2.8±0.0	23.5±0.3	66.5±0.5
	4	23	39.1±5.4	14.9±2.0	0.89±0.13	2.6±0.2	16.7±1.3	42.8±2.2
	4	65	21.0±1.0	8.00±0.4	0.33±0.02	2.6±0.0	23.9±0.2	62.9±0.9
	4	144	23.9±0.9	7.3±0.1	0.36±0.04	3.3±0.1	20.5±2.3	67.4±8.5
4	262	18.00±0.7	6.2±0.4	0.23±0.01	2.9±0.1	27.6±1.5	79.7±3.3	

The permeability results of PES/pNA(4%)/ZIF-8(10%) mixed matrix membranes on the Robeson's upper bound curves for H₂/CO₂, CO₂/CH₄ and H₂/CH₄ pairs were presented in Figure.4.10. For H₂/CO₂ and H₂/CH₄ gas pairs, separation performances of MMMs were close to the upper bound curve with decreasing particle size of ZIF-8 except of 14 nm ZIF-8 loaded MMM. For CO₂/CH₄ gas pair, the mixed matrix membranes had similar selectivity values with increasing particle size of ZIF-8. It was clearly seen in Figure.4.10 that 23 nm ZIF-8 loaded MMM had good gas separation performances in the 10% ZIF-8 loaded MMM.

In Figure.4.11, the gas separation performances of 20% ZIF-8 loaded MMMs on the upper bound curves for H₂/CO₂, CO₂/CH₄ and H₂/CH₄ pairs were given. For H₂/CO₂ gas pair, the membrane performance was close to upper bound curve in the trade-off line. The permeabilities of H₂ increased with the similar H₂/CO₂ ideal selectivity that may be a result of poor interaction and formation of nonselective voids between PES matrix and filler material. For CO₂/CH₄ and H₂/CH₄ pairs, the trends of membrane performances were not improved due to decreased selectivities. This could be explained by the occurrence of the interfacial non-selective voids and their expansion with increasing number of particles in the polymer matrix, so gas molecules passed through membrane, easily.

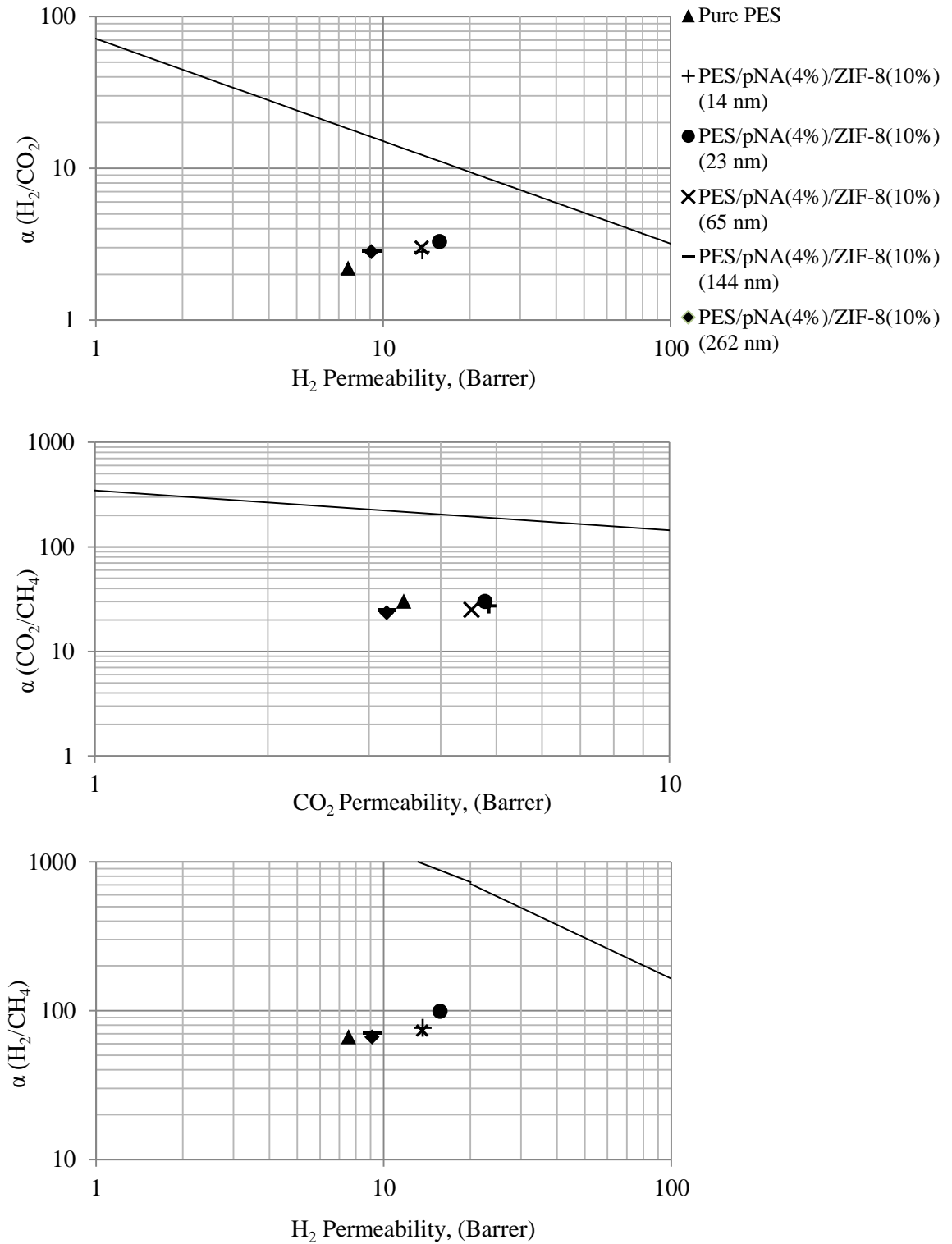


Figure.4.10 The permeation results of PES/pNA(4%)/ZIF-8(10%) MMMs on the Robeson's upper bound curves for H_2/CO_2 , CO_2/CH_4 and H_2/CH_4 gas pairs

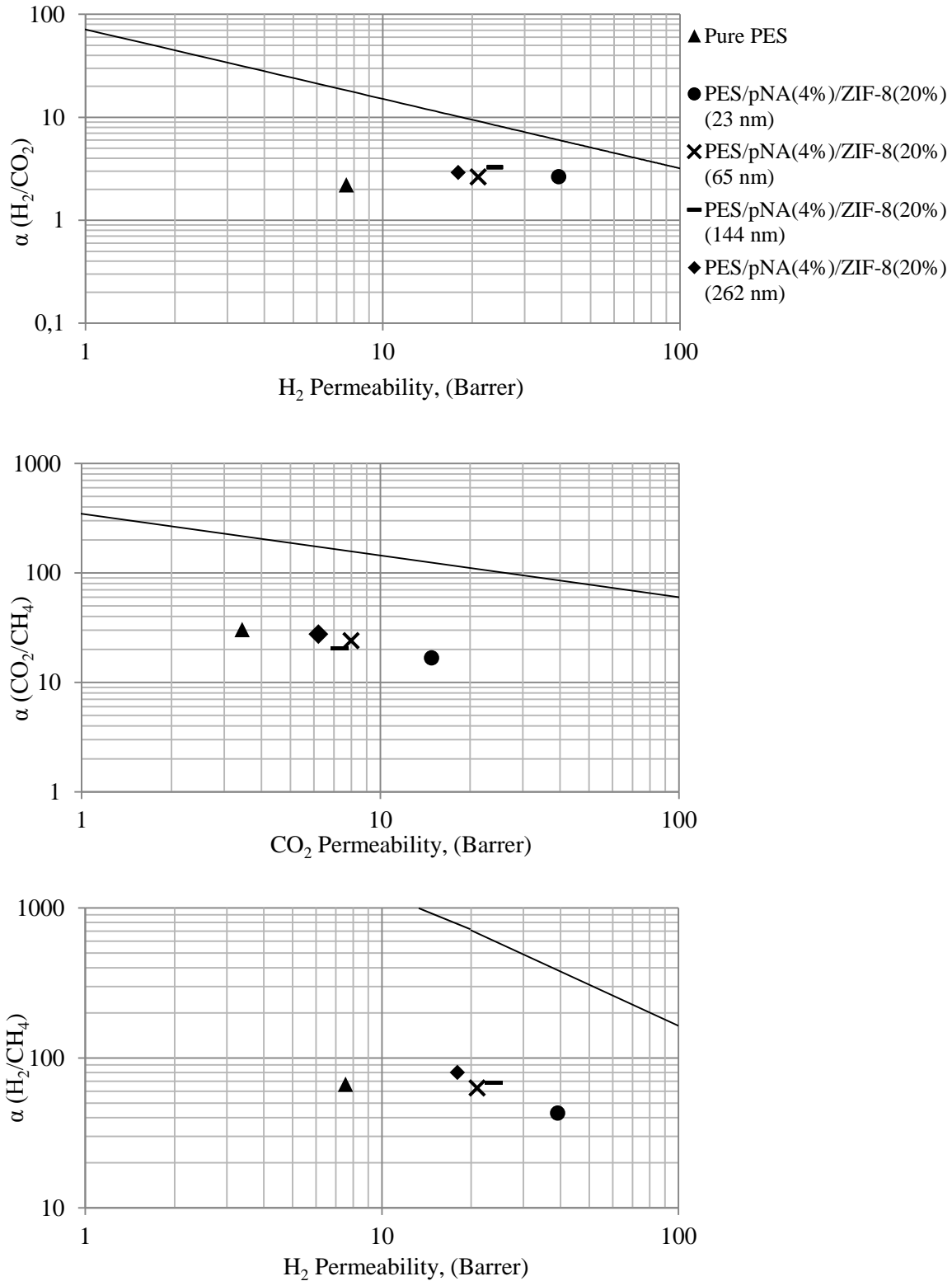


Figure.4.11 The permeation results of PES/pNA(4%)/ZIF-8(20%) MMMs on the Robeson's upper bound curves for H₂/CO₂, CO₂/CH₄ and H₂/CH₄ gas pairs

The comparisons of the permeation results of 10 wt% and 20 wt% ZIF-8 (23 nm) loaded PES/pNA(4%) MMMs were presented for H₂/CH₄ gas pair in Figure.4.12. The ideal selectivity of 20 wt % ZIF-8 (23 nm) loaded MMM decreased for H₂/CH₄ gas pair, significantly, although the permeation of H₂ increased which could be caused by non-selective voids around the filler interfaces. On the other hand, both the permeabilities and ideal selectivities improved for 10 wt % ZIF-8 (23 nm) loaded MMM when compared to pure PES membrane. This behavior related to the good compatibility between polymer and filler also non-defect membrane morphology. Therefore, it was clearly seen in Figure.4.12 that 10 wt% ZIF-8 loaded MMM had better gas separation performances.

The similar behavior of the effect of filler loading on separation performances was reported in literature. Keser et al. [19] reported that the permeability values of all gases were improved with increasing amount of ZIF-8 into the ZIF-8/HMA(4 wt%)/PES MMMs that could be due to enhance non-selective interfacial voids. Also, the ideal selectivity values of all gas pairs decreased with increasing amount of ZIF-8. The same behavior was also shown in some research [10, 18, 21].

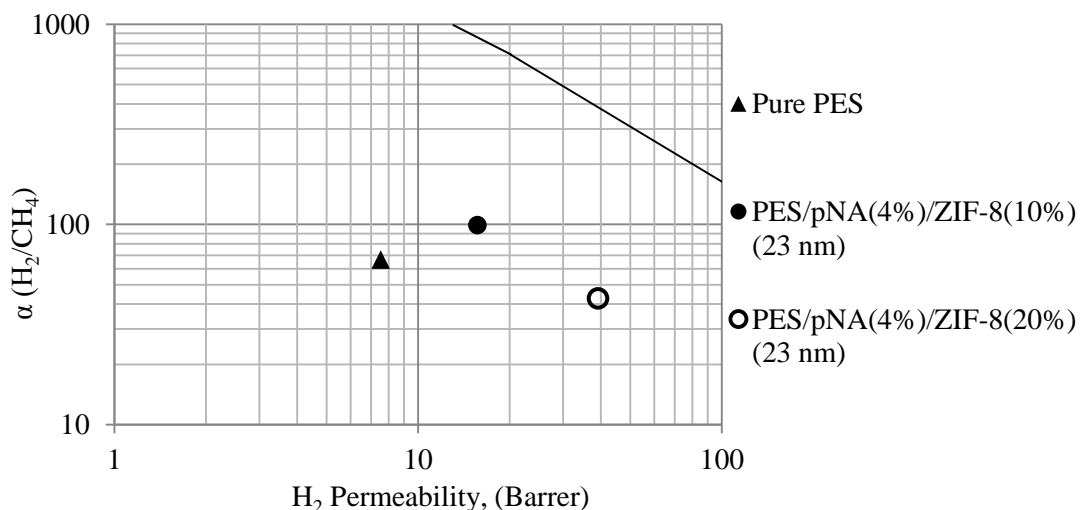


Figure.4.12 The permeation results of PES/pNA(4%)/ZIF-8(10%) (23 nm) and PES/pNA(4%)/ZIF-8(20%) (23 nm) MMMs on the Robeson's upper bound curves for H₂/CH₄ gas pair

4.4 Effect of Feed Pressure on the Gas Separation Performance of PES/pNA(4%)/ZIF-8(10%, 23 nm)

In industrial scale, the processes such as CO₂ removal from high pressure natural gas and separation of H₂ from gas mixtures should be able to operate at high feed pressures due to economic reasons. Most of research did not investigate the effects of feed pressure on the separation performance of MMMs. Limited numbers of research examined the separation performances at high pressure ranges. It was claimed that the behavior of the structure of membranes and the characteristics of filler materials could change depending on the feed pressure [60]. It can be useful to examine the effects of feed pressure on the separation performances to obtain information about behavior of MMMs.

In this study, PES/pNA(4%)/ZIF-8(10%) (23 nm) MMM, which showed the better separation performance for single gas permeation experiments, was chosen to study the effects of feed pressure on the gas separation performance. The high pressure measurements were conducted at 6, 10, 12 and 15 bar (absolute) feed pressures. The permeability values of H₂, CO₂ and CH₄ for PES/pNA(4%)/ZIF-8(10%) (23 nm) MMM were reported for different feed pressures in Figure.4.13. It was seen that the permeability of H₂ was not affected by changing feed pressure, which was nearly 15.8 barrer for all pressures. The permeabilities of CO₂ and CH₄ decreased with increasing feed pressure. When the feed pressure was increased from 3 bar to 15 bar, the permeabilities of CO₂ and CH₄ changed from 4.9 to 3.9 and 0.16 to 0.1, respectively. The percent decreases in CO₂ and CH₄ were 20% and 38%. The kinetic diameter of H₂ molecule is smaller than CO₂ and CH₄ gas molecules. In the glassy state, PES chains pack more efficiently with increasing upstream pressure; therefore, the free volume was decreased. Also, the transport mobility decreased for big gas molecules. It may be speculated that the biggest gas molecules may slowly pass through the membrane with packing effect of PES molecules [60, 61]. In addition, the plasticizing effect of CO₂ can be shown for glassy polymer membranes at higher feed pressures. The more CO₂

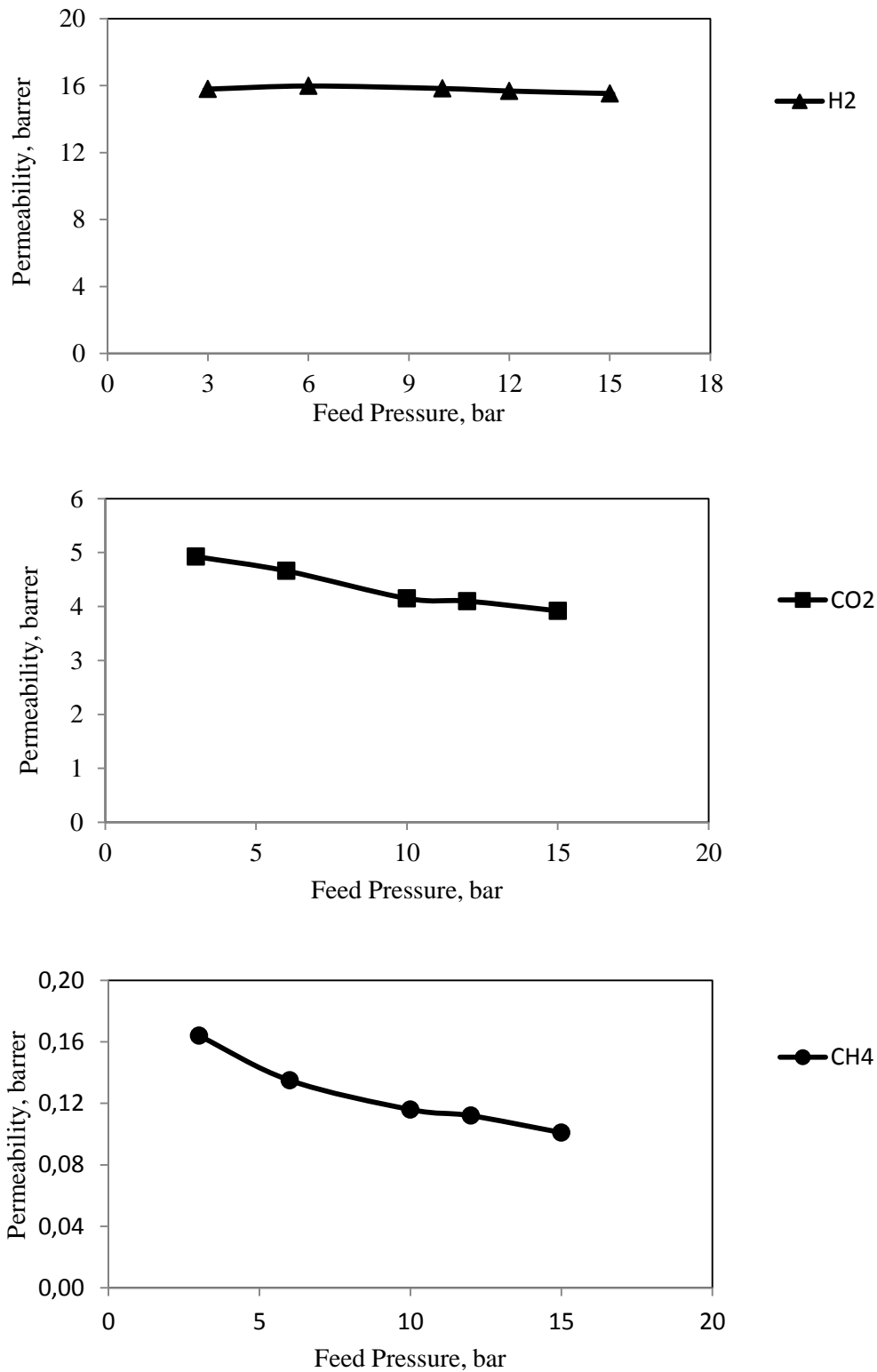


Figure.4.13 The permeabilities for H₂, CO₂ and CH₄ for PES/pNA(4%)/ZIF-8(10%) (23 nm) MMM with different feed pressures

sorption leads to excessive swelling of the polymer matrix at higher feed pressures. It may increase mobility of the polymer chains and the plasticization that increases the permeabilities of slower components [69, 70]. In this study, it could be seen that the increase in permeability was not observed, and the feed pressures were below the pressures of the plasticization effect of CO₂.

Figure.4.14 presented the change in the ideal selectivities for H₂/CO₂, CO₂/CH₄ and H₂/CH₄ for PES/pNA(4%)/ZIF-8(10%) (23 nm) MMM with different feed pressures. The ideal selectivity values of all gas pairs were increased with increasing feed pressure. The ideal selectivity for H₂/CO₂, CO₂/CH₄ and H₂/CH₄ gas pairs changed from 3.2 to 4.0, from 30.2 to 39.1 and from 96.3 to 154.1, respectively, with increasing feed pressure from 3 bar to 15 bar. The percent increases in the ideal selectivity values for H₂/CO₂, CO₂/CH₄ and H₂/CH₄ pairs were 24%, 22.8% and 60%, respectively. This was related to fact that the permeabilities of big gas molecules changed significantly due to the pressure effect.

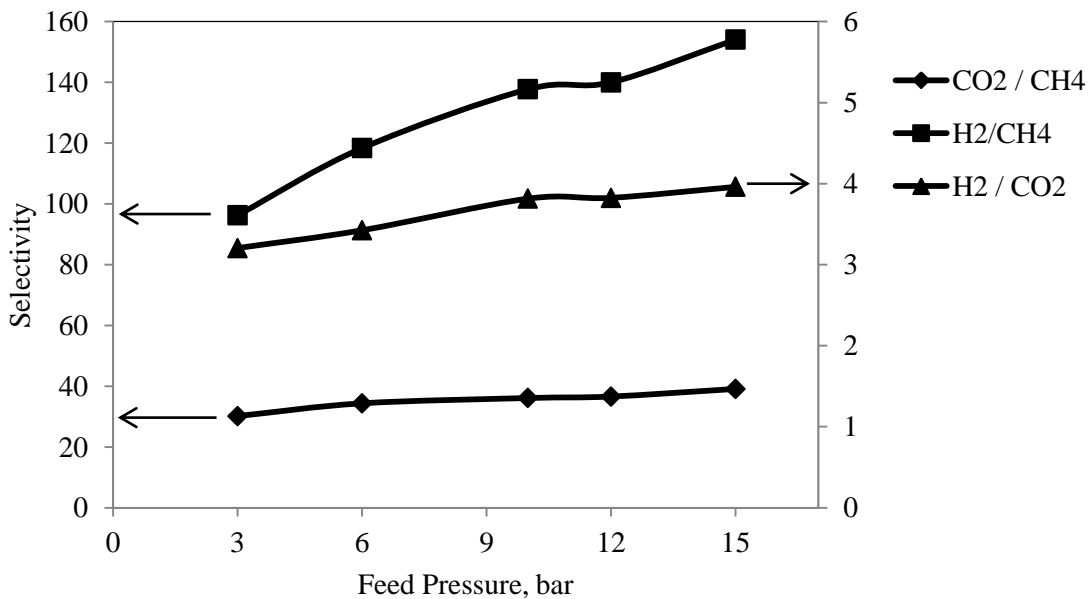


Figure.4.14 The ideal selectivities for H₂/CO₂, CO₂/CH₄ and H₂/CH₄ gas pairs for PES/pNA(4%)/ZIF-8(10%) (23 nm) MMM with different feed pressures

The similar behavior of the MMM at high feed pressure was also shown in Keser et al. [19] study which were investigated between 3 and 12 bar feed pressures. The different membrane compositions were used to investigate the effect of the feed pressure. The permeabilities of CO₂ and CH₄ were reduced with increasing feed pressure. However, the permeability of H₂ was independent from feed pressure. The selectivities for gas pairs were increased with increasing feed pressure, especially H₂/CH₄ gas pair.

In Figure.4.15, Robeson's upper bound curves for H₂/CO₂, CO₂/CH₄ and H₂/CH₄ gas pairs were given together for results of high pressure permeation analysis. For H₂/CO₂ and H₂/CH₄ pairs, the ideal selectivities increased with constant permeabilities due to almost constant permeability of H₂. In Figure.4.15, it could be observed that the separation performances for all gas pairs improved with increasing feed pressure, and PES/pNA(4%)/ZIF-8(10%) (23 nm) MMM had good gas separation performance at high pressure conditions.

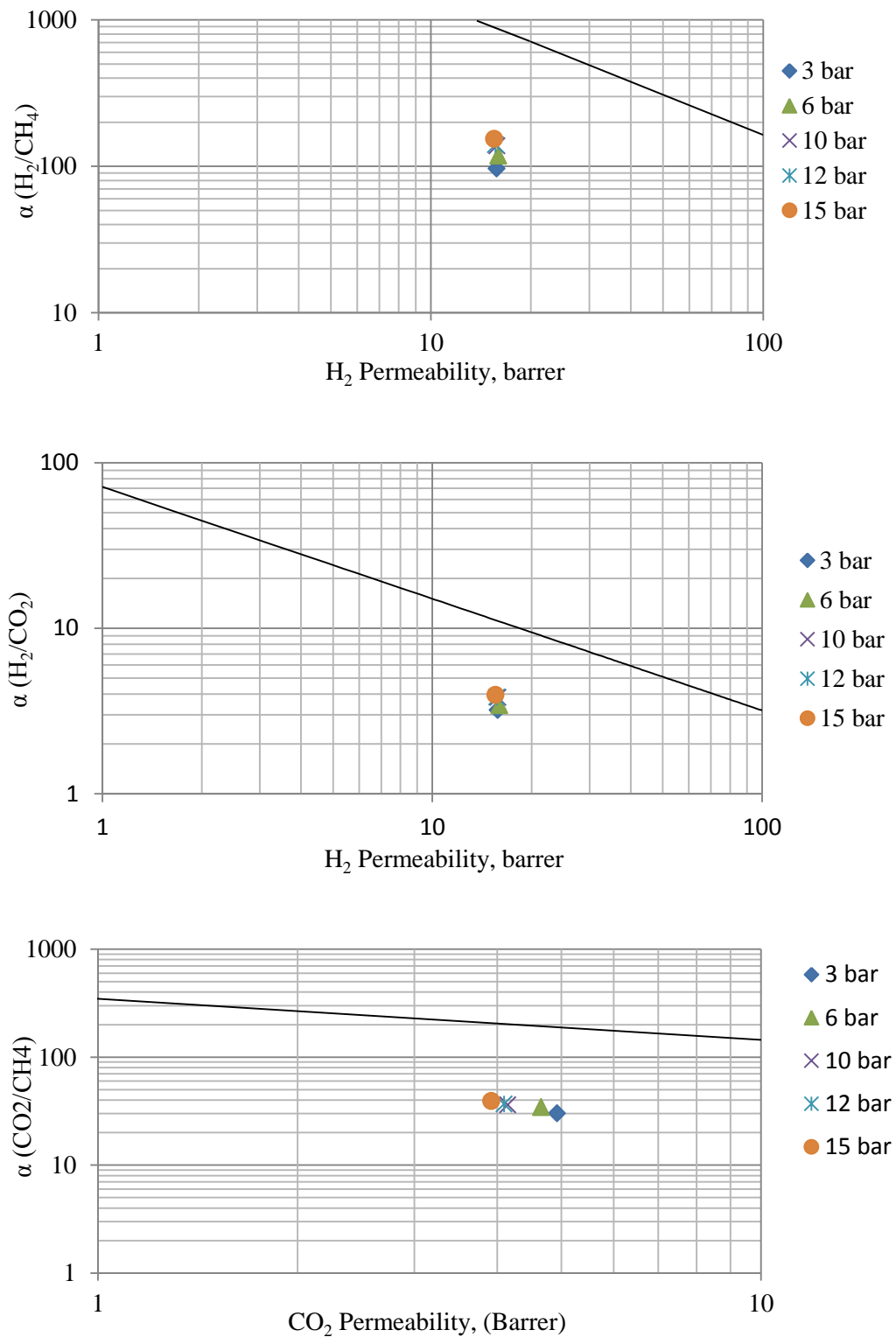


Figure.4.15 The effect of the feed pressure on PES/pNA(4%)/ZIF-8(10%) (23 nm) MMM in Robeson's upper bound curves for H_2/CO_2 , CO_2/CH_4 and H_2/CH_4 gas pairs

4.5 Binary Gas Permeation Results of PES/pNA(4%)/ZIF-8(10%, 23 nm) MMM

In this part of the study, the separation of binary gas mixtures was investigated for PES/pNA(4%)/ZIF-8(10%) (23 nm) MMM. The effect of feed composition on the gas separation performance of selected membrane was studied. The separation performance analysis of this MMM was conducted for CO₂/CH₄ gas mixture and the CO₂ in feed gas composition ranged between 10% and 50%. Also, the effect of feed pressure on the binary gas separation performances was investigated for selected membrane at 3 bar and 10 bar.

The binary gas permeabilities of the PES/pNA(4%)/ZIF-8(10%) (23 nm) MMM were reported in Figure.4.16. The permeabilities of the selected membrane increased with increasing feed composition of CO₂ due to the increased partial pressure of CO₂ in the mixture. It was expected that the mixture gas permeability values were between the pure CO₂ and CH₄ permeabilities, generally. The same result was reported by our research group [19, 20, 49]. In Figure.4.16, it was seen that the permeabilities of the selected membrane at 3 bar and 10 bar based on CO₂ composition of the feed were changed linearly with some deviations.

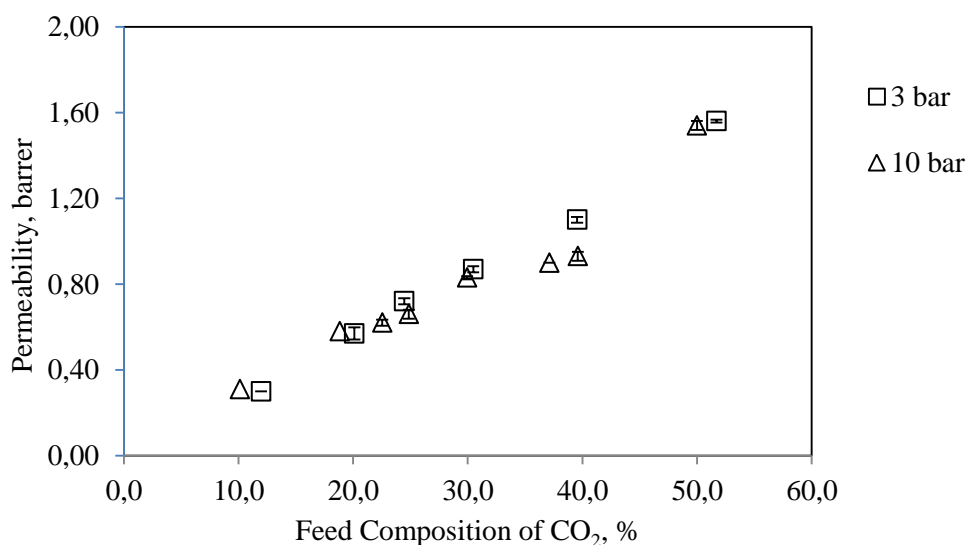


Figure.4.16 Effect of the feed composition on the permeabilities for PES/pNA(4%)/ZIF-8(10%) (23 nm) MMM

Figure 4.17 showed the change of the separation factors with increasing CO₂ percentage in the feed. The separation factor for CO₂/CH₄ of the selected membrane remained nearly constant at 3 bar. The separation factors were similar when compared with the ideal selectivity for CO₂/CH₄, 30, at 3 bar.

The separation factors at 10 bar was similar values as 3 bar when CO₂ composition of the feed was between 0% and 22.5%. The separation factors at 10 bar increased when CO₂ composition of the feed was more than 22.5% that the CH₄ content of permeate remained very small at about 3%. Both the constant CH₄ content of permeate and the increase of the feed composition of CO₂ caused the increase of the separation factors. Also, the separation factors at 10 bar were higher than the ideal selectivity with deviations, which was 36, when CO₂ composition of the feed was more than 22.5%. The reason of these deviations could be difficulties in detection sensitivity of GC due to very low CH₄ content in permeate. In Bae et al. [33] study, the measurements of binary gas mixture separation were done by using 6FDA-DAM/ZIF-90(15 wt %) MMMs. The separation selectivity of CO₂/CH₄ pair was higher than the ideal selectivities. They explained that the selective sorption and diffusion characteristics of CO₂ in ZIF-90 could cause the increase of the separation factor. Another study was Dhingra et al. [68] that pure NEW-TPI membrane had similar behavior for separation of binary CO₂/CH₄ mixture. They claimed that CO₂ had high solubility, and it was dominant effect of CO₂. The effect of CO₂ led to decrease in CH₄ permeability.

In Figure.4.17, the effect of CO₂ composition of the feed on the CH₄ content of permeate was shown for the separation of CO₂/CH₄ mixture for the PES/pNA(4%)/ZIF-8(10%) (23 nm) MMM. The CH₄ composition of the permeate was investigated in two different sections at 10 bar. In Section-I, it was observed that the CH₄ content of permeate at 10 bar decreased sharply until the feed was 25% CO₂. The CO₂ is more permeable than CH₄. Thus, it could be speculated that the small changes in CO₂ concentrations from 20% to 25% in the feed decreased the permeability of CH₄, significantly. Also, ZIF-8 had higher CO₂ adsorption capacity than CH₄ at higher pressures, which was stated in Zhang et al. study [21] in Figure.2.5. They concluded that strongly adsorbed CO₂ molecules block the diffusion pathways of CH₄. Çakal et al. [20] was speculated that the

more number of CO₂ molecules may be interact with the membrane, and this may cause pore blockage effect. Thus, the CO₂ molecules could inhibit the CH₄ molecules with increasing CO₂ concentration in the feed.

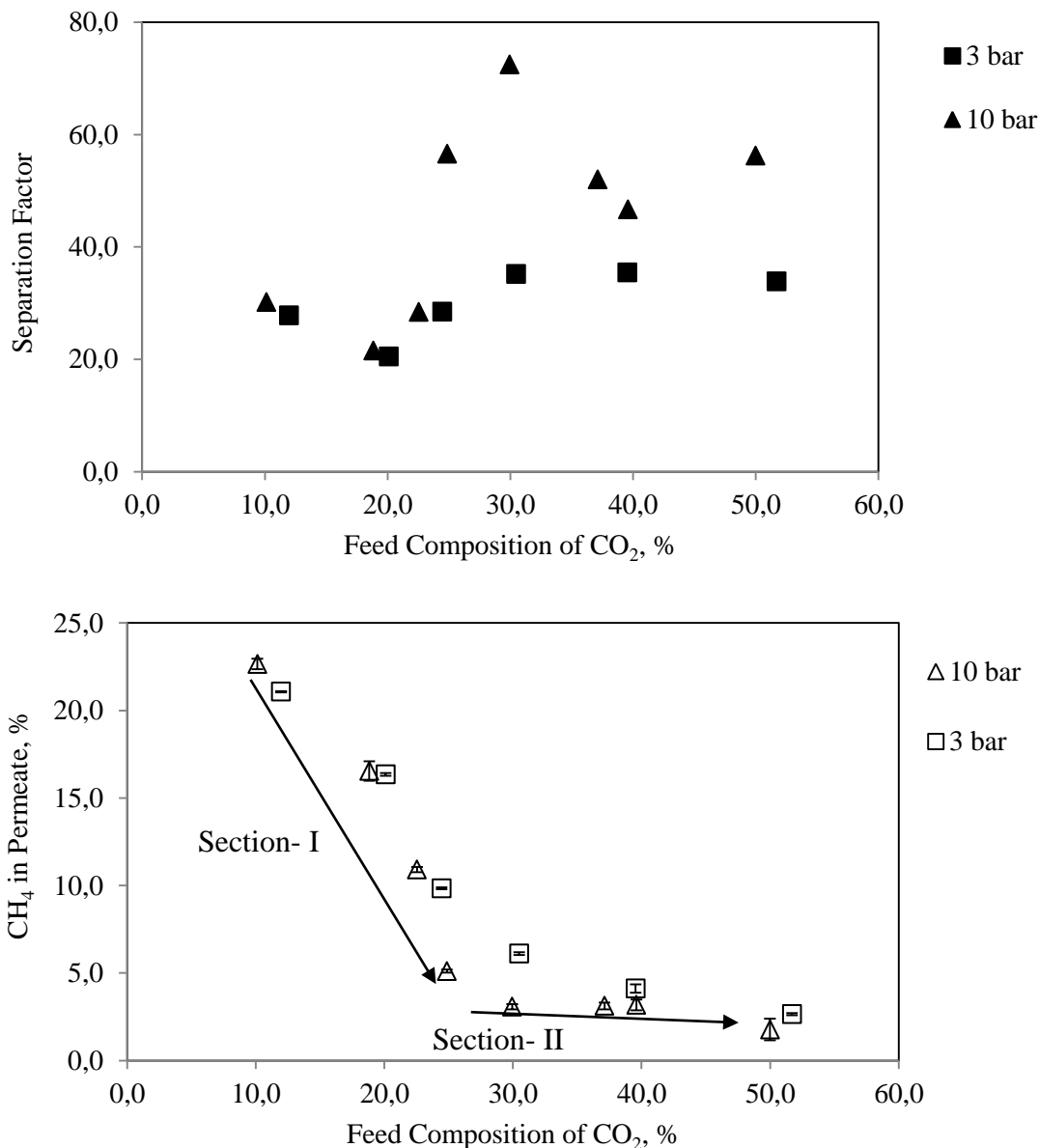


Figure.4.17 Effect of the feed composition of CO₂ on the separation factor for CO₂/CH₄ mixture and CH₄ amount in permeate for PES/pNA(4%)/ZIF-8(10%) (23 nm) MMM with different feed pressures

In Section-II, the CH₄ content of permeate was similar at about 3% when the feed composition of CO₂ was more than 25%. When the higher CO₂ concentration was considered, CO₂ molecules in the gas mixture could lead to the self-inhibition. Therefore, the similar permeate compositions of CH₄, Section-II, might be due to the self-inhibition of the CO₂ molecules. Also, the permeate composition of CH₄ at 3 bar did not decrease as sharp as the ones at 10 bar. This behavior could be explained by that the low operation pressure allowed slower transportation than high operation pressures.

CHAPTER 5

CONCLUSIONS

In this study, the effect of the particle size of ZIF-8 on the gas separation performance of MMMs was investigated. Dense homogenous MMMs were prepared by using solvent evaporation method using PES as the polymer matrix, pNA as the low molecular weight additive and ZIF-8 as filler. The following conclusions were determined:

1. Varying particle sizes of ZIF-8 crystals with high crystallinity, which were between 14 and 262 nm, were synthesized by using 1 hour stirring method at room temperature with different MeOH/Zn⁺² molar ratio and recycling methodology. However, it was shown that the particle sizes of 14 nm ZIF-8 crystals were agglomerated, highly, and these crystals behaved as if they were bigger size.
2. Pure PES, PES/pNA and PES/pNA/ZIF-8 MMMs were prepared with pNA 4% (w/w) and different amounts of ZIF-8 as 10 and 20% (w/w). In MMMs, the particle sizes of 14, 23, 65, 144 and 262 nm ZIF-8 crystals were used to investigate the effect of the particle size of ZIF-8 on the gas separation performance.
3. The incorporation of pNA into the membrane reduced permeabilities of H₂, CO₂ and CH₄, and increased ideal selectivities when compared to pure PES membrane. When the low molecular weight additive was used, the segmental movement of polymer matrix and free volume between polymer chains and filler reduced, so the gas separation performance of membranes improved.

4. The 10% (w/w) ZIF-8 loaded MMMs showed high compatibility as it was seen in SEM analysis. One gram of the particle size of 23 nm ZIF-8 crystals had approximately 1478 times greater number of particle than one gram of the particle size of 262 nm ZIF-8 crystals. The addition of the smaller particle sizes of ZIF-8 crystals increased the permeabilities and ideal selectivities for 10% (w/w) ZIF-8 loaded MMMs. Also, the single gas permeabilities of the 20% (w/w) ZIF-8 loaded MMMs showed higher permeabilities than 10% (w/w) ZIF-8 loaded MMMs; however, they had lower selectivities. The highest permselective membrane for all gases was observed as PES/pNA(4%)/ZIF-8(10%) (23 nm) MMM.

5. The selected MMM was performed the single gas permeation measurement at feed pressure of 6, 10, 12 and 15 bar. Although the H₂ permeability was not affected by changing feed pressure, the CO₂ and CH₄ permeabilities reduced with increasing feed pressure. PES/pNA(4%)/ZIF-8(10%) (23 nm) MMM showed high gas separation performance at high feed pressures.

6. Binary gas permeation measurements of CO₂/CH₄ gas pair were conducted for PES/pNA(4%)/ZIF-8(10%) (23 nm) MMM. The effect of CO₂ composition of the feed was investigated for the selected MMM at 3 and 10 bar. The separation factors at 3 bar were constant, and it were similar when compared to the ideal selectivity. The behavior of the separation factors at 10 bar had two section. Firstly, the separation factors showed similar values when compared to the analysis at 3 bar that was till the 22.5% CO₂ composition of the feed. In second section, the separation factors at 10 bar were higher than the ideal selectivity.

CHAPTER 6

RECOMMENDATIONS

1. The different type of low molecular weight additives with multifunctional groups can be used to investigate the effects of the LMWA on the gas separation performances of ternary MMMs.
2. PES/pNA/ZIF-8 MMMs can be prepared by using different preparation method such as phase inversion method to see effects on the membrane structure and the gas separation performances of MMMs.
3. In this study, ternary MMMs were prepared based on the changing ratios of the filler to polymer with constant LMWA to polymer ratio. Ternary MMMs can be prepared by using constant filler to LMWA ratio with changing amounts of materials to investigate the effect on the gas separation performance.
4. For binary gas mixture permeation measurements, different gas components, such as hydrogen, nitrogen etc., can be investigated to see behavior of the MMMs for the different gas mixture systems.

REFERENCES

- [1] Mulder, M., “Basic Principles of Membrane Technology”, *Kluwer Academic Publishers*, Second Edition, Dordrecht, 1997.
- [2] Ismail, A.F., Ridzuan, N., Rahman, S.A., “Latest development on the membrane formation for gas separation”, *Songklanakarin J. Sci. Technology*, 24, 1025-1043, 2002.
- [3] Bastani, D., Esmaeili, N., Asadollahi, M., “Polymeric mixed matrix membranes containing zeolites as a filler for gas separation applications: A review” *Journal of Industrial and Engineering Chemistry*, 19, 375-393, 2013.
- [4] Li, H., Freeman, B.D., Ekiner, O.M., “Gas permeation properties of poly(urethane-urea)s containing different polyethers”, *Journal of Membrane Science*, 369, 49-58, 2011.
- [5] Yampolskii, Y., “Polymeric Gas Separation Membranes”, *Macromolecules*, 45, 3298-3311, 2012.
- [6] Javaid, A., “Membranes for solubility-based gas separation applications”, *Chemical Engineering Journal*, 112, 219-226, 2005.
- [7] Goh, P.S., Ismail, A.F., Sanip, S.M., Ng, B.C., Aziz, M., “Recent advances of inorganic fillers in mixed matrix membrane for gas separation”, *Separation and Purification Technology*, 81, 243-264, 2011.
- [8] Erucar, I., Keskin, S., “Computational screening of metal organic frameworks for mixed matrix membrane applications”, *Journal of Membrane Science*, 407-408, 221-230, 2012.
- [9] Robeson, L.M., “The upper bound revised”, *Journal of Membrane Science*, 320, 390-400, 2008.
- [10] Ordonez, M.J.C., Balkus, K.J., Ferraris, J.P., Musselman, I.H., “Molecular sieving realized with ZIF-8/Matrimid mixed matrix membranes”, *Journal of Membrane Science*, 361, 28-37, 2010.
- [11] Aroon, M.A., Ismail, A.F., Matsuura, T., Montazer-Rahmati, M.M., “Performance studies of mixed matrix membranes for gas separation: A review”, *Separation and Purification Technology*, 75, 229-242, 2010.

- [12] Sen, D., Yilmaz, L., Kalipcilar, H., “Development of polycarbonate based zeolite 4A filled mixed matrix gas separation membranes”, *Journal of Membrane Science*, 303, 194- 203, 2007.
- [13] Yong, H.H., Park, N.C., Kang, Y.S., Won, J., Kim, W.N., “Zeolite filled polyimide membrane containing 2,4,6-triaminopyrimidine”, *Journal of Membrane Science*, 188, 151–163, 2001.
- [14] Ferraris, J.P., Musselman, I.H., Balkus, K.J., “Mixed matrix membranes based on metal organic frameworks”, *Advanced Materials for Membrane Preparation*, Chapter 6, 83-93, 2012.
- [15] Venna, S.R., Carreon, M.A., “Highly permeable zeolite imidazolate framework-8 membranes for CO₂/CH₄ separation”, *J. Am. Chem. Soc.*, 132, 76-78, 2010.
- [16] Venna, S.R., Jasinski, J.B., Carreon, M.A., “Structural evolution of zeolitic imidazolate framework-8”, *J. Am. Chem. Soc.*, 132, 18030-18033, 2010.
- [17] Bux, H., Liang, F., Li, Y., Cravillon, J., Wiebcke, M., Caro, J., “Zeolitic imidazolate framework membrane with molecular sieving properties by microwave-assisted solvothermal synthesis”, *J. Am. Chem. Soc.*, 131, 16000-16001, 2009.
- [18] Diaz, K., Lopez-Gonzalez, M., del Castillo, L., F., Riande, E., “Effect of zeolitic imidazolate frameworks on the gas transport performance of ZIF-8-poly(1,4-phenylene ether-ether-sulfone) hybrid membranes”, *Journal of Membrane Science*, 383, 206-213, 2011.
- [19] Keser, N., “Production and performance evaluation of ZIF-8 based binary and ternary mixed matrix gas separation membranes”, Master Thesis, Middle East Technical University, August 2012.
- [20] Çakal, Ü., “Natural Gas Purification by Zeolite Filled Polyethersulfone Based Mixed Matrix Membranes”, Ms Thesis, Middle East Technical University, October, 2009.
- [21] Song, Q., Nataraj, S.K., Roussenova, M.V., Tan, J.C., Hughes, D.J., “Zeolitic imidazolate framework (ZIF-8) based polymer nanocomposite membranes for gas separation”, *Energy Environ. Sci.*, 5, 8359-8369, 2012.
- [22] Liu, C., “Recent Progress in Mixed-Matrix Membranes, Advanced Membrane Technology and Applications”, *Wiley: Hoboken, NJ.*, 787 – 819, 2008.
- [23] Huang, Z., Li, Y., Wen, R., Teoh, M.M., Kulprathipanja, S., “Enhanced gas separation properties by using nanostructured PES-zeolite 4A mixed matrix membranes”, *Journal of Applied Polymer Science*, 101, 3800-3805, 2006.
- [24] Koros, W.J., M.R. Coleman, D.R.B. Walker., “Controlled Permeability Polymer Membranes”, *Annu. Rev. Mater. Sci.*, 22, 47-89, 1992.

- [25] Kesting, R.E., Fritzsche, A.K., "Polymeric gas separation membranes", *Wiley Interscience Publishers*, New York, 416, 1993.
- [26] Zimmerman, C. M., Singh, A., Koros, W.J., "Tailoring mixed matrix composite membranes for gas separations", *J. Membr. Sci.*, 137, 145-154, 1997.
- [27] Robeson, L. M., "Polymer membranes for gas separation", *Curr. Opin. Solid State Mater. Sci.*, 4, 549-552, 1999.
- [28] Ismail, A. F., David, L. I. B., "A review on the latest development of carbon membranes for gas separation", *J. Membr. Sci.*, 193, 1-18, 2001.
- [29] Mahajan, R., "Formation, characterization and modeling of mixed matrix membrane materials", PhD thesis, The University of Texas at Austin, 2000.
- [30] Reid, B.D., Ruiz-Treviño, F.A., Musselman, I.H., Balkus Jr., K.J., Ferraris, J.P., "Gas permeability properties of polysulfone membranes containing mesoporous molecular sieve MCM-41", *Chem. Mater.*, 13, 2366–2373, 2001.
- [31] Huang, Z., Li, Y., Wen, R., Teoh, M.M., Kulprathipanja, S., "Enhanced gas separation properties by using nanostructured PES-zeolite 4A mixed matrix membranes", *Journal of Applied Polymer Science*, 101, 3800-3805, 2006.
- [32] Perez, E.V., Balkus, K.J., Ferraris, J.P., Musselman, I.H., "Mixed-matrix membranes containing MOF-5 for gas separations", *Journal of Membrane Science*, 328, 165–173, 2009.
- [33] Bae, T.H., Lee, J.S., Qiu, W., Koros, W.J., Jones, C.W., Nair, S., "A High-Performance Gas- Separation Membrane Containing Submicrometer-Sized Metal–Organic Framework Crystals", *Angew. Chem. Int. Ed.*, 49, 9863 –9866, 2010.
- [34] Sürer, M.G., Baç, N., Yilmaz, L., "Gas permeation characteristics of polymer-zeolite mixed matrix membranes", *Journal of Membrane Science*, 91, 77-86, 1994.
- [35] Moore, T.T., Mahajan, R., Vu, D.Q., Koros, W.J., "Hybrid membrane materials comprising organic polymers with rigid dispersed phases", *AIChE J.*, 50, 311–321, 2004.
- [36] Ismail, A.F., Rahim, R.A., Rahman, W.A.W.A., "Characterization of polyethersulfone/Matrimid 5218 miscible blend mixed matrix membranes for O₂/N₂ gas separation", *Separation and Purification Technology*, 63, 200-206, 2008.
- [37] Duval, J.M., Kemperman, A.J.B., Folkers, B., Mulder, M.H.V., Desgrandchamps G., Smolders, C.A., "Preparation of zeolite filled glassy polymer membrane", *Journal of Applied Polymer Science*, 54, 409-418, 1994.

- [38] Karatay, E., Kalıpcılar, H., Yılmaz, L., “Preparation and performance assessment of binary and ternary PES-SAPO 34-HMA based gas separation membranes”, *Journal of Membrane Science*, 364, 75–81, 2010.
- [39] Duval, J.M., Folkers, B., Mulder, M.H.V., Desgrandchamps, G. and Smolders, CA. “Adsorbent filled membranes for gas separation. Part 1. Improvement of the gas separation properties of polymeric membranes by incorporation of microporous adsorbents”, *Journal of Membrane Science*, 80(1), 189-198, 1993.
- [40] Bushell, AF, Attfield, MP, Mason, CR, Budd, PM; Yampolskii, Y, Starannikova, L, Rebrov, A; Bazzarelli, F, Bernardo, P, Jansen, JC, Lanc, M, Friess, K, Shantarovich, V, Gustov, V, Isaeva, V.,”Gas permeation parameters of mixed matrix membranes based on the polymer of intrinsic microporosity PIM-1 and the zeolitic imidazolate framework ZIF-8”, *Journal Of Membrane Science*, 427, 48-62, 2013.
- [41] Zhang Y, Musselman IH, Ferraris JP, Balkus KJ.,”Gas permeability properties of Matrimid membranes containing the metal organic framework Cu–BPY–HFS”, *Journal of Membrane Science*, 313, 170–181, 2008.
- [42] Adams, R., Carson, C., Ward, J., Tannenbaum, R., Koros, W., “Metal organic framework mixed matrix membranes for gas separations”, *Microporous and Mesoporous Materials*, 131, 13–20, 2010.
- [43] McCarthy, M.C., Varela-Guerrero, V., Barnett, G. V., Jeong, H.K., “Synthesis of zeolitic imidazolate framework films and membranes with controlled microstructures”, *Langmuir*, 26, 14636–14641, 2010.
- [44] Zhang, L., Wu, G., Jiang, J., ”Adsorption and Diffusion of CO₂ and CH₄ in Zeolitic Imidazolate Framework-8: Effect of Structural Flexibility”, *J. Phys. Chem.*, 118, 8788-8794, 2014.
- [45] Basu, S., Odena, A.C., Vankelecom, I.F.J., “MOF-containing mixed-matrix membranes for CO₂/CH₄ and CO₂/N₂ binary gas mixture separations”, *Separation and Purification Technology*, 362,478, 2010.
- [46] Y.Dai, J.R. Johnson, O. Karvan, D.S. Sholl, W.J. Koros, “Ultem®/ZIF-8 mixed matrix hollow fiber membranes for CO₂/N₂ separations”, *Journal of Membrane Science*, 401– 402, 76– 82, 2012.
- [47] Thang, H.V., Kaliaguine, S., “Predictive Models for Mixed Matrix Membrane Performance: A Review”, *Chem. Rev.*, 113, 4980-5028, 2013.
- [48] Battal, T., Baç, N., Yılmaz, L., “Effect of feed composition on the performance of polymerzeolite mixed matrix gas separation membranes”, *Separation Science and Technology*, 30, 2365- 2384, 1995.
- [49] Şen, D., Yılmaz, L., Kalıpcılar, H.,”Effect of Feed Composition on the Gas Separation Performance of Binary and Ternary Mixed Matrix Membranes”, *Separation Science and Technology*, 48, 859-866, 2013.

- [50] Cakal, U., Yilmaz, L., Kalipcilar, H., “Effect of feed gas composition on the separation of CO₂/CH₄ mixtures by PES-SAPO34-HMA mixed matrix membranes”, *Journal of Membrane Science*, 417-418, 45-51, 2012.
- [51] Tantekin-Ersolmaz, Ş.B., Atalay-Oral, Ç., Tatlier, M., Erdem-Şenatalar, A., Schoeman, B., Sterte, J., “Effect of zeolite particle size on the performance of polymer-zeolite mixed matrix membranes”, *Journal of Membrane Science*, 175, 285-288, 2000.
- [52] Şen, D., “Polycarbonate Based Zeolite 4A Filled Mixed Matrix Membranes: Preparation, Characterization, and Gas Separation Performances”, PhD Thesis, Middle East Technical University, February 2008.
- [53] Park, K.S., Ni, Z., Cote, A.P., Choi, J.Y., Huang, R., Uribe-Romo, F.J., Chae, H.K., O’Keeffe, M., Yaghi, O.M., “Exceptional chemical and thermal stability of zeolitic imidazolate frameworks”, *Proc. Natl. Acad. Sci. U.S.A.*, 103, 10186–10191, 2006.
- [54] Pan, Y., Liu, Y., Zeng, G., Zhao, L., Lai, Z., “Rapid Synthesis of Zeolitic Imidazolate Framework-8 (ZIF-8) Nanocrystals in an Aqueous System”, *Chem. Commun.*, 47, 2071-2073, 2011.
- [55] Zhao, Z., Ma, X., Li, Z., Lin, Y.S., “Synthesis, characterization and gas transport properties of MOF-5 membranes”, *Journal of Membrane Science*, 382, 82–90, 2011.
- [56] Cravillon, J., Schröder, C.A., Nayuk, R., Gummel, J., Huber, K., Wiebcke, M., “Fast Nucleation and Growth of ZIF-8 Nanocrystals Monitored by Time-Resolved In Situ Small-Angle and Wide-Angle X-Ray Scattering”, *Angew. Chem. Int. Ed.*, 50, 8067–8071, 2011.
- [57] Li, Y., Chung, T., Cao, C., Kulprathipanja, S., “The effects of polymer chain rigidification, zeolite pore size and pore blockage on polyethersulfone (PES)-zeolite 4A mixed matrix membranes”, *Journal of Membrane Science*, 260, 45-55, 2005.
- [58] Şen, D., “Effect of Compatibilizers on the Gas Separation Performance of polycarbonate based Membranes”, Ms thesis, Middle East Technical University, 2003.
- [59] Şen, D., Kalipcilar, H., Yilmaz, L., “Gas Separation performance of polycarbonate membranes modified with multifunctional low-molecular weight additives”, *Separation Science and Technology*, 41, 1813–1828, 2006.
- [60] Chiou, J.S., Maeda, Y., Paul, D.R., “Gas Permeation in Polyethersulfone”, *Journal of Applied Polymer Science*, 33, 1823-1828, 1987.
- [61] Hamed, K., Hossein, K., Hossein, N., Mohammad, R. M., Seyed, M. B., “Fabrication of Homogenous Polymer-Zeolite Nanocomposites as Mixed-Matrix Membranes for Gas Separation”, *Chemical Engineering & Technology*, 35, 885-892, 2012.

- [62] Yong, H.H., Park, N.C., Kang, Y.S., Won, J., Kim, W.N., “Zeolite filled polyimide membrane containing 2,4,6-triaminopyrimidine”, *Journal of Membrane Science*, 188, 151–163, 2001.
- [63] Ruiz-Treviño, F.A., Paul, D.R., “Modification of polysulfone gas separation membranes by additives”, *Journal of Applied Polymer Science*, 66, 1925-1941, 1997.
- [64] Moore, T.T., Koros, W.J., “Non-ideal effects in organic–inorganic materials for gas separation membranes”, *Journal of Molecular Structure*, 739, 87–98, 2005.
- [65] Sridhar, S., Smitha, B., Ramakrishna, M., Aminabhavi, T.M., “Modified poly(phenylene oxide) membranes for the separation of carbon dioxide from methane”, *Journal of Membrane Science*, 280, 202-209, 2006.
- [66] Keser Demir, N., Topuz, B., Yılmaz, L., Kalıpçılar, H., “Synthesis of ZIF-8 from Recycled Mother Liquors”, *Microporous and Mesoporous Materials*, 2014.
- [67] Qi Shi, Zhaofeng Chen, Zhengwei Song, Jinping Li, and Jinxiang Dong, “Synthesis of ZIF-8 and ZIF-67 by Steam-Assisted Conversion and an Investigation of Their Tribological Behaviors”, *Angew. Chem.*, 122, 1 – 5, 2010.
- [68] Dhingra, S.S., Marand, E., “Mixed gas transport through polymeric membranes”, *Journal of Membrane Science*, 141, 45-63, 1998.
- [69] Shahid, S., Nijmeijer, K., “High pressure gas separation performance of mixed matrix polymer membranes containing mesoporous Fe(BTC)”, *Journal of Membrane Science*, 4591, 33-44, 2014.
- [70] Wessling, M., Schoeman, S., van der Boomgaard, Th., Smolders, C., A., “Plasticization of gas separation membranes”, Gas Separation International, Austin, TX, USA, 22-24, April 1991.

APPENDIX A

THE AMOUNTS OF CHEMICALS FOR THE SYNTHESIS OF ZIF-8

Table A.1 Weights of used chemicals during the synthesis of ZIF-8 with different average particle sizes

Average Particle Size based on SEM, (nm)	Zn(NO₃)₂.6H₂O, (g)	Hmim, (g)	MeOH, (g)	NaOH, (g)	Mother Liquor, (g)
14	4.1	-	-	-	322.1
23	-	-	-	13	356.6
65	4.8	10.6	361.6	-	-
144	4.8	10.6	179.4	-	-
262	4.8	10.6	44.9	-	-

APPENDIX B

THE AMOUNTS OF MATERIALS IN MEMBRANE PREPARATION

Table B.1 Weights of used polymer, filler, low molecular weight additive and volume of solvent during the preparation of membranes

Membrane Type	PES, (g)	ZIF-8, (g)	pNA, (g)	DMF, (ml)
Pure PES	2.0	-	-	10
PES/pNA(4%)	2.0	-	0.08	10
PES/ZIF-8(14nm)(10%)/pNA(4%)	2.0	0.2	0.08	10
PES/ZIF-8(23nm)(10%)/pNA(4%)	2.0	0.2	0.08	10
PES/ZIF-8(65nm)(10%)/pNA(4%)	2.0	0.2	0.08	10
PES/ZIF-8(144nm)(10%)/pNA(4%)	2.0	0.2	0.08	10
PES/ZIF-8(262nm)(10%)/pNA(4%)	2.0	0.2	0.08	10
PES/ZIF-8(23nm)(20%)/pNA(4%)	2.0	0.4	0.08	10
PES/ZIF-8(65nm)(20%)/pNA(4%)	2.0	0.4	0.08	10
PES/ZIF-8(144nm)(20%)/pNA(4%)	2.0	0.4	0.08	10
PES/ZIF-8(262nm)(20%)/pNA(4%)	2.0	0.4	0.08	10

APPENDIX C

CALCULATION OF SINGLE PERMEABILITIES

The pressure change at the permeate side were recorded with respect to time by computer software. The simulated pressure change versus time curve was given in Figure.C.1. Time intervals of the gases H₂, CO₂ and CH₄ were 5s, 10s and 30s, respectively. The permeabilities were calculated by using algorithm that given in Figure C.1.

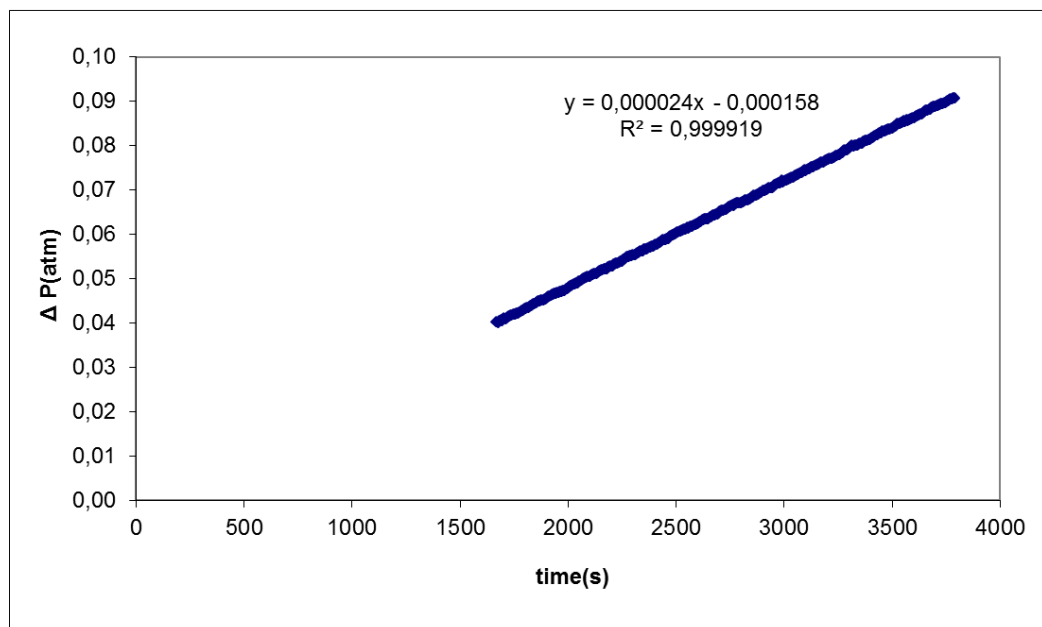


Figure C.1 The pressure change versus time graph for H₂ permeation test for PES/ZIF-8(144nm)(10%)/pNA(4%)

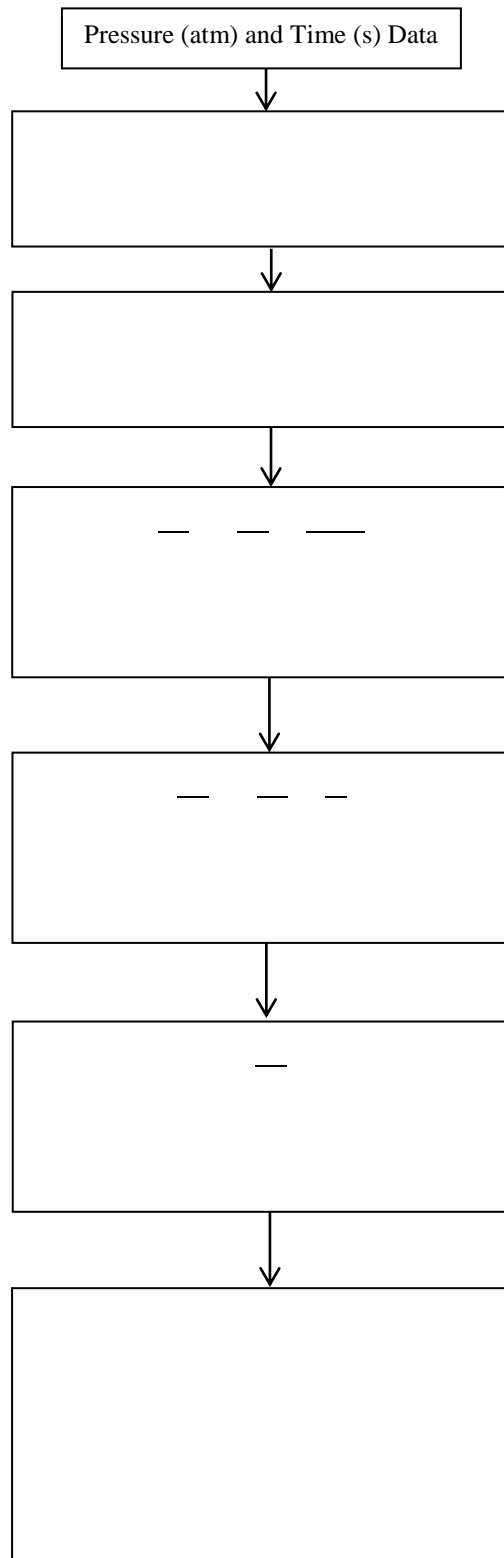


Figure C.2 Algorithm for single gas permeability calculation

APPENDIX D

CALIBRATION OF GAS CHROMATOGRAPHY

Gas chromatograph was calibrated for CO₂ and CH₄ gases to analyze gas compositions of feed and permeate side. The calibration curves were obtained by analyzing pure components in GC at certain pressure. The pressure versus area under the peak curves was obtained for CO₂ and CH₄ gases. CO₂ and CH₄ were fed to GC several times at different pressures between 0 and 100 Torr. After analysis, the area values under the curves were obtained. The amount of each gas in gas mixtures was determined by using GC data and calibrating curves. The calibration curves for CO₂ and CH₄ were given in Figure D.1 and Figure D.2, respectively.

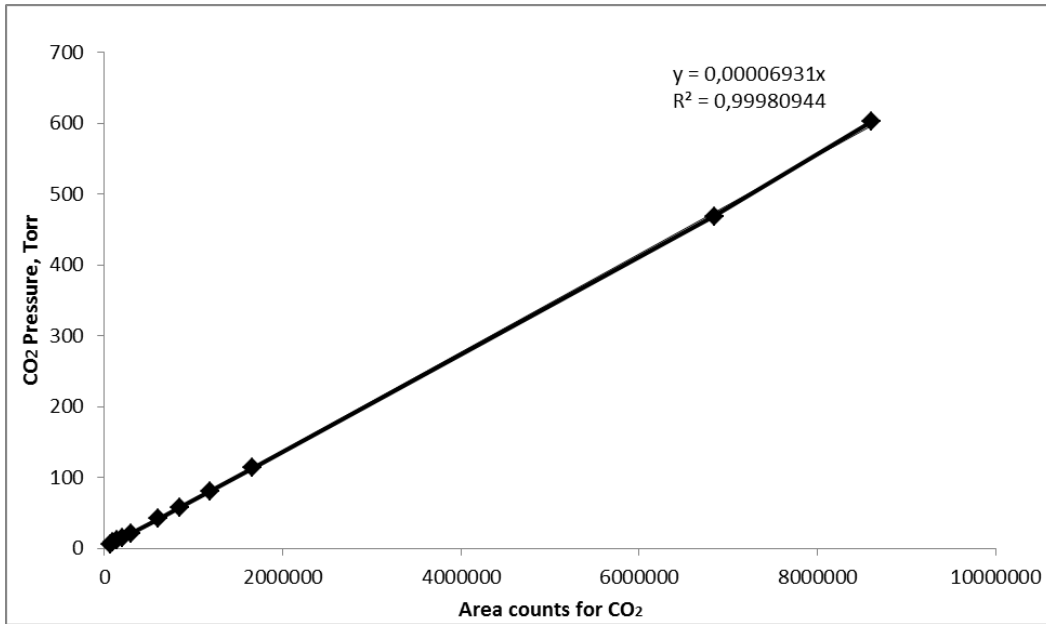


Figure D.1 The calibration curve of CO₂

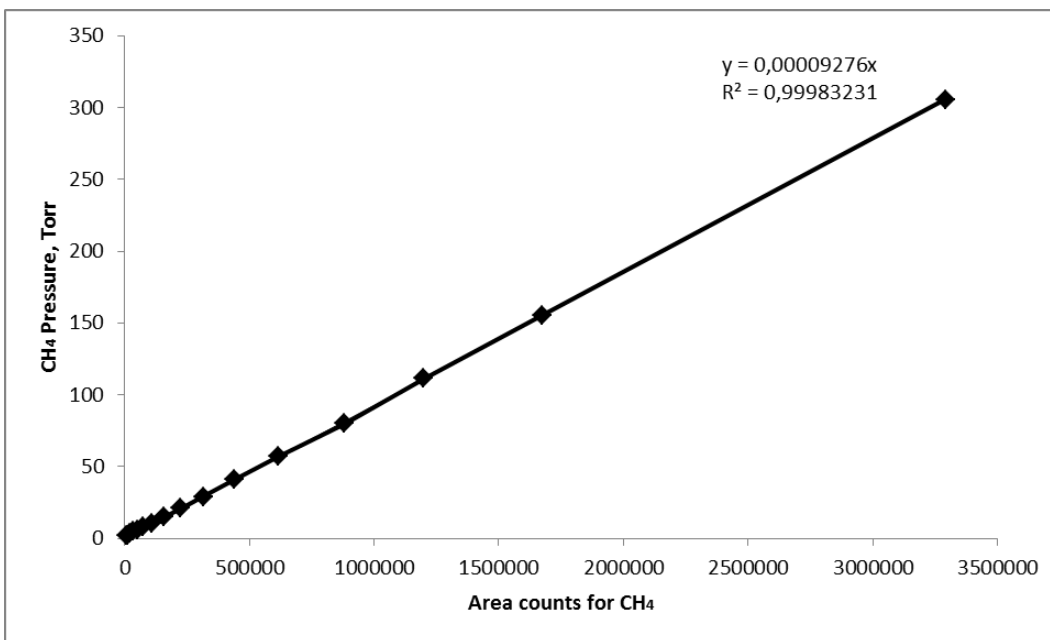


Figure D.2. The calibration curve of CH₄

APPENDIX E

A SAMPLE CALCULATION FOR DETERMINATION OF PERMEABILITIES AND SELECTIVITIES OF BINARY GAS MIXTURES

Membrane: PES/ZIF-8(20nm)(10%)/pNA(4%)

Membrane thickness: 65 μm

Gas mixture & Feed Composition: CO_2/CH_4 & 50:50

System Temperature: 35 $^\circ\text{C}$

Feed side analysis; 1st analysis at 64.6 Torr.

GC outputs: Area counts for CH_4 = 351786

Retention time for CH_4 = 1.62 s

Area counts for CO_2 = 463850

Retention time for CO_2 = 2.33 s

Partial pressure of $\text{CO}_2 = P_{\text{CO}_2,\text{feed}} = 0.00006913 \times (\text{Area counts for } \text{CO}_2)$

Partial pressure of $\text{CH}_4 = P_{\text{CH}_4,\text{feed}} = 0.00009276 \times (\text{Area counts for } \text{CH}_4)$

$$P_{\text{CO}_2,\text{feed}} = 0.00006913 \times 463850 = 32.07$$

$$P_{\text{CH}_4,\text{feed}} = 0.00009276 \times 351786 = 32.63$$

$$X_{\text{CO}_2,\text{feed}} = P_{\text{CO}_2,\text{feed}} / (\text{feed pressure}) = 32.07 / 64.6 = 0.4964 \text{ (49.64 \%)}$$

$$X_{\text{CH}_4,\text{feed}} = P_{\text{CH}_4,\text{feed}} / (\text{feed pressure}) = 32.63 / 64.6 = 0.5051 \text{ (50.51\%)}$$

Feed side analysis; 2nd analysis at 46.1 Torr.

GC outputs: Area counts for CH₄= 250514

Retention time for CH₄= 1.63 s

Area counts for CO₂= 335716

Retention time for CO₂= 2.33 s

$$\text{Partial pressure of CO}_2 = P_{\text{CO}_2,\text{feed}} = 0.00006913 \times (\text{Area counts for CO}_2)$$

$$\text{Partial pressure of CH}_4 = P_{\text{CH}_4,\text{feed}} = 0.00009276 \times (\text{Area counts for CH}_4)$$

$$P_{\text{CO}_2,\text{feed}} = 0.00006913 \times 335716 = 23.21$$

$$P_{\text{CH}_4,\text{feed}} = 0.00009276 \times 250514 = 23.24$$

$$X_{\text{CO}_2,\text{feed}} = P_{\text{CO}_2,\text{feed}} / (\text{feed pressure}) = 23.21 / 46.1 = 0.5034 \text{ (50.34 \%)}$$

$$X_{\text{CH}_4,\text{feed}} = P_{\text{CH}_4,\text{feed}} / (\text{feed pressure}) = 23.24 / 46.1 = 0.5041 \text{ (50.41 \%)}$$

Permeate side analysis; 1st analysis at 83.4 Torr.

GC outputs: Area counts for CH₄= 13319

 Retention time for CH₄= 1.63 s

 Area counts for CO₂= 1194983

 Retention time for CO₂= 2.30 s

$$P_{\text{CO}_2, \text{permeate}} = 0.00006913 \times 1194983 = 82.61$$

$$P_{\text{CH}_4, \text{permeate}} = 0.00009276 \times 13319 = 1.24$$

$$X_{\text{CO}_2, \text{permeate}} = P_{\text{CO}_2, \text{permeate}} / (\text{permeate pressure}) = 82.61 / 83.4 = 0.9905 \text{ (99.05 \%)}$$

$$X_{\text{CH}_4, \text{permeate}} = P_{\text{CH}_4, \text{permeate}} / (\text{permeate pressure}) = 1.24 / 83.4 = 0.015 \text{ (1.5 \%)}$$

Permeate side analysis; 2nd analysis at 59.3 Torr.

GC outputs: Area counts for CH₄= 9828

 Retention time for CH₄= 1.63 s

 Area counts for CO₂= 845366

 Retention time for CO₂= 2.31 s

$$P_{\text{CO}_2, \text{permeate}} = 0.00006913 \times 845366 = 58.44$$

$$P_{\text{CH}_4, \text{permeate}} = 0.00009276 \times 9828 = 0.91$$

$$X_{\text{CO}_2, \text{permeate}} = P_{\text{CO}_2, \text{permeate}} / (\text{permeate pressure}) = 58.44 / 59.3 = 0.9855 \text{ (98.55 \%)}$$

$$X_{\text{CH}_4, \text{permeate}} = P_{\text{CH}_4, \text{permeate}} / (\text{permeate pressure}) = 0.91 / 59.3 = 0.015 \text{ (1.5 \%)}$$

Separation Selectivity:

$$\alpha_{ij} = \frac{\left(\frac{X_i}{X_j}\right)_{permeate}}{\left(\frac{X_i}{X_j}\right)_{feed}}$$

Separation selectivity is the ratio of mol fractions of gases in the permeate side to feed side.

$$\alpha_{CO_2/CH_4} = \frac{\left(\frac{0.9881}{0.0177}\right)}{\left(\frac{0.4999}{0.5046}\right)}$$

$$\alpha_{CO_2/CH_4} = 56.35$$

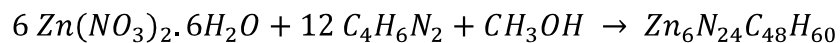
APPENDIX F

SAMPLE CALCULATION OF YIELD AND COMPOSITIONS OF ZIF-8 SYNTHESIS SOLUTIONS

All amounts of materials were calculated for every step of synthesis. The consumed and remained amounts of $Zn(NO_3)_2 \cdot 6H_2O$ and $C_4H_6N_2$ were calculated by using initial amounts of materials and synthesized ZIF-8 amount.

Calculation of Original Synthesis Solution;

Reaction of the synthesis,



Synthesis solution,

- 4.8g $Zn NO_3 \cdot 2.6H_2O$
- 10.56g $C_4H_6N_2$
- 361.6g CH_3OH

Also materials,

- $MW_{Zn NO_3 \cdot 2.6H_2O} = 297.49 \text{ g/mole}$
- $MW_{C_4H_6N_2} = 82.11 \text{ g/mole}$
- $MW_{CH_3OH} = 32.11 \text{ g/mole}$

➤ $Mw_{Zn_6N_{24}C_{48}H_{60}} = 1365.51 \text{ g/mole}$

✓ 1.29 g ZIF-8 was obtained from the batch synthesis of first day. Consumed and remained amounts of materials were calculated from these data as,

Consumed amount of Zn^{+2}

$$= \frac{1.29 \text{ g ZIF} - 8}{1365.51 \frac{\text{g}}{\text{mole ZIF} - 8}} \cdot \frac{6 \text{ mole } Zn^{+2}}{1 \text{ mole ZIF} - 8} \cdot \frac{297.49 \text{ g}}{1 \text{ mole } Zn^{+2}}$$

$$= 1.69 \text{ g}$$

Remained amount of Zn^{+2} =

$$\begin{aligned} & \text{Initial amount of } Zn^{+2} - \\ & \text{Consumed amount of } Zn^{+2} \\ & = 4.8 \text{ g} - 1.69 \text{ g} = 3.11 \text{ g} \end{aligned}$$

Consumed amount of Hmim

$$= \frac{1.29 \text{ g ZIF} - 8}{1365.51 \frac{\text{g}}{\text{mole ZIF} - 8}} \cdot \frac{12 \text{ mole Hmim}}{1 \text{ mole ZIF} - 8} \cdot \frac{82.11 \text{ g}}{1 \text{ mole Hmim}}$$

$$= 0.93 \text{ g}$$

Remained amount of Hmim =

$$\begin{aligned} & \text{Initial amount of Hmim} - \\ & \text{Consumed amount of Hmim} \\ & = 10.56 \text{ g} - 0.93 \text{ g} = 9.63 \text{ g} \end{aligned}$$

Remained amount of MeOH =

$$= 376.96 \text{ g} - 1.29 \text{ g} - 3.11 \text{ g} - 9.63 \text{ g} = 362.93 \text{ g}$$

Theoretically produced amount of ZIF-8 was calculated as,

$$\begin{aligned} \text{ZIF-8}_{\max} &= \frac{4.8 \text{ g Zn}^{+2}}{297.49 \frac{\text{g}}{\text{mole ZIF-8}}} \cdot \frac{1 \text{ mole ZIF-8}}{6 \text{ mole Zn}^{+2}} \cdot \frac{1365.51 \text{ g/mole}}{1 \text{ mole ZIF-8}} \\ &= 3.67 \text{ g} \end{aligned}$$

$$\begin{aligned} \text{Yield, \%} &= \frac{\text{Obtained amount of ZIF-8}}{\text{Maximum amount of ZIF-8}} \cdot 100 \\ &= \frac{1.29 \text{ g ZIF-8}}{3.69 \text{ g ZIF-8}} \\ &= \boxed{35.2 \%} \end{aligned}$$

1st Step of the synthesis of second day;

The composition of the synthesis solution was calculated by using the remaining amounts of Zn^{+2} , Hmim and MeOH from the first day synthesis.

$$\text{Remaining amount of Zn}^{+2} = \frac{3.11 \text{ g Zn}^{+2}}{297.49 \frac{\text{g}}{\text{mole}}} = 0.010 \text{ mole}$$

$$\text{Remaining amount of Hmim} = \frac{9.63 \text{ g Hmim}}{82.11 \frac{\text{g}}{\text{mole}}} = 0.117 \text{ mole}$$

$$\text{Remaining amount of MeOH} = \frac{362.93 \text{ g MeOH}}{32.11 \frac{\text{g}}{\text{mole}}} = 11.303 \text{ mole}$$

$$\text{Zn}^{+2} / \text{Hmim} / \text{MeOH} = 0.010 / 0.117 / 11.303$$



0.63 g NaOH was added into the 1st Mother Liquor, and 1.67 g ZIF-8 was synthesized from this step.

Theoretically produced amount of ZIF-8 was calculated as,

$$\begin{aligned} \text{ZIF-8}_{max} &= \frac{3.11 \text{ g Zn}^{+2}}{297.49 \frac{\text{g}}{\text{mole ZIF-8}}} \cdot \frac{1 \text{ mole ZIF-8}}{6 \text{ mole Zn}^{+2}} \cdot \frac{1365.51 \text{ g/mole}}{1 \text{ mole ZIF-8}} \\ &= 2.38 \text{ g} \end{aligned}$$

$$\begin{aligned} \text{Yield, \%} &= \frac{\text{Obtained amount of ZIF-8}}{\text{Maximum amount of ZIF-8}} \cdot 100 \\ &= \frac{1.67 \text{ g ZIF-8}}{2.38 \text{ g ZIF-8}} \\ &= \boxed{70.2 \%} \end{aligned}$$

Consumed amount of Zn^{+2}

$$\begin{aligned} &= \frac{1.67 \text{ g ZIF-8}}{1365.51 \frac{\text{g}}{\text{mole ZIF-8}}} \cdot \frac{6 \text{ mole Zn}^{+2}}{1 \text{ mole ZIF-8}} \cdot \frac{297.49 \text{ g}}{1 \text{ mole Zn}^{+2}} \\ &= 2.18 \text{ g} \end{aligned}$$

Remained amount of Zn^{+2} =

$$\begin{aligned} &\text{Initial amount of Zn}^{+2} - \\ &\text{Consumed amount of Zn}^{+2} \\ &= 3.11 \text{ g} - 2.18 \text{ g} = 0.93 \text{ g} \end{aligned}$$

Consumed amount of Hmim

$$\begin{aligned} &= \frac{1.67 \text{ g ZIF} - 8}{1365.51 \frac{\text{g}}{\text{mole ZIF} - 8}} \cdot \frac{12 \text{ mole Hmim}}{1 \text{ mole ZIF} - 8} \cdot \frac{82.11 \text{ g}}{1 \text{ mole Hmim}} \\ &= 1.21 \text{ g} \end{aligned}$$

Remained amount of Hmim =

$$\begin{aligned} &\text{Initial amount of Hmim} - \\ &\text{Consumed amount of Hmim} \\ &= 9.63 \text{ g} - 1.21 \text{ g} = 8.42 \text{ g} \end{aligned}$$

Remained amount of MeOH =

$$= 362.93 \text{ g} + 0.63 \text{ g} - 1.67 \text{ g} = 361.89 \text{ g}$$

2nd Step of the synthesis of second day;

The composition calculation,

$$\text{Remaining amount of Zn}^{+2} = \frac{0.93 \text{ g Zn}^{+2}}{297.49 \frac{\text{g}}{\text{mole}}} = 0.0031 \text{ mole}$$

$$\text{Remaining amount of Hmim} = \frac{8.42 \text{ g Hmim}}{82.11 \frac{\text{g}}{\text{mole}}} = 0.103 \text{ mole}$$

$$\text{Remaining amount of MeOH} = \frac{361.89 \text{ g MeOH}}{32.11 \frac{\text{g}}{\text{mole}}} = 11.27 \text{ mole}$$

$$\text{Zn}^{+2}/\text{Hmim}/\text{MeOH} = 0.003/0.103/11.27$$

$$\text{Zn}^{+2}/\text{Hmim}/\text{MeOH} = 1/34.3/3635$$

In this step, initial amount of $Zn NO_3 \cdot 2.6H_2O$ was added into the second mother liquor. 1.15 g ZIF-8 was synthesized in this step.

Theoretically produced amount of ZIF-8 was calculated as,

$$\begin{aligned} ZIF - 8_{max} &= \frac{4.11 + 0.93 \text{ g } Zn^{+2}}{297.49 \frac{\text{g}}{\text{mole ZIF} - 8}} \cdot \frac{1 \text{ mole ZIF} - 8}{6 \text{ mole } Zn^{+2}} \cdot \frac{1365.51 \text{ g/mole}}{1 \text{ mole ZIF} - 8} \\ &= 3.86 \text{ g} \end{aligned}$$

$$\begin{aligned} \text{Yield, \%} &= \frac{\text{Obtained amount of ZIF} - 8}{\text{Maximum amount of ZIF} - 8} \cdot 100 \\ &= \frac{1.15 \text{ g ZIF} - 8}{3.86 \text{ g ZIF} - 8} \\ &= \mathbf{29.8 \%} \end{aligned}$$

Consumed amount of Zn^{+2}

$$\begin{aligned} &= \frac{1.15 \text{ g ZIF} - 8}{1365.51 \frac{\text{g}}{\text{mole ZIF} - 8}} \cdot \frac{6 \text{ mole } Zn^{+2}}{1 \text{ mole ZIF} - 8} \cdot \frac{297.49 \text{ g}}{1 \text{ mole } Zn^{+2}} \\ &= 1.5 \text{ g} \end{aligned}$$

Remained amount of Zn^{+2} =

$$\begin{aligned} &\text{Initial amount of } Zn^{+2} - \\ &\text{Consumed amount of } Zn^{+2} \\ &= 4.11 \text{ g} + 0.83 \text{ g} - 1.5 \text{ g} = 3.5 \text{ g} \end{aligned}$$

Consumed amount of Hmim

$$\begin{aligned} &= \frac{1.15 \text{ g ZIF} - 8}{1365.51 \frac{\text{g}}{\text{mole ZIF} - 8}} \cdot \frac{12 \text{ mole Hmim}}{1 \text{ mole ZIF} - 8} \cdot \frac{82.11 \text{ g}}{1 \text{ mole Hmim}} \\ &= 0.83 \text{ g} \end{aligned}$$

Remained amount of Hmim =

$$\text{Initial amount of Hmim} -$$

Consumed amount of Hmim

$$= 8.42 \text{ g} - 0.83 \text{ g} = 7.59 \text{ g}$$

Remained amount of MeOH =

$$= 361.89 \text{ g} + 4.11 \text{ g} - 1.15 \text{ g} = 364.85 \text{ g}$$

1st Step of the synthesis of third day;

The composition calculation,

$$\text{Remaining amount of Zn}^{+2} = \frac{3.5 \text{ g Zn}^{+2}}{297.49 \frac{\text{g}}{\text{mole}}} = 0.0117 \text{ mole}$$

$$\text{Remaining amount of Hmim} = \frac{7.59 \text{ g Hmim}}{82.11 \frac{\text{g}}{\text{mole}}} = 0.0924 \text{ mole}$$

$$\text{Remaining amount of MeOH} = \frac{364.85 \text{ g MeOH}}{32.11 \frac{\text{g}}{\text{mole}}} = 11.36 \text{ mole}$$

$$\text{Zn}^{+2}/\text{Hmim}/\text{MeOH} = 0.0117/0.0924/11.36$$

$$\text{Zn}^{+2}/\text{Hmim}/\text{MeOH} = 1/7.89/970$$

1.12 g NaOH was added into the 1st Mother Liquor, and 1.67 g ZIF-8 was synthesized from this step.

Theoretically produced amount of ZIF-8 was calculated as,

$$\begin{aligned} \text{ZIF-8}_{\max} &= \frac{3.5 \text{ g Zn}^{+2}}{297.49 \frac{\text{g}}{\text{mole ZIF-8}}} \cdot \frac{1 \text{ mole ZIF-8}}{6 \text{ mole Zn}^{+2}} \cdot \frac{1365.51 \text{ g/mole}}{1 \text{ mole ZIF-8}} \\ &= 2.71 \text{ g} \end{aligned}$$

$$\begin{aligned}
 \text{Yield, \%} &= \frac{\text{Obtained amount of ZIF - 8}}{\text{Maximum amount of ZIF - 8}} \cdot 100 \\
 &= \frac{1.67 \text{ g ZIF - 8}}{2.71 \text{ g ZIF - 8}} \\
 &= \mathbf{61.6 \%}
 \end{aligned}$$

Consumed amount of Zn⁺²

$$\begin{aligned}
 &= \frac{1.67 \text{ g ZIF - 8}}{1365.51 \frac{\text{g}}{\text{mole ZIF - 8}}} \cdot \frac{6 \text{ mole Zn}^{+2}}{1 \text{ mole ZIF - 8}} \cdot \frac{297.49 \text{ g}}{1 \text{ mole Zn}^{+2}} \\
 &= 2.18 \text{ g}
 \end{aligned}$$

Remained amount of Zn⁺² =

$$\begin{aligned}
 &\quad \text{Initial amount of Zn}^{+2} - \\
 &\quad \text{Consumed amount of Zn}^{+2} \\
 &= 3.5 \text{ g} - 2.18 \text{ g} = 1.32 \text{ g}
 \end{aligned}$$

Consumed amount of Hmim

$$\begin{aligned}
 &= \frac{1.67 \text{ g ZIF - 8}}{1365.51 \frac{\text{g}}{\text{mole ZIF - 8}}} \cdot \frac{12 \text{ mole Hmim}}{1 \text{ mole ZIF - 8}} \cdot \frac{82.11 \text{ g}}{1 \text{ mole Hmim}} \\
 &= 1.21 \text{ g}
 \end{aligned}$$

Remained amount of Hmim =

$$\begin{aligned}
 &\quad \text{Initial amount of Hmim} - \\
 &\quad \text{Consumed amount of Hmim} \\
 &= 7.59 \text{ g} - 1.21 \text{ g} = 6.38 \text{ g}
 \end{aligned}$$

Remained amount of MeOH =

$$= 364.85 \text{ g} + 1.12 \text{ g} - 1.67 \text{ g} = 364.3 \text{ g}$$

2nd Step of the synthesis of third day;

The composition calculation,

$$\text{Remaining amount of } Zn^{+2} = \frac{1.32 \text{ g } Zn^{+2}}{297.49 \frac{\text{g}}{\text{mole}}} = 0.0108 \text{ mole}$$

$$\text{Remaining amount of Hmim} = \frac{6.38 \text{ g Hmim}}{82.11 \frac{\text{g}}{\text{mole}}} = 0.0778 \text{ mole}$$

$$\text{Remaining amount of MeOH} = \frac{364.3 \text{ g Hmim}}{32.11 \frac{\text{g}}{\text{mole}}} = 11.35 \text{ mole}$$

$$Zn^{+2}/Hmim/MeOH = 0.0108/0.0778/11.35$$

$$Zn^{+2}/Hmim/MeOH = 1/7.2/1051$$

In this step, initial amount of $Zn \text{ NO}_3 \cdot 2.6H_2O$ was added into the second mother liquor. 0.97 g ZIF-8 was synthesized in this step.

Theoretically produced amount of ZIF-8 was calculated as,

$$\begin{aligned} ZIF - 8_{max} &= \frac{3.52 + 1.32 \text{ g } Zn^{+2}}{297.49 \frac{\text{g}}{\text{mole } ZIF - 8}} \cdot \frac{1 \text{ mole } ZIF - 8}{6 \text{ mole } Zn^{+2}} \cdot \frac{1365.51 \text{ g/mole}}{1 \text{ mole } ZIF - 8} \\ &= 3.7 \text{ g} \end{aligned}$$

$$\text{Yield, \%} = \frac{\text{Obtained amount of } ZIF - 8}{\text{Maximum amount of } ZIF - 8} \cdot 100$$

$$= \frac{0.97 \text{ g ZIF-8}}{3.70 \text{ g ZIF-8}}$$

$$= \boxed{26.2 \%}$$

Consumed amount of Zn^{+2}

$$= \frac{0.97 \text{ g ZIF-8}}{1365.51 \frac{\text{g}}{\text{mole ZIF-8}}} \cdot \frac{6 \text{ mole Zn}^{+2}}{1 \text{ mole ZIF-8}} \cdot \frac{297.49 \text{ g}}{1 \text{ mole Zn}^{+2}}$$

$$= 1.27 \text{ g}$$

Remained amount of $\text{Zn}^{+2} =$

$$\text{Initial amount of Zn}^{+2} -$$

$$\text{Consumed amount of Zn}^{+2}$$

$$= 4.84 \text{ g} + 1.27 \text{ g} - 1.5 \text{ g} = 3.57 \text{ g}$$

Consumed amount of Hmim

$$= \frac{0.97 \text{ g ZIF-8}}{1365.51 \frac{\text{g}}{\text{mole ZIF-8}}} \cdot \frac{12 \text{ mole Hmim}}{1 \text{ mole ZIF-8}} \cdot \frac{82.11 \text{ g}}{1 \text{ mole Hmim}}$$

$$= 0.70 \text{ g}$$

Remained amount of Hmim =

$$\text{Initial amount of Hmim} -$$

$$\text{Consumed amount of Hmim}$$

$$= 6.38 \text{ g} - 0.70 \text{ g} = 5.68 \text{ g}$$

Remained amount of MeOH =

$$= 364.3 \text{ g} + 3.53 \text{ g} - 0.97 \text{ g} = 366.86 \text{ g}$$

APPENDIX G

SAMPLE CALCULATION OF PARTICLE SIZE BY USING SCHERRER EQUATION

The particle size of materials can be calculated by using Scherrer equation with X-ray diffraction data. This calculation can give some information about particle size of materials, theoretically. In this study, the particle sizes of five different ZIF-8 samples were calculated.

Scherrer equation,

$$D = \frac{K * \lambda}{\beta_{1/2} * \cos\theta}$$

D: Crystalline diameter, Å

λ : 1.5418 Å

K: Scherrer constant = 0.94

$\beta_{1/2}$: The full width peak at 1/2 height

θ : Bragg diffraction angle

For 65 nm ZIF-8; 2θ value of the diffraction peak at (011) plane was determined by using XRD data. Also, $\beta_{1/2}$ value was calculated by using $(2\theta)_{max}$ and $(2\theta)_{min}$ values that were Bragg angles of the diffraction peak intercepted with width of the peak at 1/2 height.

$$2\theta = 7.30$$

$$\beta_{1/2} = (2\theta)_{max} - (2\theta)_{min} = 7.475 - 7.135 = 0.34$$

$$D = \frac{K * \lambda}{\beta_{1/2} * \cos\theta} = \frac{0.94 * 1.5418}{0.34 * \frac{\pi}{180} * \cos \frac{7.30}{2} * \frac{\pi}{180}} = 244 \text{ \AA}$$

$$D = 24.4 \text{ nm}$$

APPENDIX H

REPRODUCIBILITY OF ZIF-8 SYNTHESIS

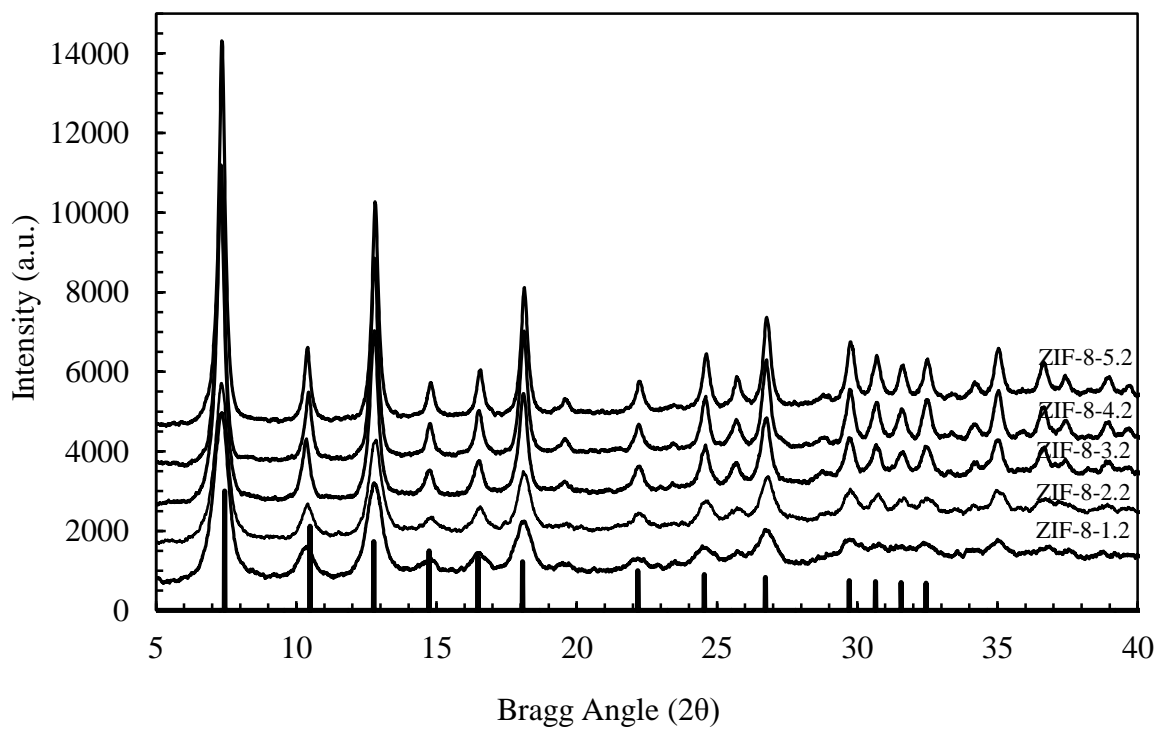


Figure.H.1 XRD patterns of the second trial synthesis of ZIF-8s

Table.H.1 Yields, crystallinities and calculated particle size of the second trial synthesis of ZIF-8 crystals with synthesis molar ratios

Sample Code	MeOH to ZnNO ₃ .6H ₂ O Molar Ratio	Yield, %	Crystallinity, %	Normalized Crystallinity, %	The Crystallite Size by using Scherrer Eqn. ((011) plane), nm
ZIF-8-1.1	1051	26.2	76.9	73.9	13
ZIF-8-2.1	1130	70.2	77.7	74.7	15
ZIF-8-3.1	695.1	35.2	97.2	93.5	24
ZIF-8-4.1	347.5	31.9	104.0	100.0	21
ZIF-8-5.1	86.9	28.9	101.0	97.1	31
ZIF-8-1.2	985	28.0	81.0	77.9	15
ZIF-8-2.2	1125.8	66.9	72.0	69.2	16
ZIF-8-3.2	695.1	36.0	95.5	92.6	21
ZIF-8-4.2	347.5	32.9	100.0	96.2	33
ZIF-8-5.2	86.9	30.2	104.0	100.0	32

APPENDIX I

THE NUMBER OF ZIF-8 PARTICLES PER GRAM CALCULATION

The number of particles was calculated by using radius of the particles and density of ZIF-8. The shapes of ZIF-8 particles were assumed as spheric. The calculation method followed as,

For 14 nm ZIF-8 particle;

$$\rho_{\text{ZIF-8}} = 0.95 \text{ g/cm}^3$$

The volume of one ZIF-8 particle;

$$V = \frac{4}{3} \pi r^3 = \frac{4}{3} \pi \cdot 7 \text{ nm} \cdot \frac{10^{-9} \text{ m}}{1 \text{ nm}}^3 = 1.437 \times 10^{-24} \text{ m}^3 / \text{particle}$$

The number of particle per gram;

$$0.95 \frac{\text{g}}{\text{cm}^3} \times \frac{1 \text{ cm}^3}{10^{-6} \text{ m}^3} \times \frac{1.437 \times 10^{-24} \text{ m}^3}{\text{particle}} = 1.365 \times 10^{-18} \text{ g/particle}$$

$$\frac{1}{1.365 \times 10^{-18} \text{ g/particle}} = 7.33 \times 10^{17} \text{ particles/gram}$$

APPENDIX J

DETERMINATION OF AVERAGE PARTICLE SIZES OF ZIF-8 BY USING SEM IMAGES

The particle sizes were determined in each SEM image of ZIF-8 crystals, which was given in Figure.J.1, by counting the length of 18 to 30 particles for each sample. The Image-J Software was used for counting and particle sizes of crystals were given in Table.J.1.

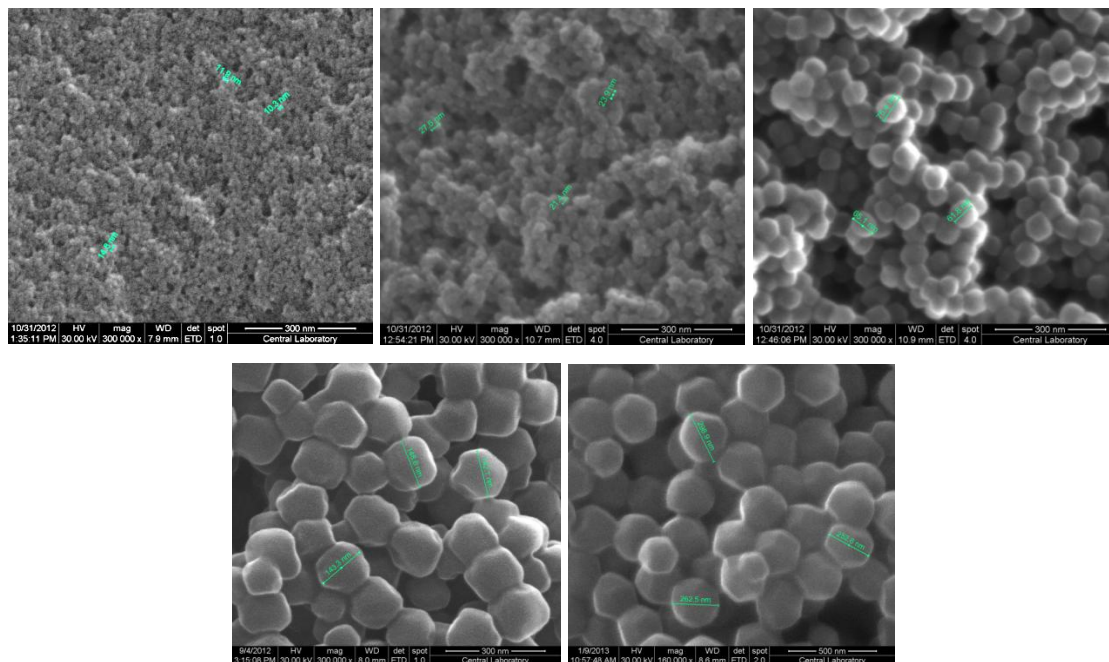


Figure.J.1 Used SEM images for counting particle sizes of ZIF-8 crystals

Table.J.1 Particle sizes of each crystals and average particle sizes of ZIF-8 samples

	Particle Size				
	ZIF-8-1	ZIF-8-2	ZIF-8-3	ZIF-8-4	ZIF-8-5
	11,9	27,6	61,8	149	299
	10,3	23,9	65,3	142	253
	14,8	21,4	75,4	143	263
	13,9	23,3	70,0	146	265
	13,9	23,4	66,0	140	252
	16,8	21,8	73,0	146	278
	16,5	19,9	68,0	142	292
	15,0	19,6	69,0	158	225
	15,9	19,8	64,7	149	252
	13,3	17,6	71,5	152	255
	15,9	21,5	71,0	156	247
	15,6	23,7	63,4	157	277
	12,0	19,6	61,6	158	252
	14,1	23,1	69,5	139	257
	14,7	22,2	61,6	122	248
	12,6	23,7	66,6	146	272
	15,6	22,7	58,5	144	264
	14,9	24,1	56,4	123	282
	15,1	26,9	63,7	144	242
	14,4	21,0	65,3	126	-
	11,7	21,6	60,1	145	-
	17,9	27,1	60,8	140	-
	12,0	26,3	60,3	152	-
	13,3	25,7	52,5	137	-
	11,7	27,1	62,7	149	-
	-	-	64,2	-	-
	-	-	68,2	-	-
	-	-	59,7	-	-
	-	-	65,8	-	-
	-	-	63,4	-	-
	-	-	61,7	-	-
Average	14,2±1,9	23,0±2,7	64,6±5,0	144,0±10	262±18

APPENDIX-K

SEM IMAGES OF ZIF-8 SAMPLES

The bigger sizes of SEM images of ZIF-8 crystals were given in Figure.K.1.

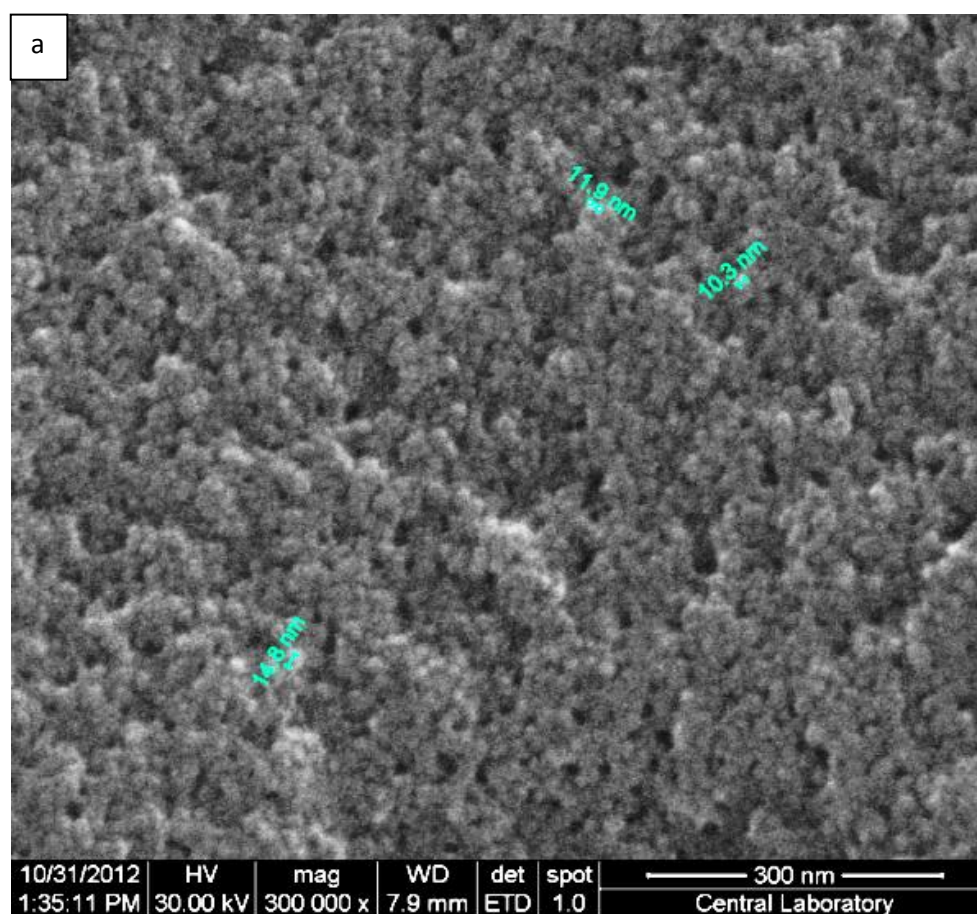


Figure.K.1 SEM images of ZIF-8 crystals (a) 14 nm, (b) 23 nm, (c) 65 nm, (d) 144 nm, (e) 262 nm

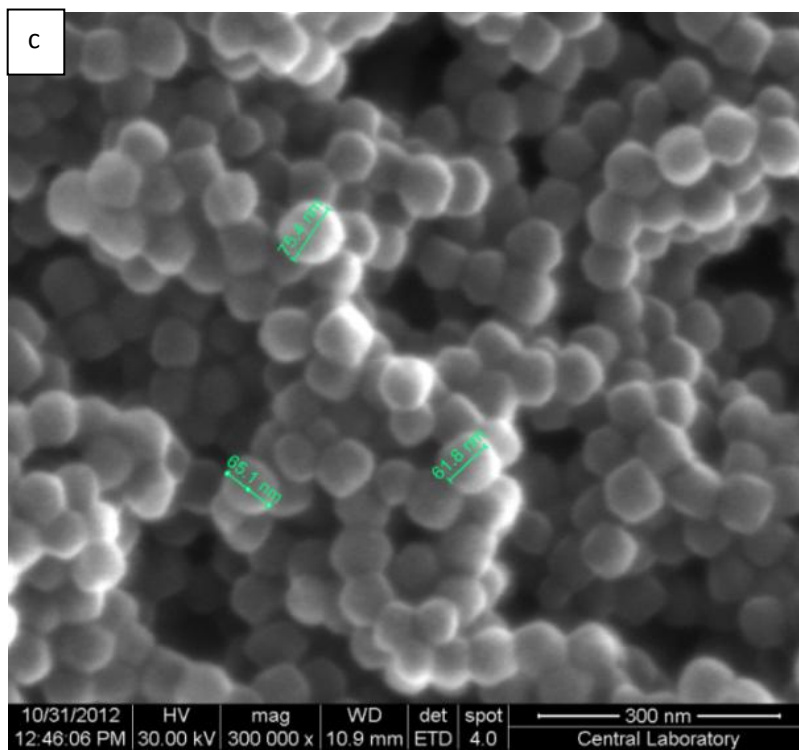
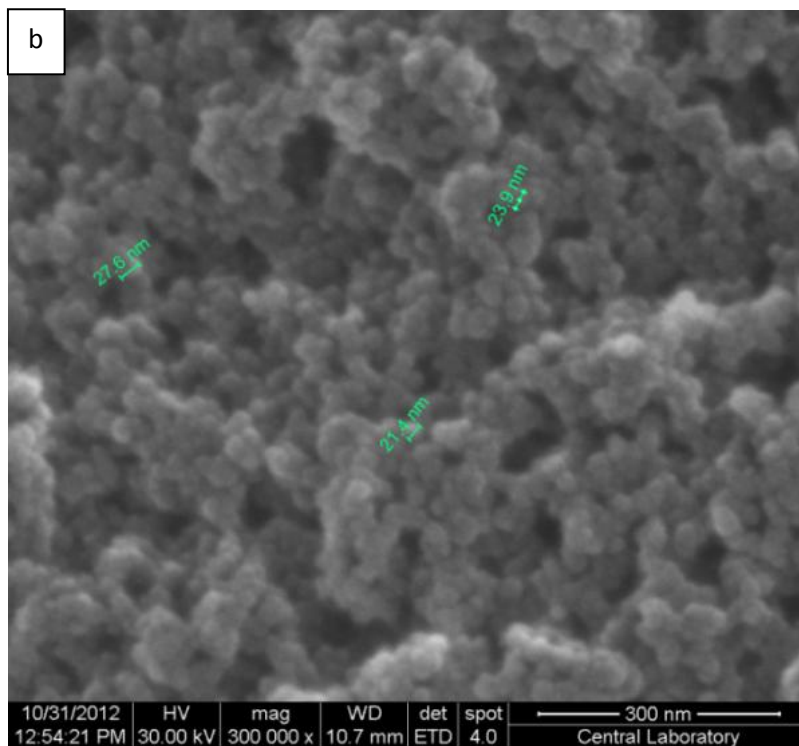


Figure.K.1 SEM images of ZIF-8 crystals (a) 14 nm, (b) 23 nm, (c) 65 nm, (d) 144 nm, (e) 262 nm (cont.)

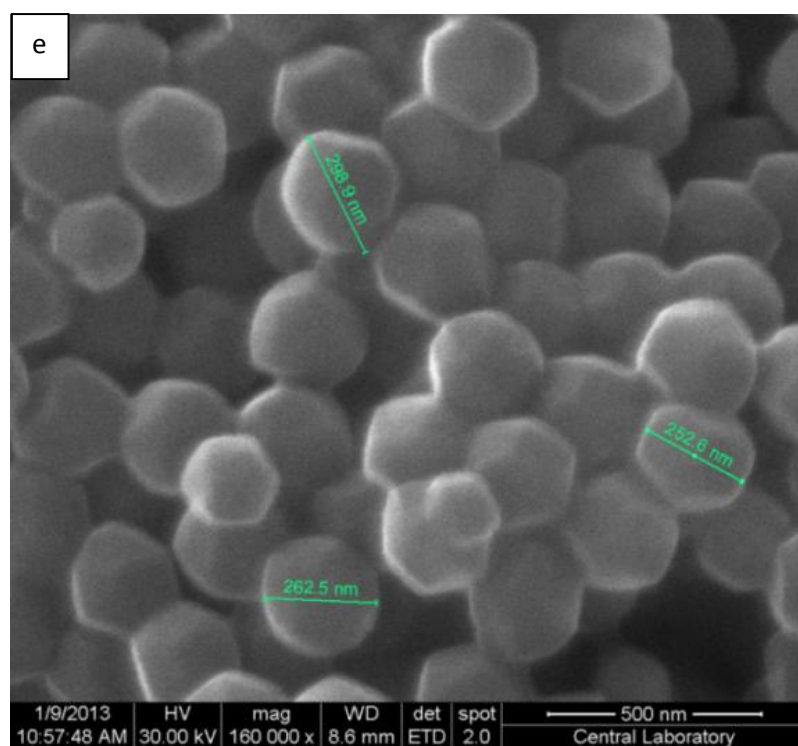
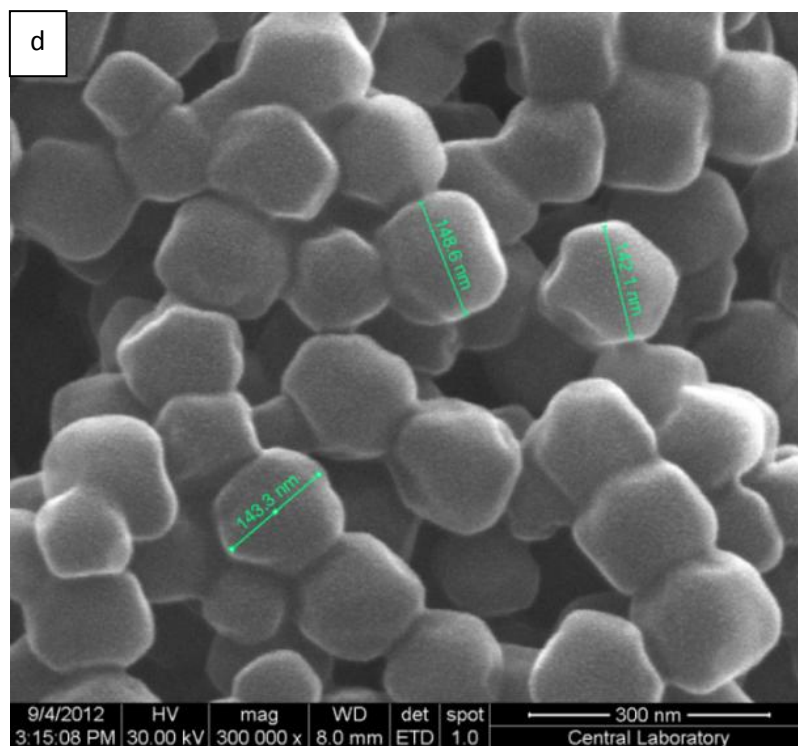


Figure.K.1 SEM images of ZIF-8 crystals (a) 14 nm, (b) 23 nm, (c) 65 nm, (d) 144 nm, (e) 262 nm (cont.)

APPENDIX-L

SEM IMAGES OF PES/pNA(4%)/ZIF-8(10%, 23nm) MMM

The bigger sizes of SEM images of PES/pNA(4%)/ZIF-8(10%, 23nm) were given in Figure.L.1.

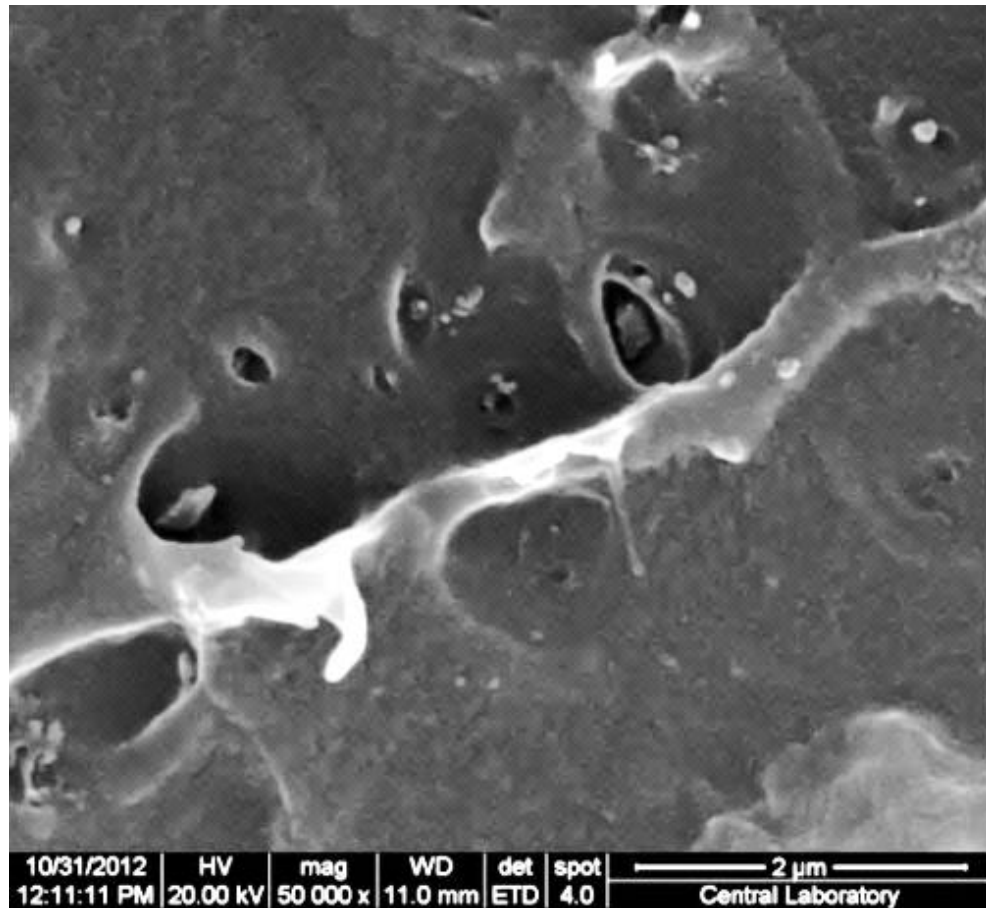


Figure.L.1 SEM images of PES/pNA(4%)/ZIF-8(10%, 23nm) MMM

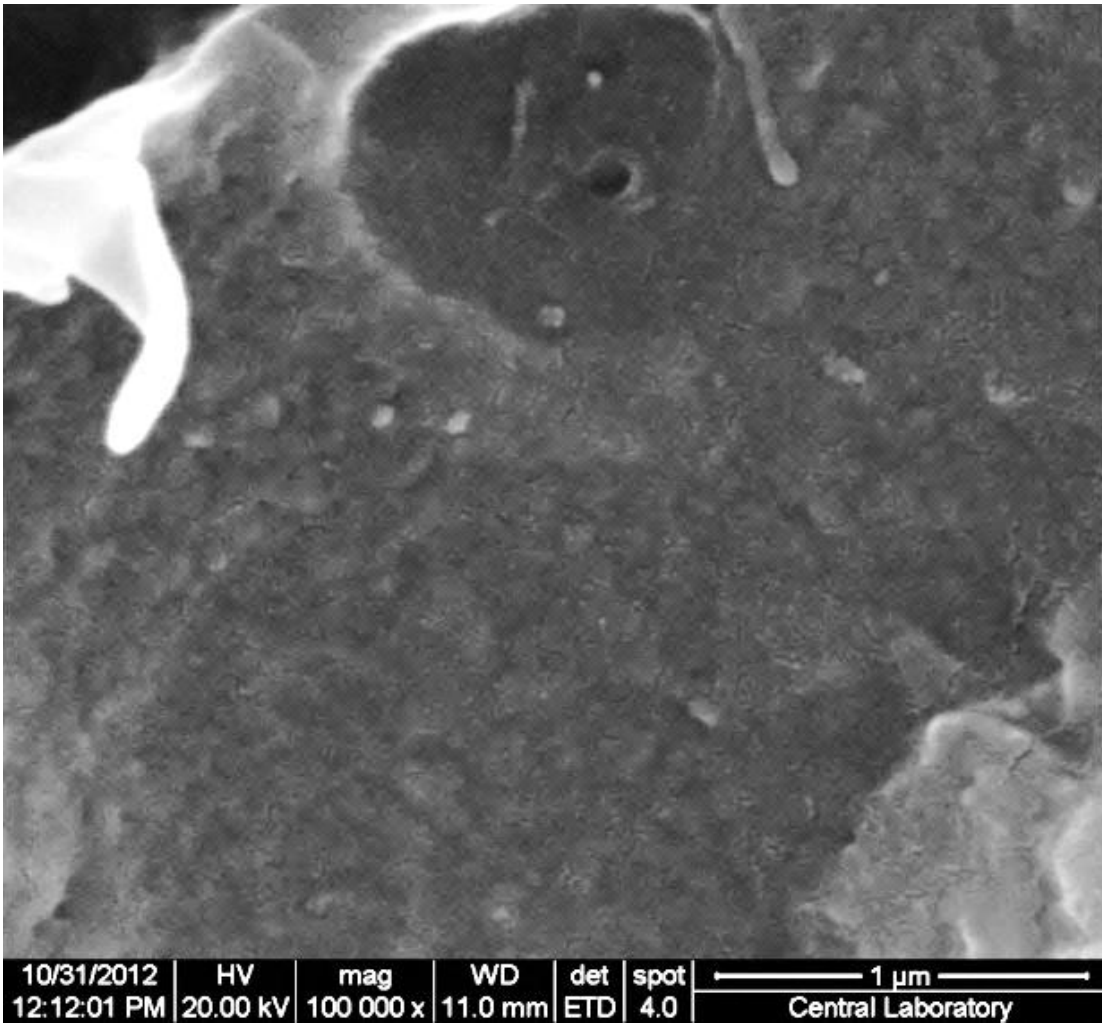


Figure.L.1 SEM images of PES/pNA(4%)/ZIF-8(10%, 23nm) MMM (cont.)

APPENDIX-M

REPRODUCIBILITIES OF SINGLE GAS PERMEATION EXPERIMENTS

Table M.1 Reproducibility data for pure PES, PES/pNA(4%) and ZIF-8 loaded PES/pNA(4%) MMMs

Membr	Cast - Part No.	Run	Permeability (barrer)			Selectivity		
			H ₂	CO ₂	CH ₄	H ₂ /CO ₂	CO ₂ /CH ₄	H ₂ /CH ₄
Pure PES	1-1	1	7,58	3,45	0,113	2,19	30,53	67,08
	1-2	2	7,60	3,45	0,115	2,20	30,00	66,09
	2-1	1	7,46	3,20	0,120	2,33	26,67	62,17
	Std. Dev.		0,08	0,13	0,00	0,07	1,74	2,12
	Avg.		7,55	3,45	0,114	2,20	30,27	66,59
PES/ pNA(4%)	1-1	1	8,34	2,68	0,061	3,11	48,36	136,72
		2	8,34	2,64		3,15		
	Std. Dev		0,00	0,03	0,00	0,03	0,00	0,00
	Average		8,34	2,66	0,061	3,13	48,36	136,72
PES/pNA(4%)/ZIF-8(10%) (14 nm ZIF-8)	1-1	1	14,18	4,87	0,167	2,91	29,16	83,41
		2	14,30	4,87		2,94		
	1-2	1	14,47	5,04	0,166	2,87	30,36	87,16
		2	14,52	5,09		2,85		
	2-1	1	12,09	4,44	0,188	2,72	23,62	64,30
		2	12,10	4,37		2,77		
	2-2	1	13,82	5,02	0,193	2,75	26,00	71,60
		2	13,73	5,08		2,70		
	Std. Dev		1,00	0,29	0,014	0,09	3,06	10,55
	Average		13,65	4,85	0,179	2,81	27,29	76,62

Table M.1 Reproducibility data for pure PES, PES/pNA(4%) and ZIF-8 loaded PES/pNA(4%) MMMs (cont'd)

Membr.	Cast - Part No.	Run	Permeability (barrer)			Selectivity		
			H ₂	CO ₂	CH ₄	H ₂ /CO ₂	CO ₂ /CH ₄	H ₂ /CH ₄
PES/pNA(4%)/ZIF-8(10%) (23 nm ZIF-8)	1-1	1	16,00	4,80	0,160	3,33	30,00	100,00
		2	15,95	4,80		3,32		
	1-2	1	15,89	4,88	0,156	3,26	31,28	101,86
		2	15,85	4,90		3,24		
	2-1	1	15,95	4,84	0,167	3,30	29,00	95,50
		2	15,90	4,84		3,29		
	2-2	1	14,95	4,56	0,151	3,28	30,20	99,00
		2	14,94	4,58		3,26		
	Avg.		15,68	4,78	0,159	3,29	30,12	99,09
	Std. Dev.		0,46	0,13	0,007	0,03	0,93	2,67
PES/pNA(4%)/ZIF-8(10%) (65 nm ZIF-8)	1-1	1	13,82	4,68	0,193	2,95	25,55	71,60
		2	13,81	4,67	0,189	2,96	24,71	73,07
	1-2	1	13,72	4,58	0,183	2,99	25,04	74,97
		2	13,65	4,51		3,02		
	2-1	1	13,43	4,57	0,185	2,94	24,70	72,60
		2	13,50	4,45		3,03		
	2-2	1	13,28	4,35	0,175	3,05	24,85	75,88
		2	13,14	4,39		2,99		
	Avg.		13,61	4,52	0,185	2,99	24,97	73,62
	Std. Dev.		0,30	0,12	0,007	0,04	0,35	1,76

Table M.1 Reproducibility data for pure PES, PES/pNA(4%) and ZIF-8 loaded PES/pNA(4%) MMMs (cont'd)

Membr.	Cast - Part No.	Run	Permeability (barrer)			Selectivity		
			H ₂	CO ₂	CH ₄	H ₂ /CO ₂	CO ₂ /CH ₄	H ₂ /CH ₄
PES/pNA(4%)/ZIF-8(10%) (144 nm ZIF-8)	1-1	1	9,13	3,24	0,136	2,82	23,82	67,13
		2	9,14	3,24		2,87		
	1-2	1	9,19	3,27	0,127	2,81	25,75	72,36
		2	9,24	3,30		2,80		
	2-1	1	9,12	3,19	0,123	2,86	25,93	74,14
		2	9,12	3,16		2,89		
	2-2	1	9,15	3,20	0,131	2,86	24,43	69,85
		2	9,11	3,24		2,81		
	Avg.		9,150	3,230	0,129	2,84	24,98	70,87
	Std. Dev.		0,04	0,05	0,006	0,03	1,02	3,05
PES/pNA(4%)/ZIF-8(10%) (262 nm ZIF-8)	1-1	1	9,08	3,22	0,136	2,82	23,67	66,76
		2	9,07	3,22		2,82		
	1-2	1	9,12	3,23	0,136	2,82	23,75	67,05
		2	9,11	3,30		2,76		
	2-1	1	9,10	3,21	0,137	2,83	23,43	66,42
		2	9,10	3,22		2,83		
	2-2	1	9,09	3,18	0,138	2,86	23,04	65,87
		2	9,06	3,18		2,85		
	Avg.		9,09	3,22	0,137	2,82	23,47	66,53
	Std. Dev.		0,02	0,04	0,001	0,03	0,32	0,51

Table M.1 Reproducibility data for pure PES, PES/pNA(4%) and ZIF-8 loaded PES/pNA(4%) MMMs (cont'd)

Membr.	Cast - Part No.	Run	Permeability (barrer)			Selectivity			
			H ₂	CO ₂	CH ₄	H ₂ /CO ₂	CO ₂ /CH ₄	H ₂ /CH ₄	
PES/pNA(4%)/ZIF-8(20%) (23 nm ZIF-8)	1-1	1	32,84	13,30	0,840	2,47	15,83	39,10	
		2	35,00	14,77		2,37			
	1-2	1	38,21	16,84	0,890	2,27	18,92	42,93	
		2	38,61	16,58		2,33			
	2-1	1	33,62	12,70	0,750	2,65	16,93	44,83	
		2	33,46	12,33		2,71			
	2-2	1	36,56	13,20	0,850	2,77	15,53	43,02	
		2	34,97	12,90		2,71			
	3-1	1	48,28	18,14	1,100	2,66	16,5	43,9	
		2	49,88	18,6		2,68			
	4-1	1	38,24	14,85	0,820	2,57	18,11	46,63	
		2	41,92	14,78		2,84			
	4-2	1	42,83	14,44	0,940	2,96	15,36	45,56	
		2	9,11	3,30		2,76			
		Avg.		39,14	14,87	0,886	2,64	16,74	42,76
		Std. Dev.		5,44	2,00	0,130	0,21	1,34	2,18

Table M.1 Reproducibility data for pure PES, PES/pNA(4%) and ZIF-8 loaded PES/pNA(4%) MMMs (cont'd)

Membr.	Cast - Part No.	Run	Permeability (barrer)			Selectivity		
			H ₂	CO ₂	CH ₄	H ₂ /CO ₂	CO ₂ /CH ₄	H ₂ /C H ₄
PES/pNA(4%)/ZIF-8(20%) (65 nm ZIF-8)	1-1	1	21,21	8,15	0,340	2,56	23,97	62,38
		2	21,30	8,28		2,57		
	1-2	1	22,10	8,42	0,356	2,62	23,65	62,08
		2	22,18	8,37		2,65		
	2-1	1	21,12	7,92	0,329	2,66	24,07	64,20
		2	20,86	7,87		2,65		
	2-2	1	19,60	7,47	0,311	2,62	24,02	63,02
		2	19,62	7,43		2,64		
	Avg.		21,00	7,99	0,334	2,62	23,93	62,92
	Std. Dev.		0,97	0,39	0,019	0,04	0,19	0,94
PES/pNA(4%)/ZIF-8(20%) (144 nm ZIF-8)	1-1	1	23,95	7,52	0,336	3,18	22,38	71,28
		2	23,46	7,44		3,15		
	1-2	1	22,96	7,23	0,420	3,17	17,21	54,67
		2	22,75	7,19		3,16		
	2-1	1	25,26	7,26	0,350	3,48	20,74	72,17
		2	25,00	7,32		3,42		
	3-1	1	23,64	7,21	0,330	3,27	21,84	71,63
		2	23,82	7,22		3,30		
	Avg.		23,86	7,30	0,359	3,27	20,54	67,44
	Std. Dev.		0,89	0,12	0,042	0,13	2,32	8,52

Table M.1 Reproducibility data for pure PES, PES/pNA(4%) and ZIF-8 loaded PES/pNA(4%) MMMs (cont'd)

Membr.	Cast - Part No.	Run	Permeability (barrer)			Selectivity		
			H ₂	CO ₂	CH ₄	H ₂ /CO ₂	CO ₂ /CH ₄	H ₂ /CH ₄
PES/pNA(4%)/ZIF-8(20%) (262 nm ZIF-8)	1-1	1	18,06	6,25	0,220	2,89	28,41	82,09
		2	17,64	6,04		2,92		
	1-2	1	18,47	6,57	0,225	2,81	29,20	82,09
		2	18,79	6,66		2,82		
	2-1	1	18,42	6,32	0,245	2,91	25,80	75,18
		2	18,60	6,38		2,92		
	2-2	1	17,00	5,75	0,214	2,96	26,87	79,44
		2	16,83	5,71		2,94		
	Avg.		17,98	6,21	0,226	2,90	27,57	79,70
	Std. Dev.		0,74	0,35	0,013	0,05	1,53	3,26

APPENDIX-N

REPRODUCIBILITIES OF HIGH PRESSURE PERMEATION EXPERIMENTS

Table N.1 Reproducibility data of high pressure permeation measurements for PES/pNA(4%)/ZIF-8(10%, 23nm) MMMs

Membr.	Pressure	Run	Permeability (barrer)			Selectivity		
			H ₂	CO ₂	CH ₄	H ₂ /CO ₂	CO ₂ /CH ₄	H ₂ /CH ₄
PES/pNA(4%)/ZIF-8(10%) (23 nm ZIF-8)	3	1	15,79	4,95	0,164	3,19	30,18	96,28
		2	15,8	4,9		3,22		
	6	1	15,98	4,64	0,135	3,44	34,37	118,37
		2	15,98	4,69		3,41		
	10	1	15,81	4,16	0,118	3,8	35,25	133,98
		2	15,85	4,14	0,112	3,83	36,96	141,52
	12	1	15,68	4,1	0,112	3,82	36,6	140
		2	15,68	4,09		3,83		
	15	1	15,56	3,95	0,101	3,94	39,1	154,06
		2	15,5	3,89		3,98		

APPENDIX-O

REPRODUCIBILITIES OF BINARY GAS PERMEATION EXPERIMENTS

Table O.1 Reproducibility data of binary gas permeation measurements for PES/pNA(4%)/ZIF-8(10%, 23nm) MMMs

Feed Pres., bar	CO ₂ in feed, %	Analysis / Run	Perm. , barrer	Permeate Composition			Separation Factor	
				X _{CO2}	X _{CH4}	X _{Total}		
10	50.0	1-1	1.54		0.9905	0.0148	1.0053	56.2
		1-2			0.9855	0.0154	1.0009	
		2-1	1.53		0.9884	0.0201	1.0085	
		2-2			0.9879	0.0206	1.0086	
				Avg.	0.9881	0.0177	1.0058	
				Std.Dev.	0.0021	0.0031	0.0036	
	39.6	1-1	0.94		0.9617	0.0337	0.9953	46.6
		1-2			0.9595	0.0345	0.9940	
		2-1	0.92		0.9650	0.0357	1.0007	
		2-2			0.9694	0.0236	0.9930	
				Avg.	0.9639	0.0319	0.9958	
				Std.Dev.	0.0043	0.0055	0.0034	
	37.1	1-1	0.89		0.9704	0.0304	1.0008	52.0
		1-2			0.9693	0.0312	1.0005	
		1-3			0.9661	0.0337	0.9997	
		2-1	0.91		0.9675	0.0293	0.9968	
		2-2			0.9660	0.0305	0.9965	
		2-3			0.9630	0.0322	0.9953	
			Avg.	0.9670	0.0312	0.9983		
			Std.Dev.	0.0026	0.0015	0.0024		

Table O.1 Reproducibility data of binary gas permeation measurements for PES/pNA(4%)/ZIF-8(10%, 23nm) MMMs (cont.)

Feed Pres., bar	CO ₂ in feed, %	Analysis / Run	Perm., barrer	Permeate Composition			Separation Factor		
				X _{CO2}	X _{CH4}	X _{Total}			
10	30.0	1-1	0.84		0.9621	0.0320	72.5		
		1-2			0.9657	0.0315			
		1-3			0.9611	0.0311			
		1-4			0.9596	0.0298			
		2-1	0.82		0.9688	0.0311		0.9999	
		2-2			0.9634	0.0302		0.9936	
		2-3			0.9685	0.0298		0.9983	
				Avg.		0.9642		0.0308	0.9949
				Std.Dev.		0.0036		0.0009	0.0037
	24.9	1-1	0.68		0.9546	0.0492	56.6		
		1-2			0.9510	0.0501			
		1-3			0.9498	0.0510			
		2-1	0.64		0.9591	0.0533		1.0124	
		2-2			0.9566	0.0522		1.0088	
		2-3			0.9528	0.0509		1.0037	
				Avg.		0.9540		0.0511	1.0051
				Std.Dev.		0.0035		0.0015	0.0046
	22.5	1-1	0.62		0.9082	0.1104	28.4		
		1-2			0.8971	0.1108			
		1-3			0.8986	0.1110			
		2-1	0.62		0.9092	0.1091		1.0184	
		2-2			0.9057	0.1063		1.0120	
		2-3			0.9023	0.1074		1.0097	
				Avg.		0.9035		0.1092	1.0127
				Std.Dev.		0.0050		0.0020	0.0047
	18.8	1-1	0.58		0.8363	0.1598	21.5		
		1-2			0.8328	0.1664			
		1-3			0.8304	0.1690			
2-1		0.57		0.8252	0.1649	0.9901			
2-2				0.8329	0.1667	0.9997			
2-3				0.8306	0.1659	0.9965			
			Avg.		0.8314	0.1655		0.9968	
			Std.Dev.		0.0037	0.0031		0.0036	
10.1	1-1	0.31		0.7816	0.2241	30.2			
	1-2			0.7627	0.2191				
	2-1	0.30		0.7779	0.2329		1.0107		
	2-2			0.7716	0.2302		1.0018		
			Avg.		0.7734		0.2266	1.0000	
			Std.Dev.		0.0082		0.0062	0.0126	

Table O.1 Reproducibility data of binary gas permeation measurements for PES/pNA(4%)/ZIF-8(10%, 23nm) MMMs (cont.)

Feed Pres., bar	CO ₂ in feed, %	Analysis / Run	Perm., barrer	Permeate Composition			Separation Factor	
				X _{CO2}	X _{CH4}	X _{Total}		
3	51.7	1-1	1.54		0.9722	0.0267	0.9989	33.8
		1-2			0.9712	0.0264	0.9976	
		1-3			0.9713	0.0261	0.9974	
		2-1	1.57		0.9722	0.0270	0.9992	
		2-2			0.9709	0.0269	0.9978	
		2-3			0.9702	0.0263	0.9965	
				Avg.	0.9714	0.0266	0.9979	
				Std.Dev.	0.0008	0.0003	0.0010	
	30.5	1-1	0.87		0.9462	0.0618	1.0080	35.2
		1-2			0.9420	0.0617	1.0038	
		1-3			0.9464	0.0612	1.0077	
		2-1	0.87		0.9485	0.0608	1.0093	
		2-2			0.9473	0.0607	1.0080	
		2-3			0.9493	0.0606	1.0099	
				Avg.	0.9466	0.0611	1.0078	
				Std.Dev.	0.0025	0.0005	0.0021	
	24.5	1-1	0.71		0.9087	0.0986	1.0073	28.5
		1-2			0.9060	0.0985	1.0045	
		1-3			0.9046	0.0982	1.0028	
		2-1	0.72		0.9059	0.0982	1.0052	
		2-2			0.9038	0.0992	1.0023	
		2-3			0.9024	0.0976	1.0021	
				Avg.	0.9052	0.0984	1.0037	
				Std.Dev.	0.0022	0.0005	0.0017	
	20.1	1-1	0.55		0.8460	0.1603	1.0063	20.5
		1-2			0.8441	0.1640	1.0081	
		1-3			0.8407	0.1665	1.0072	
		2-1	0.58		0.8442	0.1637	1.0079	
2-2				0.8439	0.1627	1.0066		
2-3				0.8323	0.1603	0.9926		
			Avg.	0.8438	0.1635	1.0072		
			Std.Dev.	0.0050	0.0024	0.0060		
12.0	1-1	0.29		0.7939	0.2115	1.0054	27.8	
	1-2			0.7918	0.2111	1.0030		
	1-3			0.7911	0.2103	1.0014		
	2-1	0.31		0.7941	0.2109	1.0050		
	2-2			0.7929	0.2100	1.0030		
	2-3			0.7939	0.2099	1.0038		
			Avg.	0.7928	0.2108	1.0035		
			Std.Dev.	0.0012	0.0006	0.0015		

Table O.1 Reproducibility data of binary gas permeation measurements for PES/pNA(4%)/ZIF-8(10%, 23nm) MMMs (cont.)

Feed Pres., bar	CO ₂ in feed, %	Analysis / Run	Perm., barrer	Permeate Composition			Separation Factor		
				X _{CO2}	X _{CH4}	X _{Total}			
3	39.5	1-1	1.08		0.9566	0.0401	0.9967	35.4	
		1-2			0.9582	0.0407	0.9989		
		1-3			0.9579	0.0411	0.9990		
		2-1	1.11		0.9539	0.0412	0.9952		
		2-2			0.9555	0.0419	0.9974		
		2-3			0.9575	0.0424	0.9998		
				Avg.		0.9566	0.0412		0.9978
				Std.Dev.		0.0016	0.0008		0.0017